Competing Quantum Dynamical Processes
and
Novel Facets of Coherent Population Trapping and Noise Spectroscopy

A Thesis submitted for the degree of
Doctor of Philosophy

by
LV. Jyotsna

School of Physics
University of Hyderabad
Hyderabad - 500 046
INDIA
August 1995

DECLARATION

I hereby declare that the matter embodied in this Thesis is the result of investigations carried out by me in the School of Physics, University of Hyderabad, Hyderabad - 500 046, under the supervision of Prof. G.S. Agarwal.

Place: Hyderabad

Date: 9-8-95

(I.V. Jyotsna)

CERTIFICATE

This is to certify that the work contained in this thesis entitled,**"Competing Quantum Dynamical Processes and Novel Facets of Coherent Population Trapping and Noise Spectroscopy",** has been carried out by **I.V. Jyotsna,** under my supervision for the full period prescribed under Ph.D. ordinances of the University and the same has not been submitted for the award of research degree of any University.

Place: *Hyderabad/Ahmedabad*

Date: *9-8-95*

G S Agarwal
Thesis supervisor

Dean *9.8.95*

School of Physics,
University of Hyderabad,
Hyderabad - 500 046, INDIA.

To my father who has always been my source of inspiration. . . . . .

To my mother whose ambition for me and whose sacrifices have made this day possible. . . . . .

To my brother whose faith in me has always boosted my morale. . . . . .

ACKNOWLEDGEMENTS

I would like to express my gratitude to Prof. G. S. Agarwal for his excellent guidance and supervision. His enthusiasm for physics and his hard work have always been my source of inspiration. Working with him has been a unique and illuminating experience.

I thank the Dean, School of Physics, for allowing me to avail the facilities in the School.

I thank all the non-teaching staff in the School of Physics who helped me in different capabilities at different stages of my research work.

I thank Dr. S. Dutta Gupta for all the times he patiently helped me resolve computational difficulties.

I thank Prof. V. Srinivasan for his everflowing 'milk' of kindness and affection. I thank Prof. S. Chaturvedi for being so pleasant and concerned.

I remember Vinod here for all the help rendered. Without his help in the C. C. some of the numerical calculations in this thesis could not have been pursued at all.

I thank Ananthalakshmi my friend and philosopher for being what she is. I sincerely thank Suneel for just being there whenever I am in dire straits.

I take this opportunity to sincerely thank all my teachers in school, in Bachelors and Masters degree programs who laid the foundations for my education.

I reminisce here the good research times I shared with Shanta, Tara, Jolly and Arun, Samba, Ramana, Ashok, Gautam, Han, Harsha, Nirmal and scores of others who cannot all be named here. I owe a special thanks to all of them as each of them has invested a part of themselves in me.

I thank my friend Srinivas without whom the thesis would not have materialized at all.

I thank my parents-in-law who have been very accommodating about all the oddities in pursuing my thesis.

Lastly I acknowledge Jaganath, my husband whose presence in the last throes of research acted as a motivation.

Name	:	**I.V. JYOTSNA**
Nationality	:	**INDIAN**

Educational Qualifications

Ph.D.	:	submitted thesis in August 1995
		School of Physics, University of Hyderabad
		Hyderabad, India
Thesis Supervisor	:	Prof. G.S. Agarwal
Master's Degree	:	May 1989, M.Sc. in Physics
		Indian Institute of Technology Madras, India
Bachelor's Degree	:	May 1987, B.Sc. in Mathematics, Physics, **Chemistry**
		Osmania University, Hyderabad, India

Fellowships, Awards and Medals

1987	A rolling cup for standing first in all **faculties** in **the** Bachelors Degree at college level.
1987	A gold medal for standing first in Bachelors Degree in Science (B.Sc.) at college level.
1987	A second gold medal for standing first in Physics in B.Sc. at College level.
1987	National Merit Scholarship, Ministry **of** Education, Government **of** India.
1990	Junior Research Fellowship of the Council **for** Scientific and Industrial Research (CSIR), New Delhi, India.
1992	Senior Research Fellowship of **CSIR, New Delhi, India.**

List of Publications

1. *The Jaynes-Cummings Model with Continuous External Pumping.*
   I.V. Jyotsna and G.S. Agarwal, Optics Commun. 99, 344 (1993).

2. *Competing Three Photon and Single Photon Transitions in Cavity QED.*
   I.V. Jyotsna and G.S. Agarwal, Phys. Rev. **A50,** 1770 (1994).

3. *Derivation of Spectroscopic Information from Intensity-Intensity Correlations.*
   I.V. Jyotsna, G.S. Agarwal and Gautam Vemuri, Phys. Rev. **A51,** 3169 (1994).

4. *Coherent Population Trapping at Low Light Levels.*
   I.V. Jyotsna and G.S. Agarwal, Phys. Rev. **A52,** (in press) 1995.

5. *Dynamics of Coherent Population Trapping States in Dense Systems.*
   I.V. Jyotsna and G.S. Agarwal, submitted to Phys. Rev. A.

6. *Fractional Revivals in Optical Parameteric Interactions.*
   G.S. Agarwal and I.V. Jyotsna, to be submitted to Phys. Rev. **Lett.**

Presentations in Conferences/Symposia

1. *The Jaynes-Cummings Model with Continuous External Pumping*
   i) National Laser Symposium, Indian Institute of Technology, Madras, India, February, 1993.
   ii) Recent Developments in Quantum Optics, University of Hyderabad, Hyderabad, India, March, 1993.

2. *Competing Dynamical Processes in Cavity QED.*
   i) Coherent States-New Developments and Perspectives, University of Hyderabad, Hyderabad, India, October 1993.
   ii) Winter College in Quantum Optics, International Center for Theoretical Physics, Trieste, Italy, February-March 1994.

3. *An Introductory Course in Holography.*
   Invited talk at the Workshop on Fundamentals of Lasers and Laser Applications University of Hyderabad, Hyderabad, India.

TABLE OF CONTENTS

ABSTRACT

In Chapter 1 the background and motivation for studying the various nonlinear processes investigated in the thesis is elucidated. An overview of the entire thesis is given in this chapter. A brief introduction to the semiclassical and quantum treatment of the interaction of radiation with matter is given.

The second, third and fourth chapters deal with phenomena completely explicable in the semiclassical treatment while the last two chapters deal with quantum electrodynamical competing processes which come under the purview of the fully quantum mechanical Jaynes-Cummings model (JCM).

In Chapter 2 the formation of the coherent population trapping (CPT) state at low light levels is demonstrated. A dynamical analysis of the behavior before the occurrence of CPT is done by an eigenvalue calculation, which shows that the CPT state takes longer to form for weak fields. An unusual sharp dip is discovered in the steady state response of the system for unequal decay rates. The origin of the dip is traced to the trapping conditions prevalent.

In Chapter 3 the effect of local fields on the CPT state in a dense system is studied. CPT is shown to persist undestroyed under their presence for all ranges of field strengths. A novel dispersive behavior is observed near the CPT condition in addition to the Lorentz shift. The dynamical behavior of the system at times before the occurrence of CPT is investigated. Local fields are shown to delay the formation of the CPT state. Enhancement of gain in a popular scheme of lasing without inversion is also demonstrated.

In Chapter 4 a simple analytic framework based on nonlinear response theory that uses a fluctuating laser source for probing spectroscopic data of the atomic system is presented. The idea is based on the fact that linear susceptibility has all the information

about the atomic system. A homodyne detection scheme with a phase shifter in one of the arms to distinguish between the different orders in **the electric field,** is suggested for the examination of the intensity-intensity correlations of the scattered **light from the** medium.

In Chapter 5 a numerical study of the dynamics of the atom-field **system is done in** the JCM with continuous external pumping. A simple analytical derivation is performed to support the numerical study. This model is a simple example of the two channel cavity quantum electrodynamical (QED) model where there is a classical field in one of the channels. For exact resonance of the atom, the external field and the cavity mode the dynamical properties of the atomic system are found to be identical to the properties in the standard JCM where the field enters via the initial conditions. The field properties in the two models are shown to be simply related. A complex behavior is shown to occur in the case of finite detunings.

In Chapter 6 the dynamics of a fully quantum mechanical model of the two channel cavity QED is studied. The competition between a three photon process and a single photon process occuring simultaneously between the two atomic levels is studied for various initial conditions. Even the simplest case is shown to exhibit interesting mode mixing and entanglement properties. The predictions of the quantum theory are compared and contrasted with the results obtained from various semiclassical theories. Unlike the quantum case periodicity is found to be the signature of the semiclassical results. By comparing this model with the JCM driven by an external pump studied in Chapter 5 the quantum effects are shown to be rather dominant.

Chapter 1

INTRODUCTION

The study of optics was revolutionized in a major way in two different centuries due to two fundamental causes. The first was the grand unification of the laws of electricity and magnetism with the laws of light by Maxwell [1] in the middle of the 19th century. With this, most optical phenomena like reflection, refraction, dispersion could be explained using a microscopic theory of interaction of electrons constituting matter and radiation [2]-

The other cause was the development of the laser in 1960 by Maiman [3]. The interpretation of experiments using the laser has necessitated extensions of the previously developed theory in several directions. The comparative simplicity of theoretical tools required for the treatment of light in the visible region was modified by the invention of the laser. The high intensity of laser light alongwith spatial and temporal coherence makes it possible to observe processes which are too weak to be detected with light from a conventional source. For example several nonlinear optical processes have become observable.

Laser has initiated a flood of detailed experiments of previously observed processes with conventional light sources, e.g., scattering of light. The greater detail of experimental investigation requires a more careful theoretical treatment. Also the understanding of the inner working of the laser itself requires a careful treatment of the **interaction of** atoms with electromagnetic (em) radiation.

Introduction

The study of the interaction of radiation with matter in different approximations, in different situations and at different levels comprises a major part of quantum optics and non-linear optics. The last two decades have been quite eventful for the quantum optics community, where theory has tried to keep pace with experiments and experiments were performed concurrently with the development of theory. The evolution from classical theories to the fully quantum theories and the experimental verifications performed in classical as well as most recently in the quantum domains makes an illuminating experience into the foundations of basic physics.

The interaction of radiation with matter is described in different theoretical frameworks which are based on historical development and the kind of problems one solves. In 1880 H. A. Lorentz [2] proposed the earliest theory now called the classical theory where the constituents of matter follow Newton's laws and the light fields follow Maxwell equations given by

$$\vec{\nabla}.\vec{E} = 4\pi\rho \qquad \textbf{(1a)}$$

$$\vec{\nabla}.\vec{B} = 0 \qquad \textbf{(16)}$$

$$\vec{\nabla} \times \vec{E} = -\frac{1}{c}\frac{\partial \vec{B}}{\partial t} \qquad \textbf{(1c)}$$

$$\vec{\nabla} \times \vec{B} = \frac{4\pi}{c}\vec{J} + \frac{1}{c}\frac{\partial \vec{E}}{\partial t} \quad . \qquad \textbf{(1d)}$$

where E is the electric field, B is the magnetic field, $/$ is the current density, p is the charge density and c is the velocity of light. These equations of Maxwell [1] unify the laws of electricity and magnetism with the laws of light which led to the understanding of the optical phenomena such as reflection etc. Lorentz accounted for these phenomena with the proposition of a simple model based on the interaction of elementary charges and dipoles which constitute matter with the classical electric and magnetic fields associated

with the light waves. He assumed that the charges are bound to the neutral atoms and when interacting with the em field oscillate about their mean positions. Each electron-ion pair behaves like a simple harmonic oscillator and couples to the em field through its dipole moment. The motion of such a dipole comprising the dielectric system is governed by the Lorentz equation

$$m\frac{\partial \vec{v}}{\partial t} = \vec{F} = e(\vec{E} + \frac{\vec{v}}{c} \times \vec{B}) \tag{1.2}$$

where m, e and *v* are the mass, charge and velocity of the electron, and *F* is the Lorentz force.

By the turn of the 20th century it had become clear that there were phenomena in nature which cannot be explained by existing classical theories. While studying the properties of matter scientists discovered that matter at atomic scales behaved nothing like that at large scales. The first indication that the laws of classical physics breakdown, arose with the study of the kinetic theory of gases and the black body spectrum. The subsequent work of Planck, Bohr and Einstein culminated in the development of quantum mechanics by Schrodinger, Heisenberg and Dirac. Use of quantum mechanics led to the formulation of the quantum theories of light and matter. One discovered situations where it was adequate to treat the electromagnetic field classically whereas situations involving few photons required quantized theory. These are the semiclassical and the fully quantum treatments. This thesis mainly deals with phenomena which fit into one or the other of these frameworks. The first part of the thesis deals with laser phenomena fully describable in the semiclassical regime. The second part of the thesis concerns phenomena for which a fully quantum treatment is required for a complete description of the physics. A brief introduction to the two models supported by important examples of laser phenomena, understood in these two frameworks, relevant to our thesis study is given in what follows.

1.1 First Quantization and the Semiclassical Approximation

The light field is treated classically by Maxwell's equations but matter is quantized and is treated by Schrodinger equation. The quantum theory predicts that atoms are in a superposition of energy levels and that they are like electric charges on springs i.e., dipole harmonic oscillators, when subject to an em field. The classical oscillator (Lorentz model) exhibits analog of spontaneous emission, stimulated absorption and emission. Its processes depend on the oscillator's initial phase. But in the case of the quantum dipole the incident field induces the right phase for stimulated emission irrespective of the initial phase. So the quantum dipole oscillator picture of the atom is absolutely necessary for all laser phenomena studies. The electron's motion is quantized by replacing the classical variables with operators, i.e.,

$$p\text{—}\bullet\_tW, \qquad H\text{—}{>}ihd/dt. \tag{1.3}$$

Here $h = h/27r$ where h is the Planck's constant and p is the momentum of the electron. The Hamiltonian energy H is replaced by the complex operator ihd/dt. The semiclassical Schrodinger equation for the wave function ^(r,tf) of the system is

$$
i\hbar\frac{\partial\Psi(\vec{r},t)}{\partial t} = \left\{\frac{[-i\hbar\vec{\nabla} - (\frac{\varepsilon}{c})\vec{A}(\vec{r},t)]^2}{2m} + V(\vec{r}) + e\Phi\right\}\Psi(\vec{r},t)
$$
$$
= (H_o + H_I)\Psi(\vec{r},t) \tag{1.4}
$$

where the unperturbed Hamiltonian is

$$H_o = -\frac{\hbar^2}{2m}\vec{\nabla}^2 + V(\vec{r}) + e\Phi \tag{1.5}$$

and the interaction Hamiltonian is

$$H_I = \frac{e}{2mc}\left[2i\hbar\vec{A}(\vec{r},t).\vec{\nabla} + i\hbar\vec{\nabla}.\vec{A}(\vec{r},t)\right] + \frac{e^2}{2mc^2}\vec{A}(\vec{r},t).\vec{A}(\vec{r},t). \tag{1.6}$$

Here A and $ are the vector and scalar potentials respectively. $V(r)$ is the Coulomb potential experienced by the electron. If $A \longrightarrow A' = A + \nabla *$ and $V \longrightarrow V = V + \backslash^\wedge$ there is no change in E and B. Here $\backslash$ is an arbitrary scalar function. This allows one freedom to choose a suitable gauge in different problems. One common gauge is the Coulomb gauge where $V.A = 0$ and $3> = 0$. In the Coulomb gauge Eq.(1.6) becomes

$$H_I = \frac{ie\hbar}{mc} A(\vec{r}, t).\vec{\nabla} + \frac{e^2}{2mc^2} \vec{A}(\vec{r}, t).\vec{A}(\vec{r}, t) \tag{1.7}$$

A useful approximation often used in quantum optics at this stage is the dipole approximation which puts the interaction Hamiltonian in a simpler form.

DIPOLE APPROXIMATION

The wavelength in optical and suboptical regions is very large compared to the size of the atom. So the field variables like $E(r,t)$, $A(r, t)$ are assumed to have no spatial variation in the vicinity of the atom and hence they can be replaced by $E(t),A(t)$.

In dipole approximation a transformed Hamiltonian is convenient to use instead of (1.7). Using the transformation $*(\vec{r},t) = e\&^{r'*}\backslash l)(r,t)$ in Eq. (1.7) we get

$$i\hbar\frac{\partial\psi(\vec{r}, t)}{\partial t} = \left[\frac{\hbar^2}{2m}\vec{\nabla}^2 + V(\vec{r}) - e\vec{r}.\vec{E}(t) \right] \psi(\vec{r}, t) \tag{1.8}$$

The semiclassical atom and field interaction Hamiltonian is now given by

$$H_I = -\vec{d}.\vec{E}(t) \quad . \tag{1.9}$$

where $d = er$ is the dipole moment operator. This form of interaction Hamiltonian is widely used in laser theory and nonlinear optical phenomena. However, it is very difficult to study the interaction of even one atom with light *exactly*. In laser physics other simplifications can be made depending on experimental conditions. One of them is the two-level approximation.

TWO LEVEL APPROXIMATION

If the incident radiation field is nearly monochromatic and if it almost coincides in frequency with one of the transition frequencies of the atom, this atom can be thought of approximately as a two-level atom. In reality no two-level atom exists, but many coherent resonant interactions do involve only two levels under suitable conditions. For example the spectral width of the applied field should just make the central frequency transition possible. A common mathematical notation for the two level atom is introduced below.

Let the excited and ground levels be denoted by |1) and |2) in the Dirac notation. Now |1) and |2) are the eigenstates of the unperturbed Hamiltonian, H_o, for the two-level atom. So

$$H_o = E_1|1\rangle\langle 1| + E_2|2\rangle\langle 2| \tag{1.10}$$

where E_1 and $E2$ are the energies of the levels |1) and |2) respectively.

The dipole operator is written as

$$\vec{d} = \sum_{ij} d_{ij}|i\rangle\langle j| \tag{1.11}$$

where $i,j = 1,2$ and $i \neq j$ and d_{ij} is the average of the dipole operator between the states $|i\rangle$ and |j), i.e. $d_{ij} = (2|d|j)$. $\vec{d}$ is a vector operator and has odd parity, hence no diagonal elements exists.

Let us consider the interaction of the two-level atom with a plane monochromatic em field. Using the dipole approximation the electric field is evaluated at the position of the nucleus R and is written as

$$\vec{E} = \vec{\mathcal{E}}e^{i\vec{k}.\vec{R}-i\omega t} + c.c. \tag{1.12}$$

where $\mathcal{E}$ is a constant (continuous wave). The frequency ω is chosen to be close to the transition frequency ω_0 defined as $\omega_0 = \hat{j}^{\wedge 2}$. If the origin of the energy is midway between E_1 and E_2, using Eq.(1.9) and (1.10) the total Hamiltonian of the system is

written as

$$H = \frac{\hbar\omega_o}{2}[|1\rangle\langle1| - |2\rangle\langle2|] - [d_{12}|1\rangle\langle2| + d_{21}|2\rangle\langle1|].\vec{E} \tag{1.13}$$

A two level atom is similar to a spin $|$ particle in a magnetic field. The dynamical equations for a two-level atom derived from the Schrodinger equation are the same as those for a spin $|$ particle. In the spin $\backslash$ notation the following definitions apply:

$$S^+ = |1\rangle\langle2|, \quad S^- = |2\rangle\langle1|, \quad S^z = \frac{1}{2}[|1\rangle\langle1| - |2\rangle\langle2|] \tag{1.14}$$

where S^+ and S are the raising and lowering operators and S^z is called the inversion operator. The nomenclature is appropriate because 5^+ acting on ground state $|2)$ gives the excited state $|1)$ and $S\sim$ acting on excited state $|1)$ gives the ground state $|2)$. The expectation value of S^z is related to the difference of the populations in the excited and ground states. Hence S^z is called the inversion operator. Also $S^+ = S^x$ 4- iS^y and $S\sim = S^x \sim iS^y$. From the angular momentum algebra, commutators satisfied by the atomic operators are $[S^\wedge S^*] = {}^\wedge S^*$, $[S^+,S\sim] = 2S^Z$.

Hence in the spin $|$ notation the total Hamiltonian of the interaction of a two level atom with em field is

$$H = \hbar\omega_o S^z - \left(\vec{d}_{12}S^+ + \vec{d}_{21}S^-\right).\vec{E} \tag{1.15}$$

The presence of variables changing rapidly at optical frequencies makes it difficult to understand the dynamics of the situation. To reduce the number of rapidly changing variables and to simplify the situation using the unitary operator $U = e\sim^{\text{lu/e5}}*$ a canonical transformation is made to go to a co-ordinate reference frame rotating with the frequency $u>$ where the effective Hamiltonian is given as

$$H_{eff} = \hbar(\omega_o - \omega)S^z - \hbar\left[\frac{(\vec{d}_{12}.\vec{E})}{\hbar}S^+e^{i\omega t} + h.c.\right] . \tag{1.16}$$

Taking the interaction part of $i/_e//$ and substituting (1.12) for the electric field, we get

$$\left(\frac{\vec{d}_{12}.\vec{\mathcal{E}}}{\hbar}S^+ + \frac{\vec{d}_{21}.\vec{\mathcal{E}}^*}{\hbar}S^-\right) + \left(\frac{\vec{d}_{12}.\vec{\mathcal{E}}^*}{\hbar}S^+e^{2i\omega t} + \frac{\vec{d}_{21}.\vec{\mathcal{E}}}{\hbar}S^-e^{-2i\omega t}\right) \tag{1.17}$$

As is observed above, in the rotating frame, one part of the interaction is static as it rotates with the reference frame and is thus called the rotating part, while the other part is oscillatory which is rotating in an opposite direction to the reference frame and hence is called the counter rotating part. One useful approximation in the optical domain, which is made at this juncture is the rotating wave approximation (RWA).

ROTATING WAVE APPROXIMATION

In this approximation the counter rotating part which fastly oscillates at twice the optical frequency is thrown away. Optical frequencies are $\sim 10^{15}$ Hz. But most optical detectors have a sensitivity limit of $\sim 10 \sim^{12}$ sec. Thus the counter rotating effects are essentially unobservable which justifies the RWA.

In RWA the effective Hamiltonian is given by

$$H_{eff} = \hbar \Delta S^z - \hbar(gS^+ + g^*S^-) \tag{1.18}$$

where $A = a>_o - u$ is the detuning factor between the atomic transition and the electric field and $2g = 2di2.\pounds/h$ is called the Rabi frequency, being the optical analogue of the frequency in magnetic resonance phenomena described by I.I. Rabi [4]. If the system is initially in the ground state $|2\rangle$, under the action of the effective Hamiltonian the final state of the system is given by

$$|\psi(t)\rangle = \left[\cos|\Omega|t + \frac{i\Delta \sin|\Omega|t/2}{|\Omega|}\right]|2\rangle e^{i\omega t/2} + \frac{2ig}{|\Omega|}\sin|\Omega|t/2|1\rangle e^{-i\omega t/2} \tag{1.19}$$

where $|Q|^2 = A^2 + 4|<7|^2$ is the generalized Rabi frequency. Using Eq. (1.19) many dynamical variables can be calculated. For example, inversion (S^z) in the atomic system. It is the expectation value of the inversion operator S^2 in the state $\langle i/>(t))$ i.e., $(il>(t)\backslash S^*\backslash il>(t))$. Inversion is defined in terms of the atomic excitation probability as

$$(5') = P.(t) - \backslash \tag{1.20}$$

where the probability is given by

$$P_e(t) = |\langle \psi(t) | \psi(t) \rangle|^2 = \frac{2|g|^2}{|\Omega|^2}(1 - \cos |\Omega| t) \tag{1.21}$$

This suggests that the atom undergoes sinusoidal oscillations between the ground and excited states, termed as Rabi oscillations (analogous to the magnetic resonance studies). Probability oscillates between 0 and $4|\#|^2/|\mathrm{H}|^2$.

An alternate way of studying the dynamics of the system in the semiclassical picture is to write the dynamical equations for expectation value of the atomic operators using the Heisenberg equation of motion $ihO = [0, H]$ for any operator not explicitly time dependent. At this juncture a simple assumption is made that quantum correlations between field and atom are unimportant. This is the semiclassical approximation. The equations thus obtained are called the Bloch equations [5] the solutions of which describe the dynamics of the system for all times even as the state vector approach does.

All the above description was when only a single monochromatic electric field interacts with an atom. The simultaneous application of two (or more) near resonant monochromatic radiation fields gives rise to the possibility of studying new features in nonlinear phenemena that may be shown in configurations with a larger number of levels. The three-level system interacting with two monochromatic fields is a natural extension of the two level system and is a configuration where nonlinear phenomena are greatly enhanced. The development of tunable, monochromatic dye lasers has produced an explosion of three-level investigations.

One of the consequences is that researchers working in the investigation **of the optical** properties **of nonlinear media,** have come to recognize that in the quantum mechanical evolution, coherences between atomic states play a very important role. An atomic coherence is connected to a well-defined phase relation between the atomic states.

An interesting off-shoot of atomic coherence effects was the observation of non-absorption resonances. Alzetta et al [6] discovered that the fluorescence intensity of *Na* vapour excited by a multimode dye laser when observed as a function of applied magnetic field decreased, whenever the frequency difference between the two laser modes coincided with the frequency of a hyperfine transition. Orriols [7] used the semiclassical density matrix to analyse the steady state behavior of a three-level A system using a laser constituting of two classical monochromatic fields and to realize conditions under which the narrow dip in absorption of the medium appears. He found that a transverse optical pumping aided by spontaneous emission occurs that accumulates all the atoms in a coherent superposition state of the ground states now called the coherent population trapping (CPT) state in which they are no longer able to absorb the pumping fields. He summarized that the CPT phenomenon occurs due to the simultaneous excitation pathways between the two ground levels and the excited state. Agarwal [8] had actually demonstrated quite earlier that trapping occurs in spontaneous emission when the fields are the vacuum radiation fields. The CPT state is found to be stable under the action of spontaneous decays and the two external fields. However any inclusion of collisional effects of the medium washes out the narrow coherence minimum.

CPT has been extensively studied using classical fields [7-11]. The conditions for population trapping have been explicitly derived in N-level atoms [9]. The effect of various relaxation mechanisms, strength of the laser driving fields [10], bandwidths of the fields [11] etc., have been analyzed thoroughly.

A lot of experimental work has been done on CPT which has aided in the laser manipulation of atoms. Very narrow widths of the minimum in **the** absorption **curve of the medium have been achieved** by Thomas et al [12] in atomic sodium with widths less **than the natural line** width. Such narrow resonances are used **in** frequency standards. **CPT has been** utilized in the control of atomic level populations. **Recently CPT concept**

was utilized in an efficient and selective coherent population transfer in *NO* molecules using pulsed laser [13]. Velocity selective CPT [14] is another way to control response of atoms. The basic idea is to realize pumping of atoms into a state with a given velocity where atoms are decoupled from the radiation by properly choosing the incident laser beams.

CPT has also led to the discovery of some novel, fascinating phenomena in laser physics like electromagnetically induced transparency (EIT) , lasing without inversion (LWI) and enhancement of index of refraction. EIT [15] is a more general phenomenon than CPT. It is caused by quantum interferences and unlike CPT can occur without population moving around the system. LWI utilizes the EIT/CPT. Under optimum conditions like selection of laser frequency etc., absorption to excited state is reduced to zero but stimulated emission is not affected. So with null absorption any little emission from the excited state leads to amplification of radiation without the need for population inversion at all [16]. One of the schemes for LWI [17] is based on phase dependent quantum interference arising from the utilization of external coherent fields or in other words trapping effects. LWI in CPT context is visualized as inversion existing in the basis of the absorbing (coupled) and non absorbing (uncoupled) superposition states of the ground states. The population in upper level need not exceed the total population of lower levels but only the population of the absorbing state. Recently LWI via population trapping was demonstrated [18] within the sodium *D* line using a cw dye laser. CPT has also led to the discovery of ultra high index of refraction with a low absorption [19].

In the first part of the thesis we study some of the dynamical and steady state aspects of the CPT phenomena within the three level lambda (A) configuration for different conditions.

In Chapter 2 we demonstrate the formation of CPT state even at low light levels which belies the the perturbation theory which would imply only a small amount of population

can be transferred for weak fields. A dynamical study of the formation of CPT state shows that for decreasing fields CPT takes longer and longer to occur. We perform an eigenvalue analysis to get an idea about the time scales involved. We do a perturbative calculation in the case of low fields, which shows that the minimum eigenvalue is inversely related to the sum of the decay rates from the upper level to the two lower levels. This discovery tallies with the numerically calculated system response where the system takes a longer time if one of the decay rates is increased. In the case of unequal decays steady state analysis, an unusually interesting, hitherto unfound sharp dip is discovered in the behavior of the population of the ground state, at the CPT condition. The origin of the dip is traced to the trapping conditions prevalent.

In Chapter 2 we study CPT in a dilute medium, where the effect of the neighbouring atoms could be ignored. However, for a dense medium we have to account for the effect of the neighbouring atoms (called the near dipole-dipole effect). In most optical studies we assume that the electric field acting on each atom is the macroscopic field that appears in Maxwell's equations. This is true only in the case of a medium which is so dilute that its linear dielectric constant is almost unity. The macroscopic field actually has a contribution not only from the external source but also due to the dipole moments of the other dipoles in the material. The effective field that each atom experiences is called the Lorentz local field [2].

In dense media the inclusion of near dipole-dipole effects gives rise to corrections called the the local field corrections (LFC) in the linear (Lorentz law) [2] and non linear susceptibility [20]. A nonlinear relation between atomic polarization and macroscopic susceptibility is defined which has enormous implications on the optical properties of the medium. This relation has led to the discovery of new effects.

Recently the LFC were incorporated into the optical Bloch equations [21] and the response of the atom to a strong near-resonant pump field was studied. **A novel** intensity

dependent spectral shift called the dynamic Lorentz shift that varied throughout the resonance line shape was found. For weak fields a static Lorentz shift was observed and for strong fields the response was independent of the LFC. In a recent nice experiment [22] the optical response of a dense potassium vapour under conditions where local field effects become important was measured. The results confirmed the predictions of the linear and nonlinear response theories. It was also demonstrated that the densities required for the local field effects to be important are not large.

The generalized theory of the processes of LWI and enhancement of index of refraction in a three level system by inclusion of local fields was studied in Ref.[23]. Their work predicts a novel enhancement of inversionless gain and absorptionless index of refraction by more than two orders of magnitude for certain values of atomic density. As was discussed in the preceding pages CPT is closely associated with LWI and enhancement of index of refraction. Hence it is important to study the influence of local fields on the formation of CPT state. It would also be fruitful to get an idea about the effect of LFC on the dynamics before steady state occurs.

In Chapter 3 we investigate the characteristics of the CPT state in a dense medium. We incorporate the local field effects into the density matrix equations. We illustrate how CPT persists undestroyed in the presence of LFC for all ranges of field strengths. In addition to the Lorentz shift in the steady state response we demonstrate a novel dispersive behavior near the CPT condition besides important asymmetries and shifts of the Autler-Townes peaks in absorption spectra for strong fields. For weak fields we show that the LFC shift the minimum of the sharp dip which was predicted in Chapter 2 for unequal decay rates near the CPT condition, without destroying the CPT itself. We also study the effect of local fields on the dynamics before CPT occurs and show that the evolution to the CPT state is delayed due to the local fields. In this chapter we demonstrate enhancement of gain with the inclusion of LFC in a popular scheme of LWI.

The absorption minimum occurring due to the CPT is a good pinpointer of the particular two levels involved in the trapping phenomenon. The minimum gives valuable spectroscopic information of the atomic system under consideration. However two laser fields are required for this technique to be used. It would be advantageous to utilize just a single field to derive atomic level information. Recently, Yabuzaki and coworkers [24] used diode lasers to demonstrate that field fluctuations can be useful in extracting atomic spectroscopic information. Diode lasers have a power spectrum that has sufficient spectral density in the tails to excite an atomic transition and produce a field that has a stable amplitude with large phase fluctuations. When such a field propagates through a medium the atomic resonances convert phase fluctuations into amplitude fluctuations and the transmitted field has excess intensity fluctuations compared to the input field. The excess fluctuations contain information about the atomic lines.

In Chapter 4 we present a new simple analytical framework based on linear response theory that uses a fluctuating laser source for probing the properties of the atomic medium. The idea is based on the fact that a fluctuating field would induce a fluctuating polarization in the medium which in turn would give rise to a fluctuating radiated field. We exploit the fact that linear suceptibility contains all the atomic structure information in it. We use a detection scheme where the radiated field is homodyned with the incident field and examine the power spectrum of the resulting intensity-intensity correlation function. It is shown that by including a phase shifter in the detection apparatus one can isolate the contributions to the correlation function that are linear and quadratic in the radiated field. While the quadratic contribution is shown to lead to Lorentzian shaped resonances, the linear contribution exhibits dispersive-shaped resonances. A three-level V-system is used for the atomic model where there are two resonances in the spectrum corresponding to the two allowed transitions. The analysis we present is very general and can be applied to a wide variety of atomic and molecular systems.

1.2 Second Quantization and the Quantum Model

Another level of interaction of radiation and matter is the fully quantum mechanical model where not only matter but also em radiation is quantized. A brief outline of quantization of radiation in a cavity is given below using Fermi's simple approach to electrodynamics.

Working in the coulomb gauge and using the relations

$$\vec{E} = -\frac{1}{c}\frac{\partial \vec{A}}{\partial t} \tag{1.22}$$

$$\vec{B} = \vec{\nabla} \times \vec{A} \tag{1.23}$$

in Eq.(lc) gives

$$\vec{\nabla}^2 \vec{A} = \frac{1}{c^2}\frac{\partial^2 \vec{A}}{\partial t^2} . \tag{1.24}$$

This is the wave equation which determines the propagation of em fields in vacuum. The total energy H of the field inside the cavity is

$$H = \frac{1}{8\pi} \int \left(\vec{E}^2 + \vec{B}^2 \right) dV \tag{1.25}$$

where dV is the volume element and the integration is over the entire volume of the cavity.

It is convenient to represent fields in terms of plane traveling waves. The vector potential is written as a linear superposition of plane waves in the form

$$A(\vec{r}, t) = \sum_a \sum_{\sigma=1}^{2} \sqrt{\frac{2\pi\hbar c^2}{\omega_a V}} \hat{e}_{a\sigma} \left\{ a_{a\sigma} e^{i(\vec{k}_a.\vec{r} - \omega_a t)} + a_{a\sigma}^\dagger e^{-i(\vec{k}_a.\vec{r} - \omega_a t)} \right\} \tag{1.26}$$

where $a = 1,2$ are the two directions of polarization, and vector e_{oa} specifies the polarization. The numbers a_{aa} and $a_{\backslash a}$ are constants. We choose $e_a\backslash$ _L e_a2- k_a is the direction of propagation of the plane wave and if $k\backslash = w\backslash l<?$ each term in the series satisfies the wave equation in (1.24). From the Coulomb gauge condition $e_{aa}.k_a = 0$. Hence E and A are transverse to the direction of propagation.

The electric and magnetic fields are determined from the three components of $\vec{A}$, A_x, A_y and A_z at each point (x,y,z) and at time t. Hence an uncountably infinite number of variables have to be specified. If the cavity boundary conditions are imposed on the fields the wave equation in (1.24) has infinite, discrete and a complete set of normal mode solutions orthogonal to one another. The number of variables is countable now. We now show that $A(r,t)$ and $E(r,t)$ can be expressed in terms of canonically conjugate variables. We let

$$a_{a\sigma}(t) = a_{a\sigma}e^{-i\omega_a t} \quad , \quad a_{a\sigma}^\dagger(t) = a_{a\sigma}^\dagger e^{i\omega_a t} \tag{1.27}$$

and

$$\vec{U}_{a\sigma}(\vec{r}) = \frac{\hat{e}_{a\sigma}e^{i\vec{k}_a.\vec{r}}}{\sqrt{V}} \quad , \quad \vec{U}_{a\sigma}^* = \frac{\hat{e}_{a\sigma}e^{-i\vec{k}_a.\vec{r}}}{\sqrt{V}} \tag{1.28}$$

which satisfy the orthonormality conditions

$$\int_{cavity} \vec{U}_{a\sigma}^*(\vec{r}).\vec{U}_{a'\sigma'}(\vec{r})dV = \delta_{aa'}\delta_{\sigma\sigma'} \ . \tag{1.29}$$

The variables $a_{a\sigma}(t)$ and $a_{a\sigma}^\dagger(t)$ can be used to describe the field. We introduce the real variables p_{aa} and q_{aa} by

$$
\begin{aligned}
a_{a\sigma} &= \frac{1}{\sqrt{2\hbar\omega_a}}(\omega_a q_{a\sigma} + ip_{a\sigma}) \\
a_{a\sigma}^\dagger &= \frac{1}{\sqrt{2\hbar\omega_a}}(\omega_a q_{a\sigma} - ip_{a\sigma}) \ .
\end{aligned} \tag{1.30}
$$

Using Eqs.(1.22) and (1.26), the electric field is expressed as

$$\vec{E}(\vec{r},t) = i\sum_{a\sigma}\sqrt{\frac{2\pi\hbar\omega_a}{V}}\hat{e}_{a\sigma}\left[a_{a\sigma}(t)e^{i\vec{k}_a.\vec{r}} - a_{a\sigma}^\dagger(t)e^{-i\vec{k}_a.\vec{r}}\right] \ . \tag{1.31}$$

From Eqs.(1.25) and (1.29) the Hamiltonian for the cavity is

$$
\begin{aligned}
H &= \frac{1}{2}\sum_{a\sigma}\hbar\omega_a(a_{a\sigma}a_{a\sigma}^\dagger + a_{a\sigma}^\dagger a_{a\sigma}) \\
&= \frac{1}{2}\sum_{a\sigma}(p_{a\sigma}^2 + \omega_a^2 q_{a\sigma}^2) \ . \\
&= \sum_{a\sigma}H_{a\sigma} \ .
\end{aligned} \tag{1.32}
$$

But H_{aa} is the energy of a harmonic oscillator of frequency $u>_a$ and so the field energy is equal to an infinite set of uncoupled radiation oscillators. p_{aa} and q_{aer} are canonically conjugate momentum and position variables satisfying the canonical Hamiltonian equations of motion. The choice of multiplication constant $\sqrt{2\pi\hbar c^2/\omega_a V}$ in Eq.(1.26) was to take care that H would have units of energy, huj_a.

To quantize the em field, energy of each of the infinite set of oscillators is quantized. We associate Hermitian operators with the conjugate variables q_{aa} and $p_{a(r}$ and as it is experimentally known that photons are bosons they satisfy the bosonic commutation rules. In terms of the non-Hermitian operators a_{ao} and $a_{\backslash a}$, the commutation relations are

$$\left[a_{a\sigma}, a_{a\sigma'}^{\dagger}\right] = \delta_{aa'}, \delta_{\sigma\sigma'} \quad .$$
$$[a_{a\sigma}, a_{a'\sigma'}] = 0 = \left[a_{a\sigma}^{\dagger}, a_{a'\sigma'}^{\dagger}\right] \tag{1.33}$$

The Hamiltonian for the field (1.31) with the zero point energy removed reduces to

$$H = \sum_a \hbar\omega_a a_{a\sigma}^{\dagger} a_{a\sigma} \quad . \tag{1.34}$$

In the case of only one mode being present in the cavity H is given by

$$H = \hbar\omega a^{\dagger} a \tag{1.35}$$

The operator a^*a is Hermitian. Let $|n)$ be the eigenstate of $a^{\wedge}a$ with the eigenvalue n, i.e.,

$$a^{\dagger} a|n\rangle = n|n\rangle \quad , \tag{1.36}$$

where **n** denotes **the number** of photons in that particular mode ol radiation held **and** runs from 0 to oo. $a^{\wedge}a$ is called the number operator and $|n)$ is called the number state or Fock state. As observed from Eq. (1.35) $|n)$ is an eigenstate of the Hamiltonian of the system too. The eigenvalue spectrum of H consists of eigenenergies $nhuj$ where n is the

number of quanta. From the commutation relations (1.33) and simple algebra, operators
a and a* acting on the Fock state give rise to

$$\begin{aligned} a|n\rangle &= \sqrt{n}|n-1\rangle \\ a^\dagger|n\rangle &= \sqrt{n+1}|n+1\rangle \ . \end{aligned}$$ **(1.37)**

a is called the annihilation operator as it destroys a photon and lowers the state of the
radiation field from $\n)$ to $\n - 1)$ and a* is called the creation operator as it creates a
photon in the radiation mode and raises the radiation state from $\n)$ to $\n + 1)$. $a,a^\wedge$ are
also called the ladder operators.

The Fock states are an orthonormal set of vectors i.e., $(ni\ri2) = {}^\wedge m,n_2$ • The Fock
states form a Complete set of basis states. The completeness relation is given as

$$\sum_{n=0}^{\infty} |n\rangle\langle n| = 1$$ **(1.38)**

Using the non-negative and real nature of n and the property (1.37) it is seen that

$$a|0) = 0 \ .$$ **(1.39)**

where $|0)$ is the vacuum state of radiation field.

Another category of radiation states is the coherent state which is the eigenstate of
the operator a, i.e.

$$a|a) = a|a).$$ **(1.40)**

The coherent state is studied in detail in Ref.[25]. The form of $|a)$ is given in Eq. (6.22)
of Chapter 6.

Using the semiclassical Hamiltonian in Eq.(1.15) and the Hamiltonian for the quan-
tized radiation field in Eq.(1.34) the Hamiltonian for the interaction of a collection of
noninteracting, identical two-level atoms with the quantized radiation field, in dipole

approximation is given as

$$H = \hbar\omega_o \sum_i S_i^z + \hbar \sum_{a\sigma} \omega_{a\sigma} a_{a\sigma}^\dagger a_{a\sigma} - \hbar \sum_i \left[\frac{\vec{d}_{12}^{(i)} S_i^+}{\hbar} + \frac{\vec{d}_{21}^{(i)} S_i^-}{\hbar} \right] . \vec{E}_i \qquad (1.41)$$

where E_{ℓ} is the quantized electric field at the point where the 2th atom is located and $\langle ? \bullet \rangle$ is the dipole moment operator for the ith atom. Substituting for E_{ℓ} from Eq.(1.31) we get

$$H = \hbar\omega_o \sum_i S_i^z + \hbar \sum_{a\sigma} \omega_{a\sigma} a_{a\sigma}^\dagger a_{a\sigma} + \hbar \sum_{ia\sigma} \left\{ g_{a\sigma} a_{a\sigma} (S_i^+ + S_i^-) + H.C. \right\} \qquad (1.42)$$

where g_{aa} is the coupling coefficient given by

$$g_{a\sigma} = \sqrt{\frac{2\pi\omega_a}{V\hbar}} (\vec{d}_{12}.\hat{e}_{a\sigma}) \ . \qquad (1.43)$$

Usually we consider systems confined to a space whose dimensions are smaller than a wavelength *w/c*. So the spatial variation of g_{aa} can be ignored In Eq.(1.42) we have assumed that the dipole matrix element is real i.e., $d^\wedge = \langle 4i$ by making a proper choice of phase. Also as all the atoms are identical *du* is independent of the index t.

At this juncture we make the RWA where one ignores the antiresonant terms like $"aa^\wedge i"$ $^{\text{w h i c n}}$ corresponds to simultaneous creation of a photon and atomic excitation. In RWA the quantized Hamiltonian of interaction of radiation with matter is

$$H = \hbar\omega_o \sum_i S_i^z + \hbar \sum_{a\sigma} \omega_{a\sigma} a_{a\sigma}^\dagger a_{a\sigma} + \hbar \sum_{ia\sigma} \left\{ g_{a\sigma} a_{a\sigma} S_i^+ + g_{a\sigma}^* a_{a\sigma}^\dagger S_i^- \right\} \qquad (1.44)$$

The major difference between the semiclassical picture and the quantum picture is that the reaction of the spin 1/2, two-level atom on the radiation which was ignored in semi-classical picture is included in quantum Hamiltonian by quantizing the radiation field. The fully quantum Hamiltonian in Eq.(1.44) acts as the starting point for most of the quantum electrodynamical studies in quantum optics.

Irrespective of the success of the semiclassical radiation theory, quantum mechanics provides the best current picture of physical phenomena and a most complete description of the radiation field must be sought in quantum mechanical laws. Quantum theory provides rigorous expressions for observable parameters which characterize the radiation field and its interaction with atoms. In many situations classical field fails to give experimentally observed results whereas quantum field succeeds. Other situations occur when one discovers an optical problem which even though idealized, but can be solved explicitly within the framework of a quantized field theory. Such problems are rare - enough to have an importance of their own, virtually independent of their relevance to possible experimental work. If such models become realizable by experiments then there is no limit to the depths of understanding one can go to. A beautiful example of such a problem is the Jaynes-Cummings Model (JCM).

The JCM consists of the interaction of a single two-level atom with a single quantized cavity mode of the em radiation. The model is dynamically nonlinear as it signifies the coupling of a fermion (the two-level atom) with a boson (the quantized field mode). In 1963, Jaynes and Cummings [26] provided an exact solution to it and compared it with the semiclassical results. They found the stationary states and the exact eigenvalues of the coupled atom field system. They revealed the existence of Rabi oscillations in atomic excitation probabilities for fields with sharply defined energy.

Despite its ideal character JCM exhibits a rich variety of quantum phenomena. With more and more detailed research on the JCM, newer facts of the model are becoming transparent. After Jaynes and Cummings' paper in 1963 several papers extending their work appeared. Cummings and others [27] studied the short time atomic dynamics **and** field statistics in JCM for an initial coherent state where a dephasing or collapse of the sinusoidal oscillations appeared in the atomic inversion and the dipole moment in spite of the model being completely lossless. Eberly and coworkers [28] studied the long time

behavior where in addition to the collapse a revival or partial recorrelation was observed during which the initial state is almost recovered. Analytic formulas for the collapse function, the revival period and the amplitude of the revival envelope were also derived.

The physical reasoning for collapse and revivals has been understood. The collapse is due to the destructive interference of quantum Rabi oscillations at different frequencies. Such a collapse occurs even under a classical field with intensity fluctuations. However the revivals are a purely quantum effect that originate in the discreteness of the quantum states of the harmonic oscillator, the "granularity of the field" [28].

Even though JCM is too idealized and made simple it provides new insights into some of the most basic physical properties and gives unexpected results. Much effort has been directed towards extending the model to more realistic description of experiments. For a review of the JCM and its numerous extensions see Ref.[29]. JCM remained a theoretical curiosity till the mid 80's because the matrix elements describing the radiation-atom interaction are so small that the field of a single photon is not enough to lead to an atom field evolution time shorter than any other characteristic times of the system such as natural line-width, the time of flight of the atom through the cavity and cavity mode damping time.

With the making of frequency tunable lasers it is now possible to excite large population of highly excited atomic states characterized by a high principal quantum number n of the valence electron. These states are called the Rydberg states [30] as their energy levels are described by the Rydberg formula. These atoms are ideal for observing quantum effects of radiation-atom coupling due to three reasons-(l) The states are strongly coupled to the radiation field (transition rates scale as n^4). (2) Here transitions occur in *mm* wave region so that low-order mode cavities can be made large enough to allow long interaction times. (3) Rydberg states have longer lifetimes.

The idealised case of JCM was realized with the one atom maser recently [31]. In

the experimental test of the JCM, Walther and co-workers [32] used Rubidium atoms corresponding to the transition $63p_{3/2} \longrightarrow 61J_{3/2}$ in a superconducting cavity of very high quality factor $2.7\text{xl}O^8$ at a temperature of 2.5 K. A clear collapse, the quiescent interval and the revival of oscillations which now has been recognized as a purely quantum feature were observed.

Most of the literature on JCM and its generalizations is devoted to a given mode acting only on one optical transition i.e., the modes do not act simultaneously on one transition. But in realistic situations several nonlinear processes can go on at the same time if the atom is interacting with different radiation mode fields. For example pump-probe processes, quantum beats, and several other nonlinear mixing effects. Such processes come under the category of 'two-channel' phenomena.

Semi classically it is also known that if an atom interacts with different fields, competing processes occur in the system leading to interferences [33] which eventually determine the dynamics of the system. The situation is called the nonlinear optical balance [34].

The standard approach to competing processes is through Maxwell equations for the two competing fields. The polarization terms in Maxwell equations are derived from the Maxwell-Bloch equations for the atom. Such a treatment yields the evolution of mean values of the fields. But it does not lead to any information on the quantum dynamics of the competing processes. Clearly competing processes warrant a quantified field treatment and a generalization of JCM to situations where more than one field acts on the same transition. This would be especially important in understanding the quantum statistics of the generated fields.

In the second part of the thesis we study situations where the JCM has been extended and generalized to situations where two radiation fields act simultaneously between the two-states of an atom. Effectively the atom is coupled to the two-fields via 'two-channels'.

In Chapter 5 of the thesis we study the JCM where a two-level atom is being continuously pumped by an external laser field in addition to being coupled to a cavity mode. In this problem the external pump is treated classically while the cavity mode is quantized. The interaction of the atom with the cavity mode is just the single channel JCM. The presence of the external pump creates an alternate pathway between the two states of the atom. We numerically and analytically study the dynamics of the system when the external field and the cavity mode are on resonance. A one to one correspondence is established between the results for the JCM with continuous pumping and the standard JCM where the coherent field enters via the initial conditions. We show that the dynamical properties of the atomic system for the JCM which has the cavity mode in vacuum state initially but is continuously pumped by an external laser field are identical to the dynamical properties of the usual JCM with cavity mode prepared in a coherent state. The dynamics of the cavity mode in both systems is shown to be simply related. The familiar collapse and revival phenomenon is exhibited by the atomic probability. The transfer of energy between the coherent laser field and the cavity mode is mediated by the atom due to simultaneous excitation pathways of the two fields.

The JCM with a two level atom interacting independently and dynamically with two fully quantum modes via two different nonlinear processes occurring in the two simultaneous excitation channels now forms an interesting proposition. One previous work concerns the competition between Stokes and Anti-Stokes processes by Eberly and co-workers [35].

Unlike the previous chapter where one of the channels had a classical field, in Chapter 6 we present a fully quantum picture of an atomic system interacting with two modes in a lossless cavity via three photon and one photon absorption processes i.e., we present a cavity quantum electrodynamical (QED) version of the nonlinear optical balance [34]. Using a state vector approach, we study the evolution of the mean photon number of

the two modes and the atomic excitation probability for various initial conditions of the system. The most simple case is where the atom is in the ground state, the fundamental mode is in a Fock state with three photons and the third harmonic is in the vacuum state. This case exhibits the quantum Rabi oscillations with a periodic exchange of energy between the two modes with the atom acting as an intermediary. Even this simple case exhibits interesting mode mixing and entanglement properties. A comparison of the dynamical behavior is made between the cases when the system is in the Fock state and the coherent state with the predictions of the semiclassical theory where the fields evolve according to classical dynamics. The semiclassical theory predicts a periodicity reflected in the conservation laws derived, which is in contrast with the quantum results but which is similar to the semiclassical results of the standard JCM. All our study emphasizes the presence of strong quantum mechanical interference effects in the cavity with two simultaneously occurring quantum dynamical processes.

REFERENCES

1. **J.C. Maxwell,** *A Treatise on Electricity and Magnetism,* **Vol. 1 (Dover, New York,** 1954, 3rd ed.).

2. H. A. Lorentz, *The Theory of Electrons,* (Dover, New York 1952) Chap. 4.

3. T. H. Maiman, *Nature,* **187,** 493 (1960).

4. I. I. Rabi, Phys. Rev. A 51, 652 (1937).

5. F. Bloch, Phys. Rev. 70, 460 (1946).

6. G. Alzetta, A. Gozzini, L. Moi and G. Orriols, Nuovo Cimento, 36 B, 5(1976); G. Alzetta and L. Moi, *ibid,* 52 B,209(1979).

7. G. Orriols, Nuovo Cimento, 53 B, 1(1979)

8. **G. S. Agarwal,** *Quantum Statistical Theory of Spontaneous Emission,* **Springer** Tracts in Modern Physics, (Springer Verlag, Berlin, 1974) Vol. 70.

9. F. T. Hioe and C. Carroll, Phys. Rev. A 37, 3000 (1988).

10. S. Swain, J. Phys. B 15, 3405(1982).

11. P. M. Radmore and P. L. Knight, J. Phys. B 15, 561(1982); **B. J. Dalton and P. L.** Knight, J. Phys. B 15, 3997(1982).

12. J. E. Thomas, P. R. Hemma, S. Ezekiel, C. C. Leiby Jr., R. H. Picard **and** C. R. Willis, Phys. Rev. Lett. 48, 867 (1982).

13. S. Schiemann, A. Kuhn, S. Steuerwald and K. Bergmann Phys. Rev. Lett. **71,** 3637 (1993).

14. A. Aspect, E. Arimondo, R. Kaiser, N. Vansterkiste and C. Cohen-Tannoudji, Phys. Rev. Lett. 61, 826 (1988)-

15. K. J. Boiler, A. Imamoglu, S. E. harris, Phys. Rev. Lett. 66, 2593 (1991); K. Hakuta, L. Marmet and B. Stoicheff, Phys. Rev. Lett., 66, 596 (1991).

16. S. E. Harris, Phys. Rev. Lett. 62, 1022 (1989); A Imamoglu, Phys. Rev. A 40, 2835 (1989); S. E. Harris, J. E. Field and A. Imamoglu, Phys. Rev. Lett. 64, 1107 (1990).

17. 0. Kocharovskaya, F. Mauri and E. Arimondo, Op. Commun. 84, 393 (1991); O. Kocharovskaya, Phys. Rep. 219, 175-190 (1992); M. O. Scully, S. Y. Zhu and A. Gavrielides, Phys. Rev. Lett. 62, 2813 (1989).

18. E. S. Fry, X. Li, D. Nikonov, G. G. Padmabandu, M. O. Scully, A. V. Smith, F. K. Tittel, C. Wang, S. R. Wilkinson and S. Y. Zhu, Phys. Rev. Lett. 70, 3235 (1993).

19. M. Fleischhauer, C. H. Keital, M. O. Scully, C. Su and B. T. Ulrich and S. Y. Zhu, Phys. Rev. A 46, 1468 (1992); M. O. Scully, Phys. Rev. Lett. 67, 1855 (1991).

20. D. Bedeaux and N. Bloembergen, Physica 69, 57(1973).

21. R. Friedberg, S. R. Hartmann and Jamal T. Manassah, Phys. Rev. A40, 2446 (1989).

22. J. J. Maki, M. S. Malcuit, J. E. Sipe and R. W. Boyd, Phys. Rev. Lett. 67, 972 (1991).

23. J. P. Dowling and C. M. Bowden, Phys. Rev. Lett. 10, 1421(1993).

24. T. Yabuzaki, T. Mitsui and U. Tanaka, Phys. Rev. Lett. 67, 2453 (1991).

25. R. J. Glauber, Phys. Rev. A **131,** 2766 (1963).

26. E. T. Jaynes and F. W. Cummings, Proc. IEEE 1, 89 (1963).

27. F. W. Cummings Phys. Rev. A **140,** l051 (1965); P. Meystre, E. Geneux, A. Faist and A. Quattropani, Nuovo Cimento 25, 521 (1975).

28. J. H. Eberly, N. B. Narozhny and J. J. Sanchez Mondragon, Phys. Rev. Lett. **44,** 1323 (1980); N. B. Narozhny, J. J. Sanchez-Mondragon and J. H. Eberly, Phys. Rev. A3, 236 (1981).

29. B. W. Shore and P. L. Knight, J. Mod. Opt., **40,** 1195-1238, 1993.

30. S. Haroche and J. M. Raimond, *Ad. At. Mol. Phys,* Vol. 20, (Academic Press, New York 1985).

31. D. Meschede, H. Walther and G. Muller Phys. Rev. Lett. 54, 551 (1990).

32. G. Rempe, H. Walther and N. Klein, Phys. Rev. Lett. 58, 353 (1987).

33. K. Aron and P. M. Johnson, J. Chem. Phys. 67, 5099 (1977). J. C. Miller and R. N. Compton, Phys. Rev. A25, 2056 (1982)

34. D. J. Jackson and J. J. Wynne, Phys. Rev. Lett. 49, 543 (1982).

35. Liwei Wang, R. R. Puri and J. H. Eberly, Phys. Rev. **A46,** 7192 (1992); C. K. Law, Liwei Wang, and J. H. Eberly, Phys. Rev. **A45,** 5089 (1992).

Chapter 2

COHERENT POPULATION TRAPPING AT LOW LIGHT LEVELS

Atomic coherence and quantum interference effects have led to many surprising phenomena in optical physics. Use of coherence and related phenomena in the laser manipulation of atomic media has led to some path-breaking experiments. Atomic coherence is created using different techniques. For example microwave driving of the levels or Raman driving via an additional level and pulse induced coherence. With this possible novel concepts like lasing without inversion [1,2], electromagnetically induced transparency [3], efficient transfer of population from one state to the other [4] have become realistic notions.

The role that coherence plays in the behavior of a nonlinear medium was first indicated by an experimental observation in magnetic resonance experiments by Alzetta et al [5] and others [6]. Some dark resonances were observed when the fluorescence spectrum of Na atoms was scanned as a function of the applied magnetic field. This phenomenon is now called coherent population trapping (CPT). CPT is said to have occurred when a three level system with two closely spaced ground levels optically coupled to a common excited level by two coherent fields gives rise to trapping of population in a coherent superposition of the ground levels. The coherent superposition state is termed as the coherent population trapping state. This occurs under the condition that the frequency difference between the two fields is equal to the separation between the two ground levels which is called the two photon resonance (TPR) condition. The CPT state possesses

zero matrix elements of interaction with the common excited level. Thus the system eventually reaches a state in which the common level is uncoupled from the rest of the system. Hence the CPT state is the stationary state of the Hamiltonian which remains nonevolving.

The first theoretical explanation of CPT was given by Orriols [7] who studied the steady state response of a medium with three-level atoms, by writing the solution of semiclassical density matrix equations of motion. At the TPR condition a narrow minimum in the absorption spectrum was observed. This is the coherence minimum which is an indication of CPT.

Gray, Whitley and Stroud [6] discovered a constant of motion which gives rise to two superposition states which are combinations of the ground levels. One superposition is the trapping state. It is also called the nonabsorbing, nonevolving or uncoupled state. The other is the untrapped, absorbing or coupled state. The spontaneous emission in the system pumps in a few lifetimes all the population from the untrapped state to the trapped state. In steady state there is no population in the untrapped state. All of it is in the trapped state. Hioe and Carroll [8] elucidated the conditions under which a multilevel quantum system irradiated by a laser will possess invariants in the system.

The CPT has been extensively studied using classical fields [7-10] and the conditions for population trapping have been explicitly derived. The effect of the various relaxation mechanisms, strength of the laser driving fields [9], bandwidths of the fields [10] etc. have been analyzed thoroughly. Recently CPT has been dealt with in the context of quantized fields and some novel properties were discovered [11]. The CPT concept has **been utilized** in different situations. Some of the most prominent applications were the demonstration of lasing without inversion [12] and efficient transfer of population from one state to the other [4].

The form of the CPT state given in Eq.(2.19) below implies that the **laser fields** can **be**

arbitrarily small and yet the trapping state will be formed. This is sort of against one's intuition based on the perturbation theory which would imply that only a small amount of population can be transferred for weak fields. It is clearly important to understand the dynamics of the system leading to the formation of trapping states at low intensities. In this chapter we study the dynamics of the formation of CPT state in a three level system under various conditions of field intensity and spontaneous decay rates. It is found that as the field gets weaker in comparison to the decays the time taken for CPT to occur gets lengthened preventing a short-time perturbation calculation.

Another feature we study in this chapter is the effect of unequal decay rates on the steady state response of the three-level system, especially near the CPT condition. Unequal decay rates play an important role in the context of LWI [13]. In Harris' paper a necessary condition for LWI to occur is that the spontaneous emission on the transition where probe field acts must be less than that on the transition where the pump field acts. Also in most A-systems such as Cs and Rb one will encounter unequal decays. Here we demonstrate an interesting, hitlierto undiscovered sharp dip in the steady state response of the medium for unequal decays.

In Section 2.1 we analytically derive the steady state response of a three-level atomic model of Lambda (A) configuration at TPR condition using the semiclassical density matrix formalism. We then numerically demonstrate the steady state behavior of the populations and coherences (at low intensities of the laser fields) around TPR condition . We discuss the mechanism of CPT phenomenon in detail. In Section 2.2 we demonstrate an unusual dip in the ground state population in the case of unequal spontaneous decays. We give a detailed analysis of the formation of the dip using the closed form expression for the ground state population. We demonstrate that the origin of the dip is due to the trapping conditions prevalent at TPR condition. In Section 2.3 we derive the form of the CPT state and discuss its nonevolving nature. In Section 2.4 we study the effect of

various factors **like field** strengths and spontaneous emission rates on the **dynamics of the formation of the** CPT state by using a simple eigenvalue calculation **and corroborating** its prediction of the time scales involved by numerical integration of the density matrix equations. Further we perturbatively find an analytic closed form for the minimum eigenvalue which decides the relevant time scale, in the case of low light levels.

2.1 The Model and the CPT Phenomenon

Consider a three level system consisting of a single resonant excited state |1) optically coupled with two closely spaced ground sublevels |2) and |3). States |1) and |2) have energies *UUJQ* and *hujR w.r.t* the state |3). Two classical monochromatic fields of frequencies *Qi* and $Q_{,2}$ couple the transitions |1) ⇔ |3) and |1) ⇔ |2) respectively. The states |2) and |3) are not coupled directly due to parity constraints. Let 271(272) be the spontaneous emission rate from state |1) to state |3) (|2)), (Figure 2.1).

Extending the semiclassical Hamiltonian for a two-level atomic system **interacting** with a monochromatic field given in Eq. (1.13) in the introductory Chapter 1 **and** using Ref. [14] the total Hamiltonian for a three-level system interacting with two laser fields in the RWA is written as

$$H = \hbar\omega_0 A_{11} + \hbar\omega_R A_{22} \quad - \quad \vec{d}_{13} \cdot \vec{E}_1 A_{13} \exp(-i\Omega_1 t)$$
$$- \quad \vec{d}_{12} \cdot \vec{E}_2 A_{12} \exp(-i\Omega_2 t) + h.c., \qquad (2.1)$$

where A_{xy} are the atomic transition operators |x)(y|. Here *di3* (*d12*) is the atomic dipole interaction term between the states |1) and |3)(|2)) and E_u E_2 are the electric field amplitudes. Defining $G_x = $ ^^ and $G_2 = $ $^{iu\wedge z}$ the Hamiltonian in (2.1) is rewritten as

$$H = hu)oAn + ?IURA22 — hGi \exp(—iClit)Ai3 - hG2 \exp(—iQ_2t)A12 + h.c. \qquad \textbf{(2.2)}$$
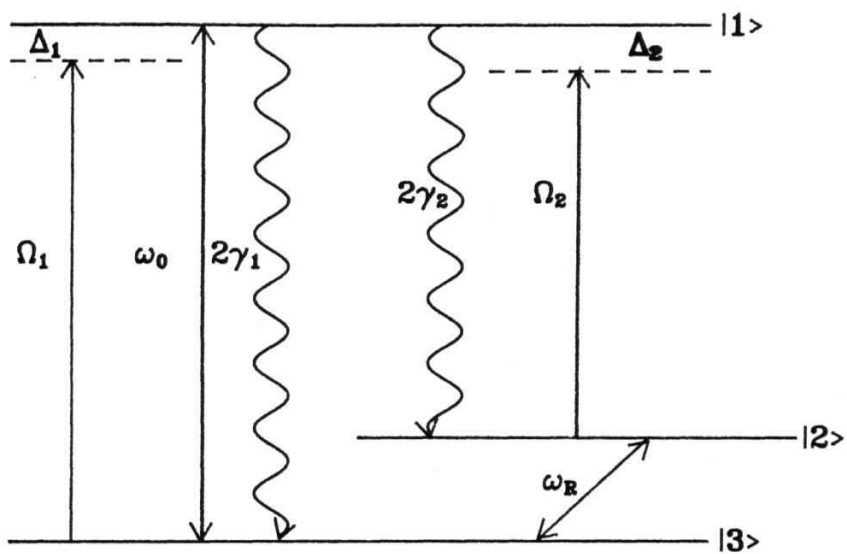
Fig. 2.1: Schematic representation of a three level lambda (A) system.

The steady state behavior is studied using the density matrix formalism. The density matrix facilitates the treatment of interacting quantum systems **for** which the state description is not very simple and for which only certain statistical properties are known. These properties are incorporated into the density matrix formulation in a simple way. The density matrix completely specifies the total system. However, sometimes it is intersting to study properties of the individual interacting systems separately. In such a case, the density operator which characterizes the system alone must be constructed. This is done by taking only those matrix elements of the total density matrix which are diagonal in the unobserved variables and summing over all of them. In other words tracing out the variables of the unobserved variable. Such a density matrix is called the reduced density matrix which contains all the information about the observed variable. Here the interest of study is the atomic system. Hence tracing over the reservoir (radiation) variables using the Born-Markov approximations, the evolution of the reduced density matrix for the atomic system is described by the master equation [15]

$$\frac{\partial \rho}{\partial t} = \frac{-i}{\hbar}[H, \rho] \quad - \quad \gamma_1(A_{13}A_{31}\rho - 2A_{31}\rho A_{13} + \rho A_{13}A_{31})$$
$$- \quad \gamma_2(A_{12}A_{21}\rho - 2A_{21}\rho A_{12} + \rho A_{12}A_{21}) \ . \tag{2.3}$$

The equations of motion for the eight components of the density matrix are obtained as

$$\dot{\rho}_{11} = -2(\gamma_1 + \gamma_2)\rho_{11} + iG_1\rho_{31}e^{-i\Omega_1 t} + iG_2\rho_{21}e^{-i\Omega_2 t} + c.c,$$
$$\dot{\rho}_{12} = -[\gamma_1 + \gamma_2 + i(\omega_0 - \omega_R)]\rho_{12} + iG_1\rho_{32}e^{-i\Omega_1 t} + iG_2(\rho_{22} - \rho_{11})e^{-i\Omega_2 t},$$
$$\dot{\rho}_{13} = -[\gamma_1 + \gamma_2 + i\omega_0]\rho_{13} + iG_2\rho_{23}e^{-i\Omega_2 t} + iG_1 e^{-i\Omega_1 t}(1 - 2\rho_{11} - \rho_{22}),$$
$$\dot{\rho}_{22} = 2\gamma_2\rho_{11} - iG_2\rho_{21}e^{-i\Omega_2 t} + c.c,$$
$$\dot{\rho}_{23} = -i\omega_R\rho_{23} - iG_1\rho_{21}e^{-i\Omega_1 t} + iG_2^*\rho_{13}e^{i\Omega_2 t} \tag{2.4}$$

The diagonal elements of the density matrix are the populations of the corresponding

levels and the off-diagonal elements determine the coherence for the corresponding transitions. The system is a closed one in the sense no population goes out of the system. Hence the conservation of population is summarized as $p_u + P22 + {}^{\wedge}33 = 1$. As $P33$ is expressible in terms of p_u and $P22$ there are only eight independent components of the density matrix.

To remove the rapidly oscillating terms in the off-diagonal elements we make the following transformation in Eq.(2.4).

$$
\begin{aligned}
{[\rho]}_{13} &= \rho_{13}e^{-i\Omega_1 t}\\
{[\rho]}_{12} &= \rho_{12}e^{-i\Omega_2 t}\\
{[\rho]}_{23} &= \rho_{23}e^{-i(\Omega_2 - \Omega_1)t}
\end{aligned}
\tag{2.5}
$$

The equations of motion in the new co-ordinate frame are given as

$$
\begin{aligned}
\dot{\rho}_{11} &= -2(\gamma_1 + \gamma_2)\rho_{11} + iG_1\rho_{31} + iG_2\rho_{21} + c.c,\\
\dot{\rho}_{12} &= -[\gamma_1 + \gamma_2 + -i\Delta_2]\rho_{12} + iG_1\rho_{32} + iG_2(\rho_{22} - \rho_{11}) ,\\
\dot{\rho}_{13} &= -[\gamma_1 + \gamma_2 - i\Delta_1]\rho_{13} + iG_2\rho_{23} + iG_1(1 - 2\rho_{11} - \rho_{22}) ,\\
\dot{\rho}_{22} &= 2\gamma_2\rho_{11} - iG_2\rho_{21} + c.c. ,\\
\dot{\rho}_{23} &= i(\Delta_1 - \Delta_2)\rho_{23} - iG_1\rho_{21} + iG_2^*\rho_{13} .
\end{aligned}
\tag{2.6}
$$

where Ai and A_2 are the detunings defined as A] = Oi - ɯ₀ and A_2 = O2 — (^0 — *UR*). AI is the frequency by which the field $E\backslash$ is detuned from the atomic transition frequency corresponding to $|1) <^*\ |2)$ and A2 is the frequency by which the field *Ei* is detuned from the atomic transition frequency corresponding to $|1) <\bullet\ |3)$.

We now study the steady state response of the medium for the case where the fields are of equal strengths i. e. symmetric fields at TPR condition. The symmetric fields case eases the analytical difficulties and demonstrates the characteristics of the medium

in a simple, clear way. The derivative of the density matrix $\dot{\rho}$, in Eq.(2.6) is set equal to zero $(\dot{\rho} = 0)$ and the set of eight simultaneous linear equations thus obtained are solved analytically. The closed form solutions of the population of the excited state $|1\rangle$, ρ_{11}, the population in one of the ground levels, (say level $|2\rangle$), ρ_{22} and the absorption characteristic of one of the fields (say G_2) i.e., $Im\rho_{12}$ are obtained as follows:

$$Im\rho_{12} = \frac{\gamma_2 \rho_{11}}{G_2} \tag{2.7}$$

$$\rho_{11} = \frac{4G_1^2 \Delta_2^2 \gamma_1^2 (\gamma_1 + \gamma_2)}{D} \tag{2.8}$$

$$\rho_{22} = \frac{1}{2} + C_1 + C_2 \ , \tag{2.9}$$

where

$$C_1 = \frac{0.125\Delta_2^4 \gamma_1^2 \gamma_2 - 0.25\Delta_2^2 G_1^2 \gamma_1^2 (\gamma_1 + \gamma_2)}{D}, \tag{2.10}$$

$$C_2 = \frac{0.125\Delta_2^{\,2} \gamma_1^{\,2} (\gamma_2 - \gamma_1)(\gamma_1 + \gamma_2)^2}{D}, \tag{2.11}$$

and

$$D = 0.25\Delta_2^4 \gamma_1^2 \gamma_2 + 0.25\Delta_2^2 \gamma_1^2 (\gamma_1 + \gamma_2)^3 + 0.5\Delta_2^2 \gamma_1^3 G_1^2 + G_1^4 \gamma_1^2 (\gamma_1 + \gamma_2). \tag{2.12}$$

In the exact resonance case $\Delta_1 = \Delta_2 = 0$ and when the decays are equal, $\gamma_1 = \gamma_2$, $\rho_{11} = 0$, $Im(\rho_{12}) = 0$, and $\rho_{22} = \frac{1}{2}$. This explicitly demonstrates that there is no population in the excited state and all the population is trapped and distributed equally in the ground levels at long times relative to the decays involved in the system. The absorption of the field G_2 is null at TPR.

Next we numerically evaluate the steady state response of the system around TPR condition for symmetric fields, $G_1 = G_2$ when the fields are weak i. e. $G_1, G_2 < \gamma_1, \gamma_2$. We present the steady state behavior for the population in level $|2\rangle$, ρ_{22}, the absorption characteristic of the field G_2 i.e., $Im\rho_{12}$, the ground state coherence behavior, $Re\rho_{23}$ and

7m/>23 as a function of the detuning A_2 to illustrate CPT in Figure 2.2. **We take** the case where $G\backslash = G2 = 0.1$, $71 = 72 = 1.0$, $71 = 0$. There is a narrow absorption minimum around TPR, $Ai = A_2 = 0$ with $Imp_{l2} = 0$ exactly at TPR as shown in Figure 2.2a. The population of level $|2)$, $/?22$ falls to a minimum value of $1/2$ (Figure 2.2b). It is found that at TPR $^33 = 1/2$ and $pu = 0$ which shows that the population is distributed symmetrically between the ground sub-levels. The whole population gets trapped in the ground states. This demonstrates that CPT occurs at low light levels too.

The ground state coherence depicted in Figure 2.2c,d shows that though it is zero at all other detunings A_2 but around TPR there is a finite coherence. A finite coherence indicates that the system is placed in a coherent superposition of the states $|2)$ and $|3)$. Another peculiar fact is that the imaginary part and real part of $/>_23$ have exchanged roles. Imaginary part is a dispersive curve and the real part is a bell-shaped absorption curve. Hence at TPR ground state coherence is $180°$ out of phase with the optical coherence. It oscillates at the frequency difference of the two laser fields ($\sim //$ wave, GHz). This coherence indirectly couples the optical coherences together through the terms in the equation for $P23$ in Eq. (2.6). These couplings show the possibility of nonlinear interference effects.

The atoms in coherent superposition of ground levels are simultaneously excited on the two optical transitions and the corresponding transition amplitudes add coherently. The consequent interference enhances or reduces the transition probability to the excited state according to the phase between the coherence $P23$ and the relative **phase of the** fields. As the phase difference is $180°$ at TPR the interference is destructive and the transition probability vanishes. This explains the absorption minimum in **Figure** 2.2a.

An important point to note is that CPT starts becoming less and less **prominent as** collisional effects become important. Collisions between atoms brings about a population movement among atoms which destroys any trapping in the ground levels.
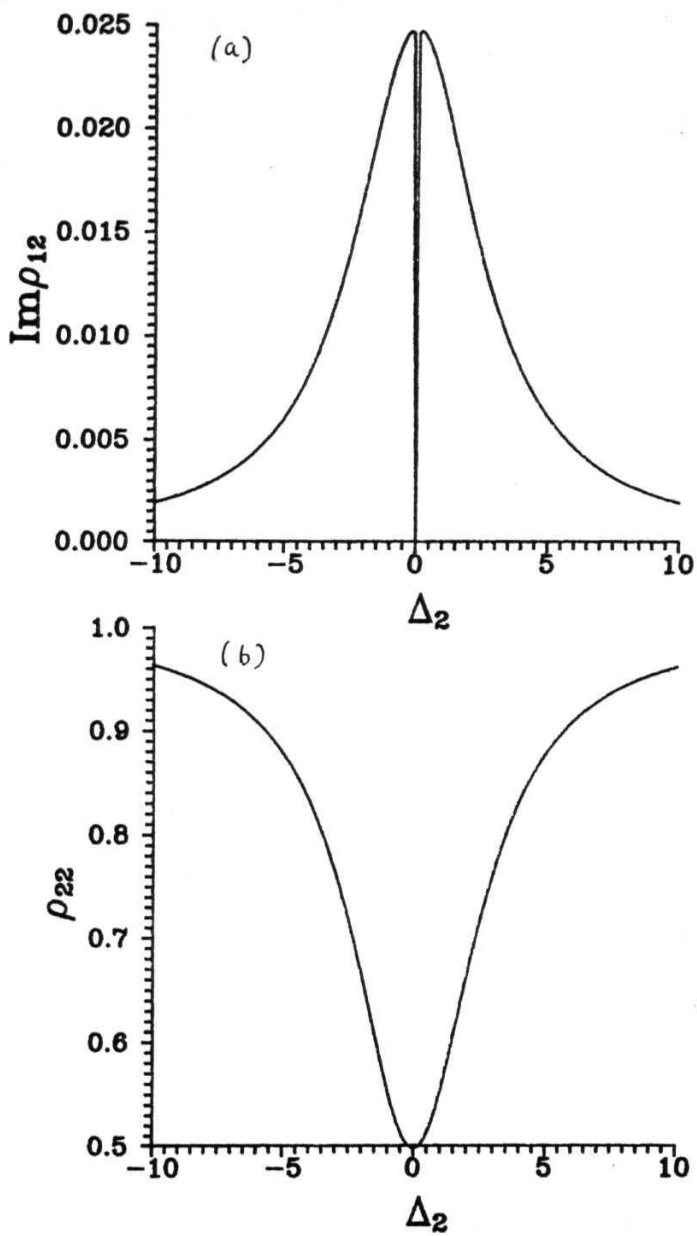
Fig. 2.2: Steady state behavior as a function of A2 of a) the absorption charac-
teristic of the medium for the transition |1) +-> |2) w. r. t field G2, *Impu,*
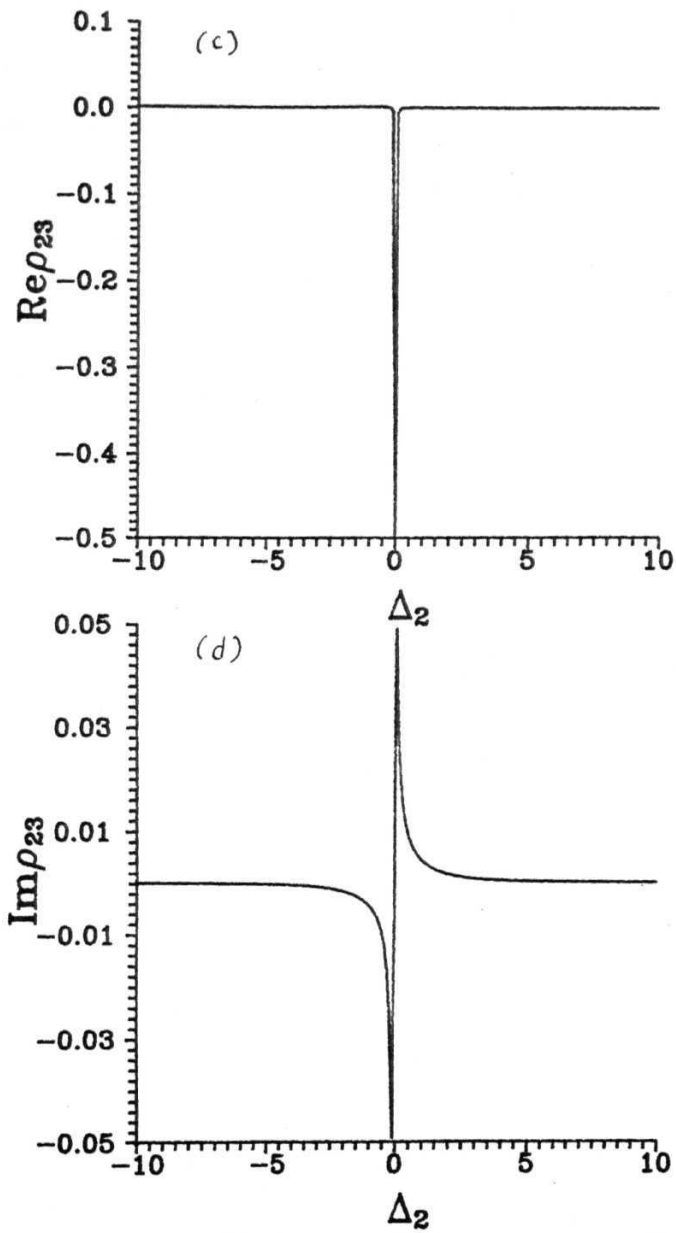b) population of the level |2), *p22.* Parameters are $G\backslash = G2 = 0.1$, A1 = 0,
7i = 72-

Fig. 2.2:Steady state behavior as a function of A2 of the real and imaginary parts of the groundstate coherence *c)Rep23* and d)/m/>23- Parameters are $6^*1 = C_2 = 0.1$, Ai = 0, 71 = 72-

2.2 Steady State Characteristics with Unequal Decays

We now study the steady state response of the medium for the case where there are unequal spontaneous emission rates from the upper level to the two ground sublevels. As in Section 2.1 the derivative of the density matrix ρ, in Eq.(2.6) is set equal to zero ($p = 0$) and the behavior of the population of state $|2\rangle$, ρ_{22} is evaluated a function of the detuning A2. Here an interesting sharp dip is observed. In the case of weak fields $\{G_1, G_2 \ll \gamma_1, \gamma_2\}$, for instance, $G_1 = G_2 = 0.1$ and for Ai $= 0$ as γ_2 is increased from being equal to γ_1 a smooth dip arises around the CPT condition (Ai $=$ A2) [Figure 2.3]. As γ_2 is increased, the height of the dip increases.

To understand the origin of the dip quantitatively a rigorous analysis is done of the analytical expression for p_{22} given in Eq. (2.9).

To explicitly evaluate and compare the individual contributions of the terms C_1 and C2, we study these as a function of A2 for the case $G_1 = G_2 = 0.1$, $\gamma_1 = 1.0$. As observed from Eq.(2.11), whenever γ_1 is equal to γ_2, $C2$ disappears. From Eq.(2.10) it is observed that in the region $G_1 < |z_2| < 1.0$, as A2 is decreased the term with the fourth power of A2 in the numerator is responsible for a decrease in Ci, eventhough the denominator, D in Eq. (2.12) (having a term of the order of A_2^4) is also reduced simultaneously. However in the region $|A_2| < G_1$ the contribution of the fourth power of A_2 is negligible compared to the term with the second power of A2. Hence the term C_1 is negative in the vicinity of the CPT condition. As $|A_2| \longrightarrow 0$ the term with the second power of A2 becomes more positive and hence it leads to the small peak with a maximum of zero at Ai $=$ A2. The term C_1 behaves in a similar manner when γ_2 is unequal to γ_1 also. This typical behavior is depicted in the Figure 2.4a for the case $\gamma_2 = 2.0$.

Once γ_2 is made unequal to γ_1, for example the case $\gamma_2 = 2.0$, the term $C2$ starts contributing. In the region $G_1 < |A2| < 1.0$, as A2 is decreased, due to the presence
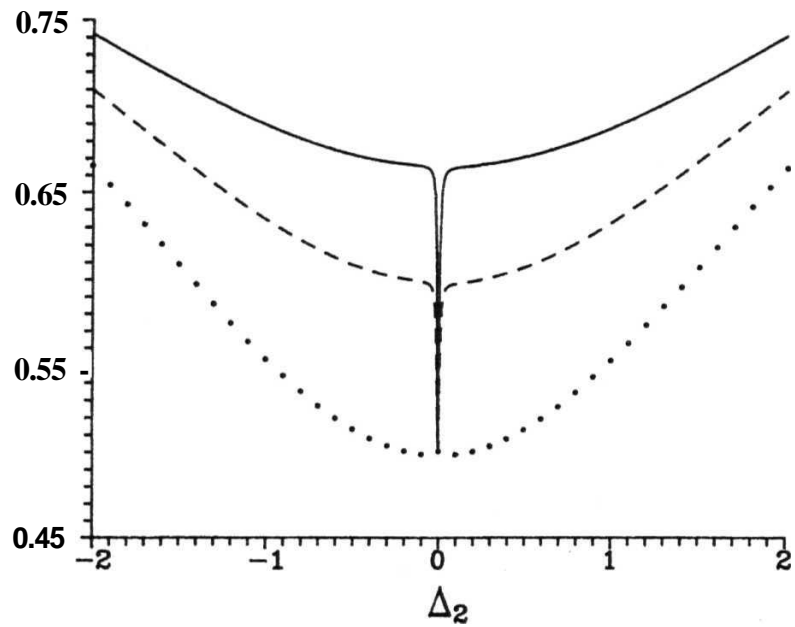
Fig. 2.3: The behavior of the population of level |2), $p_2 2$ as a function of the detuning A 2 for varying 72 values. The parameters are $G\backslash = G2 = 0.1$, Ai = 0,71 = 1.0. The dotted curve represents $72 = 1.0$, the dashed curve $72 = 1.5$ and the solid curve, $72 = 2.0$
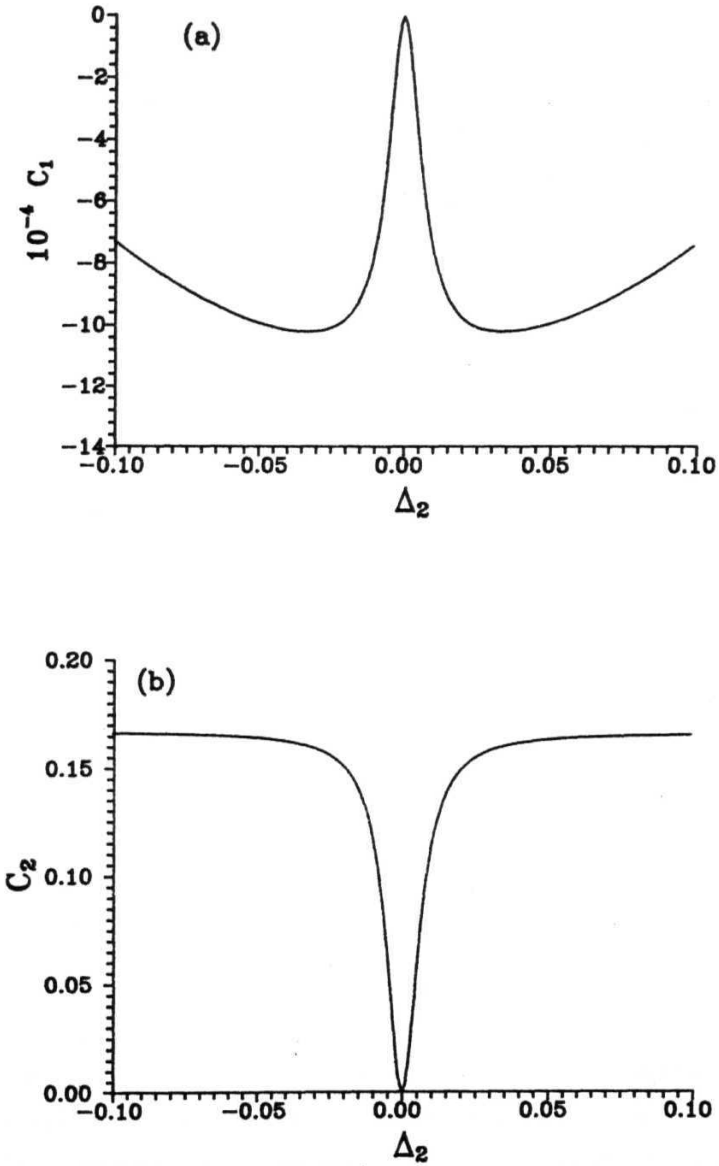
Fig. 2.4: The behavior of the two terms contributing to I_{22} as a function of the detuning A_2 in the region $|A_2| < Gi$. a) Ci and b) C_2. The parameters are $Gt=G_2 = 0.1$, $A_2 = 0$, $7_1 = 1.0$ and $7_2 = 2.0$.

of only a second order term in A2 in the numerator, the decrease in the denominator D in Eq. (2.12) increases the term CV However in the region $|A_2| < Gi$, the term of the order of the fourth power of $G\backslash$ is larger than the term with the fourth power of A_2 in denominator D. Hence any decrease in A2 results in a decrease of the numerator of C_2 without affecting the denominator D much. This gives rise to the dip in Figure 2.4b. The order of magnitude of the term C_2 is larger than Ci in the region $|A_2| < G\backslash$ and this explains the behavior of p_{22} for 72 ^ 71 (Figure 2.3).

Physically, as the spontaneous decay rate from state |1) to state |2) increases more than the spontaneous decay rate from state |1) to state |3), more and more of the population gets settled in state |2). Only at the condition, Aj = A2, the population gets distributed equally (because of the condition $G\backslash = G2)$ between the states |2) and |3). This leads to the increase in sharpness of the dip with the increase in 72. If 72 < 71, a peak is observed instead of a dip which is predicted from the Eq.(2.11).

For fields as low as 0.001 (scaled w.r.t 71) the term with the second power of $G\backslash$ in Eq.(2.10) becomes negligible and hence the peak in $C\backslash$ disappears. However for strong fields of the order of 71 this term becomes important and is responsible for the deep furrows on either side of the two photon resonance condition as depicted in Figure 2.5. But if the intensities of the fields are increased then the dip occurs only for very large 72 [Figure 2.5]. This is because the spontaneous emission from state |1) to state |2) has to be more effective than the field G_2 on the same transition to accumulate population on the level |2). The sharpness of the dip at Ai = A2 = 0, indicating a fall in the population in level |2), is manifested only when more population is there on level |2) for detunings other than Ai. For smaller 72 the decrease in ^22 at Ai = A2 gets smoothened out due to the overall low population level for the values of detuning, A_2 not equal to zero. This dip in the population of the level |2) can be observed by studying the absorption out of the level |2) using a weak probe field as for example, has been done in a different context in Ref.[4].
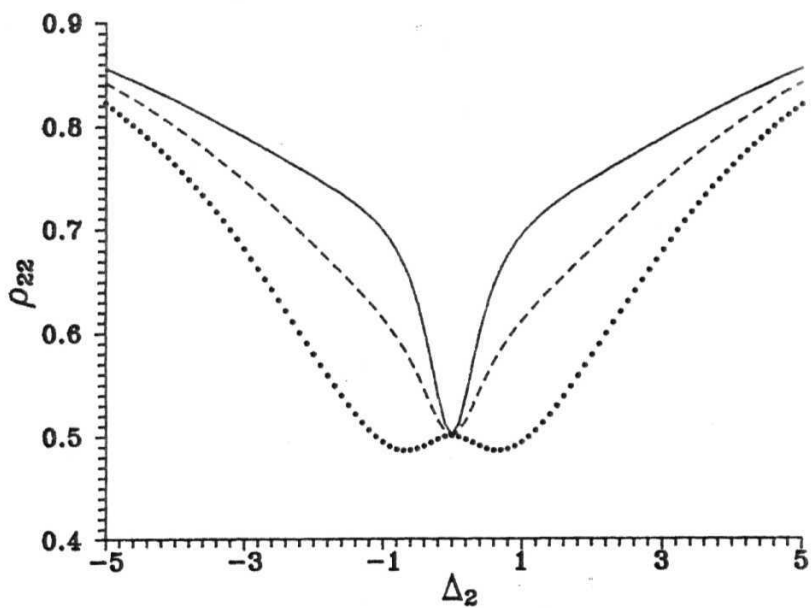
Fig. 2.5: Same as in Figure 2.3 but with parameters $d = G_2 = 1.0$, Ai $=$ 0,7i $= 1.0$. The dotted curve represents $72 = 1.5$, the dashed curve $72 = 2.5$ and the solid curve, $72 = 3.5$.

Bergmann and coworkers demonstrate efficient and selective vibrational excitation of NO molecule in its electronic ground state using pulsed lasers. The technique depends on laser coherence. The efficiency relies on a counter intuitive interacting sequence of two lasers with the medium of NO molecules with a process of stimulated Raman scattering using adiabatic passage. Optimum use of the coherence of the radiation fields is achieved by suitably delaying the pulses. This technique can be applied to a large class of atomic and molecular species such as *O2* and #2-

2.3   The CPT State

The nonevolving and noncoupling nature of the CPT phenomenon indicates some internal symmetry. The source of the symmetry and the CPT effect was demonstrated by Gray, Whitley and Stroud [6] who discovered a constant of motion at TPR condition. We derive the constant of motion at TPR here following Agarwal and Jha [14] who reported the nonabsorption resonances and derived the CPT wavefunction in a very simple manner.

The wave vector at time t corresponding to the Hamiltonian in Eq. (2.1) can be written in terms of thp basis states as

$$|\psi(t)\rangle = \sum_{n=1}^{3} b_n(t)|n\rangle. \tag{2.13}$$

Using the canonical transformation

$$M = \begin{pmatrix} b_1 \exp\{i\Omega_1 t\} \\ b_2 \exp\{i(\Omega_1 - \Omega_2)t\} \\ b_3 \end{pmatrix} \tag{2.14}$$

The Schrodinger equation for \ip) shows that

$$\dot{B} = -iMB. \tag{2.15}$$

M is expressed in the matrix form as

$$M = \begin{pmatrix} -\Delta_1 & -G_2 & -G_1 \\ -G_2^* & \Delta_2 - \Delta_1 & 0 \\ -G_1^* & 0 & 0 \end{pmatrix} . \tag{2.16}$$

The eigenvalues and eigenvectors of M will enable to predict the evolution of the system. The eigenvalues A of M are determined from the cubic equation

$$\lambda[(\lambda + \Delta_1)(\lambda - \Delta_2 + \Delta_1) - |G_1|^2 - |G_2|^2] + (\Delta_2 - \Delta_1)|G_1|^2 = 0. \tag{2.17}$$

For TPR condition, A] = A2, we find from the eigenvalue equation that one of the eigenvalues A = 0. Corresponding to the zero eigenvalue the eigenfunction is given by

$$|\psi\rangle = \left(1 + \frac{|G_2|^2}{|G_1|^2}\right)^{-1/2} [|2\rangle - G_2/G_1|3\rangle] . \tag{2.18}$$

By absorbing the phase factor we get

$$|\psi(t)\rangle = -G_1|2\rangle + G_2|3\rangle . \tag{2.19}$$

which is the trapping state. The Hamiltonian M in Eq.(2.16) acting on this state gives

$$M|\%l\rangle) = 0 \tag{2.20}$$

This implies that \ip) is a constant of motion. Hence the CPT state is stable under the action of the spontaneous decay rates of the upper levels. Once the system falls into the CPT state there is no further evolution. The entire population gets trapped in the ground level.

If $G\backslash$ = G'2, $P22 = P33 = 1/2$ irrespective of the values of $G\backslash$ and GY This implies that CPT occurs for very weak fields too as pointed out in Section 2.1. It would be interesting to study how weak fields affect the dynamics of the system and what are **the time** scales **involved.** In the next section we address some of the dynamical **questions.**

2.4 Dynamical Evolution to CPT State

Initially, at time $t = 0$, it is assumed that the atom is in the ground state and that there are no coherences *i.e.* $\wedge 33 = 1$, $p_u = p_{22} = 0$ and $p_{XJ} = 0$ where $i \wedge j$. To study the evolution of the system to CPT state from the above initial conditions the set of density matrix equations in Eq. (2.6) are numerically integrated using a fourth order Runge-Kutta method. We especially concentrate on the two photon resonance condition $Ai = A_2$.

Considering $Ai = A_2 = 0$ situation where the two external fields are exactly on resonance with the respective atomic transitions, we study the dynamical evolution to the CPT state for various field strengths and spontaneous decay rates. We specifically present the evolution of the absorption characteristic of one of the fields (say *G2) i-e., Im(pii)* and the population of the level $|2\rangle$, *p22-* For symmetric fields *i.e $G\backslash = G2$,* the steady state (relative to the decays involved) would correspond to the trapping condition if *Im(pi2) = 0* and *P22 = \-* The time is scaled as $7\wedge$.

We first study the dynamics for the strong fields situation i. e. $G\backslash$, $G2 \wedge> 7i$, 72- For a typical case, $Gi = G_2 = 10$, $71 = 72 = 1.0$, Rabi oscillations are exhibited in the evolution of the coherence *lm\pu)* and the population p_{22} [solid curves in Figure 2.6 and its inset]. To get an idea about the time scales involved we numerically perform an eigenvalue analysis of the 8×8 matrix in Eq.(2.6). For the strong fields complex eigenvalues are obtained. The complete set of eigenvalues is listed here. There are two real eigenvalues -1.0 and -2.0. The complex ones are -2.5+28.2i, -1.0+14.li, -1.0+14.1i (degeneracy) and their complex conjugates. These predict the occurrence of Rabi oscillations.This dynamical behavior shoud be observable by using the setup of Ref. 12. The real part of the complex eigenvalues is negative indicating that the system will approach steady state.
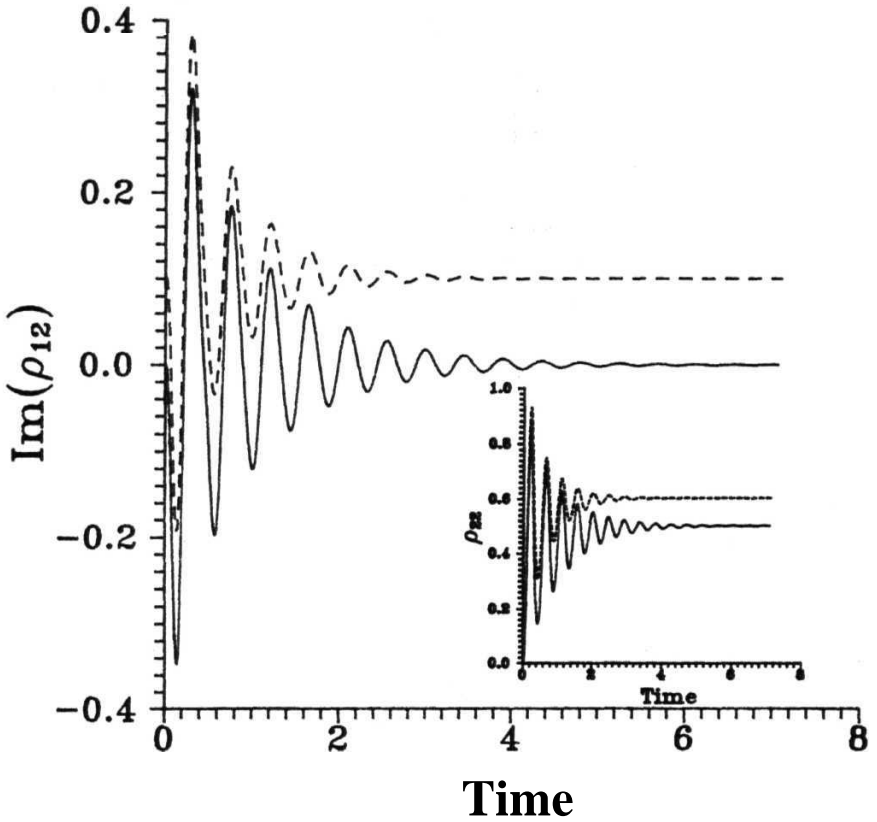
Fig. 2.6: Dynamical evolution of the absorption characteristic of the medium for the transition $|1\rangle \leftrightarrow |2\rangle$ w. r. t field G2, *Im(pu),* and population of the level $|2\rangle$, *P22* (inset). The time is scaled as *jit.* Parameters are $G\backslash = G2 - 10$, Ai = A2 = 0. The solid curves correspond to the decay rates $72 = 71 = 1.0$ and the dashed curves correspond to $72 = 2$, $71 = 1.0$. The dashed curves in the main figure and the inset have been to shifted by 0.1 units in the positive y direction for clarity.

As the field strength is lowered the eigenvalues become completely **real. For the case** $G_1 = G_2 = 0.1, 7! = 72 = $ **1.0,** the eigenvalues are -3.96,-2.02,-2.,, -1.98, -1.98, **-0.01, -0.01** (degeneracy) and -0.0099. It is also observed that the lowest **eigenvalue which dictates the time evolution** to steady state, is of the order of $G\backslash G_2$. Thus the time scale at which steady state is reached is ~ $G^\wedge$~- ^or instance when $G_1 = G_2 = 0.1$, the time scales as 1007i<. This is reflected in the dynamical evolution of *Im{pi_2)* and p_{22} as depicted in Figure 2.7 and its inset (solid curves). (Rabi oscillations have disappeared as eigenvalues are real). The steady state as observed, is nothing but as given by Eq.(2.19). This reconfirms our conclusion that the CPT state is formed even at low **light levels. But** as predicted by the analysis above, as the external field strength is reduced **the atomic system** takes longer and longer times to reach the CPT state.

The behavior of the A system is also sensitive to the relative rates of spontaneous emission on the two transitions. Therefore we study the influence of the **spontaneous** decay rates on the evolution. We again examine the eigenvalues. For strong fields, as one of the decay rates (say 72) is increased from unity it is observed that the minimum eigenvalue becomes larger. In the strong field example studied above when 72 is increased to 2.0 the minimum eigenvalue increases to -1.48 from -1.0 for the 72 = 1.0 case. In other words the time taken to reach steady state (CPT state) is relatively less. This is confirmed by the numerical integration result for the evolution shown in Figure 2.6 (dashed curves). But for **low** fields, an opposite effect occurs. As the decay rate is increased the minimum eigenvalue becomes smaller. In the low field example studied above when 72 is increased to 2.0 the minimum eigenvalue reduces to -0.0066 as compared to -0.0099 for the 72 = 1.0 case. Hence it takes longer to reach steady state as **confirmed from the dashed curves in Figure 2.7.** This is due to the build up of a small amount of coherence p_{12}, **which then slowly** decays to zero.

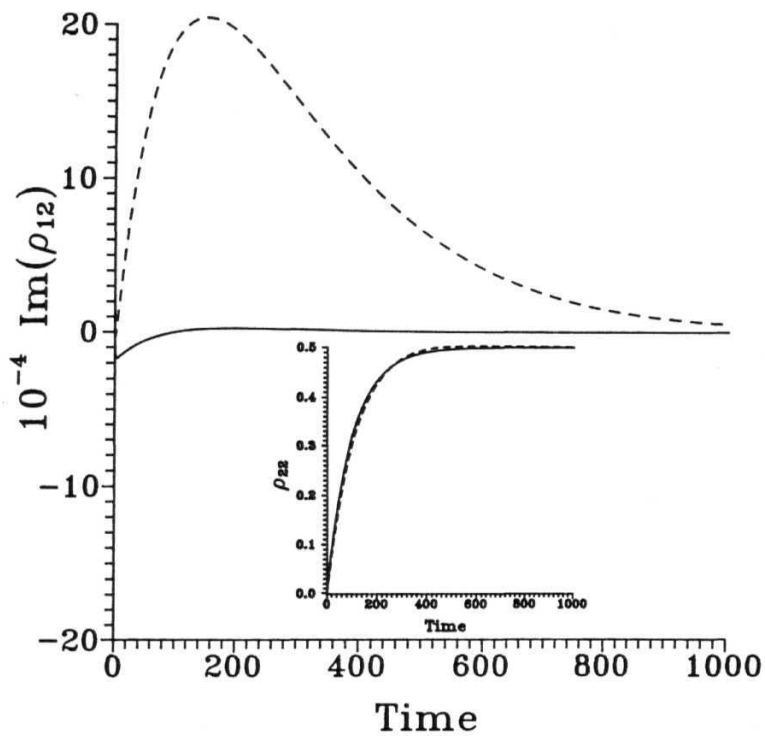**To understand the functional dependence of the minimum eigenvalue on the** decay

Fig. 2.7: Same as in Fig *1-6* with parameters $G_i = G_2 - 0.1$, $A_2 = A_j = 0$. Solid and dashed curves correspond to $y_2 = 7_i = 1.0$ and $-y_2 = 2.0, 7! = 1.0$ cases respectively.

rates and the fields we solve for the eigenvalues of the 8×8 matrix in Eq. (2.6) analytically when the fields are symmetric and when $A_i = A_2 = 0$. If A denotes the eigenvalue, then by setting $Det|p - A/| = 0$ where I is an identity matrix, an 8th order equation in A is obtained whose roots are the 8 eigenvalues. The eigenvalue equation is given as

$$(A + _7)(A^2 4- A_7 + 2 <?^2)^2 (A^3 + 3_7 A^2 + (8 <?^2 + 2_7^2)A + 4 \wedge 7) = 0. \qquad (2.21)$$

where $7 = 71 + 72$ and $g = Cn = G_2$. The first term in Eq. (2.21) gives

$$A = -7. \qquad (2.22)$$

This term can easily be identified in the numerical listing of the eigenvalues. The second term in Eq. (2.21) gives rise to a quadratic equation $A^2 - f A7 + 2g^2 = 0$ whose solutions are given by

$$\lambda = \frac{-\gamma \pm \sqrt{\gamma^2 - 8g^2}}{2}. \qquad (2.23)$$

For large g (strong fields), two complex conjugate roots are obtained (as found in the numerical analysis). But if g is small (low fields) two real roots occur. The roots in both these cases are repeated due to the square in the second term in Eq. (2.21).

The third term in Eq.(2.21) gives rise to a cubic equation given by

$$A^3 + 3_7 A^2 + (8g^2 + 2_7^2)A + 4 <7^2_7 = 0. \qquad (2.24)$$

The cubic equation accounts for the remaining three eigenvalues one of which is the minimum. The expressions for the three eigenvalues are quite involved (not given here) and do not immediately give a clear functional dependence on the fields and the decay rates. To understand the behavior of the minimum eigenvalue in the case of low fields, we perform a perturbation calculation. Introducing the scaled parameters $A = A/7$ and $g = 0/7$, Eq. (2.24) is transformed to

$$\tilde{\lambda}^3 + 3\tilde{\lambda}^2 + (8\tilde{g}^2 + 2)\tilde{\lambda} + 4\tilde{g}^2 = 0. \tag{2.25}$$

From the numerical calculation the minimum eigenvalue is found to be of the $O(g^2)$. So, we let A = $0g^2$ where *ft* is a unknown parameter which is found approximately from the perturbation calculation. In Eq. (2.25) the quadratic and cubic terms in A are ~ $O(g^4)$ and $O(g^6)$ respectively. The term $\{Sg^2 + 2\}$A is ~ $\$0\{g^4\} + 20\{g^2\}$. As *g* is quite small, retaining only the first order terms in g^2 in Eq.(2.25), we get *p* % —2. Hence $\tilde{\lambda} \approx -2\tilde{g}^2$ or

$$\lambda \approx -2\frac{g^2}{\gamma}. \tag{2.26}$$

Thus for low fields the minimum eigenvalue approximately decreases as - with the increase in one of the decay rates. In other words the system takes a longer time to reach a steady state as was discovered in the numerical calculation above.

In conclusion we have summarized the properties of the CPT state. We have demonstrated a sharp dip in the steady state response of the A system when unequal spontaneous decay rates are assumed. The origin of the dip in the behavior of the population of the ground state is due to the trapping conditions at $Ai = A_2$.

We have also demonstrated that the phenomenon of CPT persists even at low light levels [16]. Further using a simple eigenvalue calculation and corroborating its prediction of the time scales involved by numerical integration of the atomic density matrix equations for a A system, we have demonstrated how the evolution to the CPT state is dependent on the relative strengths of the fields and the spontaneous decays involved. We have shown that strong fields lead to CPT state faster. Increasing the decay rates in the case of strong fields leads to CPT faster while in the case of weak fields it leads to a relatively slow evolution to CPT.

REFERENCES

1. S. E. Harris, Phys. Rev. Lett. 62, 1022 (1989); A Imamoglu, Phys. Rev. A 40, 2835 (1989); S. E. Harris, J. E. Field and A. Imamoglu, Phys. Rev. Lett. 64, 1107 (1990); J. E. Field, K. H. Hahn and S. E. Harris, *ibid* 67, 3062 (1991).

2. O. Kocharovskaya, F. Mauri and E. Arimondo, Op. Commun. 84, 393 (1991); O. Kocharovskaya, Phys. Rep. 219, 175-190 (1992).

3. K. J. Boiler, A. Imamoglu, S. E. harris, Phys. Rev. Lett. 66, 2593 (1991); K. Hakuta, L. Marmet, B. P. Stoicheff, *ibid* 66, 596 (1991).

4. S. Schiemann, A. Kuhn, S. Steuerwald and K. Bergmann Phys. Rev. Lett. 71, 3637 (1993).

5. G. Alzetta, A. Gozzini, L. Moi and G. Orriols, Nuovo Cirnento, 36 B, 5(1976); G. Alzetta and L. Moi, *ibid.* 52 B,209(1979).

6. H. R. Gray, R. M. Whitley and C. R. Stroud Jr., Optics Lett. 3, 218 (1978); D. E. Murnick, M. S. Feld, M. M. Burns, T. U. Kuhl and P. G. Pappas *Laser Sptctroscopy* 4th ed. (Berlin, Springer Verlag, 1979), eds. H. Walther and W. Rothe, p.195.

7. G. Orriols, Nuovo Cimento, 53 B, 1(1979).

8. F. T. Hioe and C. Carroll, Phys. Rev. A 37, 3000(1988).

9. S. Swain, J. Phys. B 15, 3405(1982).

10. P. M. Radmore and P. L. Knight, J. Phys. B 15, 561(1982); B. J. Dalton and P. L. Knight, J. Phys. B 15, 3997(1982).

11. G. S. Agarwal, Phys. Rev. Lett. 71, 1351(1993); see also M. Fleischhauer, Phys. Rev. Lett. 72, 989(1994).

12. E. S. Fry, X. Li, D. Nikonov, G. G. Padmabandu, M. 0. Scully, A. V. Smith, F. K. Tittel, C. Wang, S. R. Wilkinson and S. Y. Zhu, Phys. Rev. Lett. 70, 3235 (1993).

13. A. Imamoglu, J. E. Field and S. E. Harris, Phys. Rev. Lett. 66, 1154(1991).

14. G. S. Agarwal and S. S. Jha, J. Phys. B 12 2655(1979); A. S. Manka , H. M. Doss, L. M. Narducci, P. Ru and G. L. Oppo, Phys. Rev. A 43, 3748 (1991).

15. G. S. Agarwal, *Quantum Optics,* (Berlin, Springer Verlag, 1974), Sec. 6,7,18.

16. Y. Li and M. Xiao, Phys. Rev. A51, 4959 (1995); Min Xiao and coworkers have observed the persistence of quantum interference effects at low light levels using the transitions ^{87}Rb.

Chapter 3

DYNAMICS OF COHERENT POPULATION TRAPPING STATES IN DENSE SYSTEMS

In the preceding chapter the steady state characteristics and the dynamics before the formation of the CPT state were studied in a nonlinear medium. An implicit assumption was that the medium is so dilute that the atoms constituting the medium are spaced too far apart to influence one another. However recently it has been argued that the densities which make it imperative to include the effect of neighbouring atoms (called the near dipole-dipole effect) are not very high. A density around 10^{14} $cm{\sim}^3$ is sufficient for the near dipole-dipole effects to become important. Many areas in quantum optics have ignored these effects so far.

The electric field experienced by an atom in a dense medium is not simply the macroscopic electric field. It is important to distinguish between the macroscopic electric field and the actual effective field acting on an atom. The atoms which constitute matter produce a field which has large local variations. If now an external field is applied the internal field gets modified. The macroscopic field is obtained by performing a spatial average of the total microscopic field over a region of space which is **larger than** the linear dimensions of the constituting particles. This is the field which appears in Maxwell's equations. Each particle now behaves as an electric dipole which acts as the source of a secondary field. The effective field is hence the sum of the external field produced by the source from outside the medium and the field produced near a dipole by all other dipoles

of the medium. The effective field is called the local field acting on an atom. Lorentz [1] gave a prescription to calculate the local field, called the Lorentz law given in Eq.(l) of this chapter.

The local field concept is important because it redefines the relation between macroscopic and microscopic properties of the medium. Local field effects become more important in nonlinear response with higher-order nonlinear interactions. They play a crucial role in determining nonlinear response of optical materials and large enhancement in response of semi-conductor doped glasses [2] and of metal colloids are reported. They have given rise to a lot of novel phenomena like mirrorless optical bistability [3], novel spectral shifts [4], and more recently a density dependent (i.e., piezophotonic) switching between absorption and amplification [5] and enhancement of inversionless gain and the index of refraction [6]. It has also been possible to obtain much higher atomic densities in gaseous systems by using heat pipes, atom traps or high temperature ovens so that effects from near dipole-dipole interactions become important.

At the densities needed for local fields to influence the system the absorption length of the wave traveling through the medium will be very small. But novel interference effects like CPT and EIT can substantially reduce absorption. Now EIT has been shown to enhance nonlinear wave mixing processes. For example Hakuta et al [7] have demonstrated EIT for the second harmonic 243nm light in *H2,* using dc laser fields. EIT has the potential to generate laser-like light at wavelengths where no convenient laser source exists. For efficiency in such processes laser light must propagate through a long or dense medium. Here local fields become important.

It would make an interesting study as to whether local fields affect the coherence which decides the quantum interference effects and if so, to what extent. CPT phenomenon being an important consequence of coherence and quantum interference effects [8] and also being involved in leading to LWI [9] and absorptionless index of refraction [10] where

local fields have created a large increase in gain and the refractive index, it is important to understand the influence of local fields on the formation of the CPT state.

In Section 3.1 we explicity show the relationship between macroscopic susceptibility and microscopic polarizability in the cases of linear and nonlinear dielectric media. In Section 3.2 we incorporate the local field into the semiclassical density matrices for a three-level A system and examine the nonlinear coupled equations thus obtained. In Section 3.3 we do a perturbative analysis and derive the closed form for linear and third order susceptibilities in the presence and absence of local fields. In Section 3.4 we study the steady state response for various field strengths in the presence of local fields and compare it with the behavior in the absence of them. In Section 3.5 we study the influence of local fields on the dynamics before CPT occurs. In Section 3.6 we study the gain in the presence of local fields for an inversionless gain system.

3.1 Local Field Effect on Linear and Nonlinear Response

The local field is related to the macroscopic field E and the polarization P at frequency u> in the bulk material via the Lorentz law [1]

$$\vec{E}_L(\omega) = \vec{E}(\omega) + \frac{4\pi \vec{P}(\omega)}{3} \tag{3.1}$$

The effect of local fields on the microscopic polarizability is demonstrated in the following exercise.

We first take the case of the linear response. The electric dipole moment d induced in the atom in a linear dielectric (linear in the sense the properties of the medium are directly related to the first power of the external field) is proportional to the local field as

$$\vec{d}(\omega) = \alpha(\omega)\vec{E}_L(\omega) \tag{3.2}$$

where $Qt(uj)$ is the linear polarizability of the material. If 77 is the number density of the atoms the polarization of the medium which is the total dipole moment per unit volume is given by

$$
\begin{aligned}
\vec{P}(\omega) &= \eta \vec{d}(\omega) \\
&= \eta \alpha(\omega) \vec{E}_L(\omega) \quad .
\end{aligned}
$$
(3.3)

Substituting for E_L from Eq.(3.1)

$$
\vec{P}(\omega) = \eta \alpha(\omega) \left(\vec{E}(\omega) + \frac{4\pi}{3} \vec{P}(\omega) \right)
$$
(3.4)

Expressing the polarization in terms of the linear susceptibility \M

$$
\vec{P}(\omega) = \chi^{(1)}(\omega) \vec{E}(\omega) \quad .
$$
(3.5)

Substituting this expression for polarization $P(UJ)$ into Eq.(3.4) and solving the resulting equation for x^H^) ^ *ˢ found that

$$
\chi^{(1)}(\omega) = \frac{\eta \alpha(\omega)}{1 - \frac{4\pi}{3} \eta \alpha(\omega)} \quad .
$$

The susceptibility is larger than the value $T{}Q(UJ)$ predicted by theories ignoring local fields. Also the susceptibility increases with density 77, much more rapidly than just proportionately as in the earlier theories.

Using Eq.(3.5) in Eq.(3.1) the local field is expressed in terms of the first order susceptibility as

$$
\vec{E}_L(\omega) = \left[1 + \frac{4\pi}{3} \chi^{(1)}(\omega) \right] \vec{E}(\omega)
$$
(3.7)

We now study the effect of local fields on the nonlinear response. When the medium is nonlinear i.e., the material properties vary nonlinearly with the electric field, the higher order susceptibilities are more complicatedly related to the corresponding polarizabilities. The nature of local field corrections (LFC) in nonlinear optics was elaborately

discussed by Bloembergen [11]. We illustrate here the relation between the macroscopic and microscopic using Mizrahi and Sipe's procedure [12] for the case of the four wave mixing (FWM) with the assumption that the fields are scalar. In FWM a signal field of frequency ω_1 and a probe field of frequency ω_2 impinge on a nonlinear medium. Then a phase conjugate wave of signal frequency, ω_1 is allowed to pass through the medium. The medium under appropriate phase matching conditions gives to rise a FWM signal wave of probe frequency ω_2.

Using the standard notation in nonlinear optics the total polarization at the frequency ω_2 is given by

$$P(\omega_2) = \eta\alpha(\omega_2)E_L(\omega_2) + \eta\gamma(\omega_1, -\omega_1, \omega_2)|E_L(\omega_1)|^2 E_L(\omega_2)$$ (3.8)

where $a(\omega_2)$ is the linear polarization for radiation at frequency ω_2 and $\gamma(\omega_1, -\omega_1, \omega_2)$ is the hyperpolarizability leading to FWM signal at frequency ω_2.

We next use Eqs.(3.1) and (3.7) to rewrite Eq. (3.8) as

$$P(\omega_2) = \eta\alpha(\omega_2)[E(\omega_2) + \frac{4\pi}{3}P(\omega_2)] + \eta\gamma(\omega_1, -\omega_1, \omega_2)$$
$$\times \left|1 + \frac{4\pi}{3}\chi^{(1)}(\omega_1)\right|^2 \left[1 + \frac{4\pi}{3}\chi^{(1)}(\omega_2)\right] |E(\omega_1)|^2 E(\omega_2) \quad .$$ (3.9)

The Eq.(3.9) is now solved algebraically for $P(\omega_2)$ to obtain

$$P(\omega_2) = \frac{\eta\alpha(\omega_2)E(\omega_2)}{1 - \frac{4\pi}{3}\eta\alpha(\omega_2)} + \eta\gamma(\omega_1, -\omega_1, \omega_2) \cdot \left|1 + \frac{4\pi}{3}\chi^{(1)}(\omega_1)\right|^2$$
$$\times \frac{\left[1 + \frac{4\pi}{3}\chi^{(1)}(\omega_2)\right]}{\left[1 - \frac{4\pi}{3}\eta\alpha(\omega_2)\right]}|E(\omega_1)|^2 E(\omega_2).$$ (3.10)

Identifying the first and second terms as linear and third order polarization which we represent as

$$P(\omega_2) = \chi^{(1)}(\omega_2)E(\omega_2) + \chi^{(3)}(\omega_1, -\omega_1, \omega_2)|E(\omega_1)|^2 E(\omega_2)$$ (3.11)

where in accordance with the Lorentz law and Eq. (3.6), the linear susceptibility is given as

$$\chi^{(1)}(\omega_2) = \frac{\eta\alpha(\omega_2)}{1 - \frac{4\pi}{3}\eta\alpha(\omega_2)} \tag{3.12}$$

and where third order susceptibility is given by

$$\chi^{(3)}(\omega_1, -\omega_1, \omega_2) = \frac{\left|1 + \frac{4\pi}{3}\chi^{(1)}(\omega_1)\right|^2 \left[1 + \frac{4\pi}{3}\chi^{(1)}(\omega_2)\right]}{1 - \frac{4\pi}{3}\eta\alpha(\omega_2)}$$
$$\times\ \eta\gamma(\omega_1, -\omega_1, \omega_2). \tag{3.13}$$

We can rewrite Eq.(3.12) as

$$1 + \frac{4\pi}{3}\chi^{(1)}(\omega_2) = \frac{1}{1 - \frac{4\pi}{3}\eta\alpha(\omega_2)}\ . \tag{3.14}$$

Substituting (3.14) in Eq.(3.13) the susceptibility is given as

$$\chi^{(3)}(\omega_1, -\omega_1, \omega_2) = |1 + \frac{4\pi}{3}\chi^{(1)}(\omega_1)|^2[1 + \frac{4\pi}{3}\chi^{(1)}(\omega_2)]^2\ . \tag{3.15}$$

The local field corrections (LFC) appear to the fourth order in this expression. This implies that local field effects play a vital role in defining susceptibility of higher order nonlinear interactions.

Recently Maki et al [13] studied the optical response of a dense atomic potassium vapour under conditions where LFC strongly influence in the determination of the magnitude of the optical response. Their results were in good agreement with the predictions of the Lorentz law in the linear case and with Bloembergen's prediction of the LFC to the third order susceptibility for the nonlinear case. They performed two experiments. The first experiment studied the resonant structure of the linear dielectric constant of the atomic potassium vapour [dielectric constant e is related to first order susceptibility through the relation e = 1 -f 47rx$^{(l*)}$] by measuring the spectrum of the reflectivity of the interface between the vapour and a sapphire plate that formed the window of

the cell. The properties of the atoms get modified by the sapphire surface. A highly wavelength dependent reflectivity occurs near the atomic resonance which is known as selective reflection. When the reflectivity of the interface was plotted as a function of laser frequency for several values of atomic density, the spectral variation in reflectivity became more pronounced and also as the number density was increased, a shift to lower frequencies was observed. The shift was in agreement with the theoretically predicted Lorentz red shift.

In the second experiment nonlinear response was measured by surface phase conjugation where a weak signal wave interacts with a pump normally incident on the interface. The interference of the waves produces a spatially varying intensity pattern on the surface which leads to a spatial variation in the reflection coefficient. The reflection of pump wave from this pattern creates the phase conjugate wave of the signal wave, whose intensity was ploited as a function of laser frequency for many values of atomic density. The experimental results were found to agree very well with theory. Spectral shifts of the order of 1 GHz are observed at density $\sim 10^{1'}$ atoms per cubic cm. These results of Maki and others have led to intensified research in LFC. In the next section we incorporate the local field in a dense medium of three-level atoms and study the coherence characteristics of the medium.

3.2   The Model with Local Field Corrections

We consider the same three level Lambda (A) configuration for the atomic medium as in Chapter 2. The Hamiltonian for the system is given in Eq.(2.1) of Chapter 2. The system is studied using the density matrix formalism. The semiclassical density matrix equations before the LFC are incorporated are given in Eq.(2.6) of Chapter 2.

The polarization of the medium is defined as the trace of the product of the density

matrix and the dipole moment as $\vec{P} = \mathrm{Tr}\rho\vec{d}$. Hence the fields $\vec{E}_1$ and $\vec{E}_2$ are redefined as the local fields $\vec{E}_1 + \dfrac{4\pi}{3}\eta\rho_{13}\vec{d}_{31}$ and $\vec{E}_2 + \dfrac{4\pi}{3}\eta\rho_{12}\vec{d}_{21}$ corresponding to the two transitions $|1> \leftrightarrow |3>$ and $|1> \leftrightarrow |2>$ respectively.

This inclusion of LFC modifies the frequency G_1 as $G_1 + \beta_1\rho_{13}$ and G_2 as $G_2 + \beta_2\rho_{12}$ where $\beta_1 = \dfrac{4\pi\eta|d_{13}|^2}{3\hbar}$ and $\beta_2 = \dfrac{4\pi\eta|d_{12}|^2}{3\hbar}$ are the LFC parameters for the transitions $|1> \leftrightarrow |3>$ and $|1> \leftrightarrow |2>$ respectively. Using the modified fields in the density matrix equations in Eq.(2.6) of Chapter 2, the following set of *nonlinear equations* is obtained:

$$
\begin{aligned}
\dot{\rho}_{11} &= -2(\gamma_1 + \gamma_2)\rho_{11} + iG_1\rho_{31} + iG_2\rho_{21} + c.c \;, \\
\dot{\rho}_{12} &= -[\gamma_1 + \gamma_2 - i(\Delta_2 + \beta_2(\rho_{22} - \rho_{11}))]\rho_{12} + iG_1\rho_{32} \\
&\quad + iG_2(\rho_{22} - \rho_{11}) + i\beta_1\rho_{13}\rho_{32} \;, \\
\dot{\rho}_{13} &= -[\gamma_1 + \gamma_2 - i(\Delta_1 + \beta_1(1 - 2\rho_{11} - \rho_{22}))]\rho_{13} \\
&\quad + iG_2\rho_{23} + iG_1(1 - 2\rho_{11} - \rho_{22}) + i\beta_2\rho_{12}\rho_{23} \;, \\
\dot{\rho}_{22} &= 2\gamma_2\rho_{11} - iG_2\rho_{21} + c.c. \;, \\
\dot{\rho}_{23} &= i(\Delta_1 - \Delta_2)\rho_{23} - iG_1\rho_{21} + iG_2^*\rho_{13} + i(\beta_2 - \beta_1)\rho_{13}\rho_{21} \;. \qquad (3.16)
\end{aligned}
$$

A comparison of density matrix equations without LFC (Eq. (2.6) of Chapter 2) and with LFC (Eq. 3.16) shows that the equations for populations are unaltered. This occurs because the population equations contain held terms along with their complex conjugate terms. When the LFC are added to the fields, in the population equations the complex conjugate terms of the LFC cancel each other . For example in Eq. (2.6) adding LFC to the field G2 in the equation of motion of the ground state population gives rise to the terms — $i(G_2 + hp\backslash 2)P2\backslash$ H- $*(^2$ "⊦" $02p2i)pu$ which on performing a cancellation gives the corresponding equation in Eq. (3.16).

However the coherence equations have two new kinds of terms. One term is an additional detuning term, e.g., $h\{p22 \sim P11)$ in t-[ne] second equation in Eq. (3.16) which

depends on the population inversion in the corresponding transition as **was first realized** by Hartmann and coworkers [4] in the context of two level transitions. Hartmann and coworkers incorporated LFC into optical Bloch equations for a two-level atom and studied the steady state behavior of the system. They observed that a red shift in the response was produced which was proportional to the population inversion corresponding to the two-level transition. This shift was called the dynamic Lorentz shift as it varied along the resonant line shift. The same group also studied the effect of LFC on FWM [4] in a two-level system where they found that both line shape and line shift distortions occur at intermediate intensities of the pump. For weak fields a static Lorentz shift was observed and for strong fields the response was independent of the LFC.

The second term is a nonlinear coupling between the coherences, e.g. in Eq.(3.16), the presence of *if3ipi3p32* ensures a direct coupling between $/?_{12}$ and pi_3 and not just via the term containing the ground state coherence, *iGipw* These cross couplings **indicate** a change in the kind of interference between the two pathways to the excited state.

3.3 Perturbation Calculation of Third Order Susceptibility and Polarizability

We now do a perturbation calculation of the steady state polarization corresponding to the FWM signal at frequency u_2. The relevant density matrix element is p_{i2} which consists of two orders of magnitude of the Rabi frequency G_1 and one order of **magnitude of the Rabi** frequency G_2.

Any density matrix element can be expanded in terms of the components of different orders of magnitude in G_1 and G'_2 as

$$\rho_{\alpha\beta} = \sum_{mn=0}^{\infty} \rho_{\alpha\beta}^{(m,n)} (G_1^m G_2^n) \tag{3.17}$$

where $p \pounds p$ **corresponds** to the element $p_Q p$ of the density matrix which is mth order in G_1 and nth order in G_2-

Any perturbative analysis breaks down for long times (compared to the decays in the system). To circumvent the problem we introduce the collisional decay parameter, T between the two ground state levels of the A configuration. The equation for the evolution of the ground state coherence gets modified with the addition of the term — Tp_23 on its right hand side. The rest of the equation remains unaltered.

Initially at time $/ = 0$, when there are no fields, we assume that all the population is in the ground state and that there is no polarization in the system. Hence $pf^*/^{\circ\wedge} = p^{\wedge 0 \wedge} = 0$ and $p^{(\pounds 0)} = 1$. Also the coherence $p \backslash f^{(0)} = 0$ where $i = j = 1,2,3$.

We first calculate $/>|_2'$ ^{m} the absence of LFC. The polarizability **corresponding to** the transition $|1 > <\text{-}\bullet |2 >$, which is first order in G_1, i.e., $p^{\wedge l \wedge}$ is zero as observed from Eq.(2.6). Hence

$$\alpha(\omega_2) = 0 \quad . \tag{3.18}$$

Now the polarizability corresponding to the transition $|1 > <+ |3 >$, which is first order in field G_1 is related to the corresponding coherence term by

$$\alpha(\omega_1) = \frac{|d_{13}|^2}{\hbar G_1} \rho_{13}^{(1,0)} \quad . \tag{3.19}$$

The system is now studied at steady state by setting the time derivative of the density matrix to zero (i.e., $p — 0$) for each order in G_1 and 6^*2• The third-order component corresponding to the FWM signal at $\omega 2$ is obtained from the second equation in Eq.(3.16) as

$$\rho_{12}^{(2,1)} = \frac{iG_1\rho_{32}^{(1,1)} - iG_2\rho_{11}^{(2,0)}}{k_2} \tag{U0}$$

where $k_2 = \gamma_1 + \gamma_2 - i\Delta_2$.

The lower order polarizations p_{32}' and population $p \backslash /$ are evaluated individually.

From Eq.(3.16) the population term $p_{11}^{(\prime0)}$ is found to be

$$\rho_{11}^{(2,0)} = \frac{iG_1\rho_{31}^{(0,0)} - iG_1^*\rho_{13}^{(1,0)}}{2(\gamma_1 + \gamma_2)} \quad .$$ (3.21)

The coherence term $p_{32}^{\wedge}$ which is first order in both fields is given by

$$\rho_{32}^{(1,1)} = \frac{iG_1\rho_{31}^{(1,0)}}{X_1}$$ (3.22)

where $A_1' = -T + i(A_i - A_2)$. It is clear from Eqs.(3.21) and (3.22) that the first order coherence term $p_{13}^{\wedge}$ has to be evaluated. From Eq.(2.6) it is given by

$$\rho_{13}^{(1,0)} = \frac{iG_1}{k_1}$$

where $k_i — \sim f_i + 72 — IAJ$. Substituting the complex conjugate of Eq.(3.23) i.e., $p_{13}^{\wedge(0\wedge}$ and p_{j3}' ' in Eqs.(3.21) and (3.22), the second order contributions are given by

$$\rho_{11}^{(2,0)} = \frac{|G_1|^2}{|k_1|^2}$$ (3.24)

and

$$\rho_{32}^{(1,1)} = \frac{G_1^*G_2}{X_1^*k_1^*} \quad .$$ (3.25)

Substituting Eqs.(3.24) and (3.25) in Eq.(3.20) and simplifying the resulting expression we get

$$\rho_{12}^{(2,1)} = \frac{i|G_1|^2G_2}{|k_1|^2|k_2|^2|X_1|^2} \cdot (k_1 - X_1^*)k_2^*X_1 \quad .$$ (3.26)

A similar perturbative analysis is done for the case where the LFC are included. The equations of motion are the modified density matrix equations in Eq.(3.16). **The relevant contributions** are given as

$$\rho_{12}^{(0,1)} = 0$$ (3.27)

$$\rho_{13}^{(1,0)} = \frac{iG_1}{k_1'}$$ (3.28)

$$\rho_{11}^{(2,0)} = \frac{|G_1|^2}{|k_1'|^2} \tag{3.29}$$

$$\rho_{32}^{(1,1)} = \frac{G_1^* G_2}{k_1'^* X_1^*} \ . \tag{3.30}$$

where $k_l' = k_i - ifc$.

The third order polarization with the inclusion of LFC is given by

$$\rho_{12}^{(2,1)} = \frac{[iG_1 + i\beta_1 \rho_{13}^{(1,0)}]\rho_{32}^{(1,1)} - iG_2\rho_{11}^{(2,0)}}{k_2} \ . \tag{3.31}$$

Substituting Eqs.(3.29) and (3.30) in Eq.(3.31) gives

$$\rho_{12}^{(2,1)} = \frac{i|G_1|^2 G_2}{|k_1'|^2 |k_2|^2 |X_1^2|} \cdot (k_1 - X_1^*)k_2^* X_1 \ . \tag{3.32}$$

We now check whether the polarization in the presence and absence of LFC satisfy the Bloembergen's result for nonlinear response [11]. Using the Eqs. (3.18), (3.12) along with Eqs.(3.19) and (3.14) in Eq.(3.13)

$$\chi^{(3)}(\omega_1, -\omega_1, \omega_2) = \eta\gamma(\omega_1, -\omega_1, \omega_2) \left| \frac{1}{1 - \frac{4\pi}{3}\eta\frac{i|d_{13}|^2}{\hbar k_1}} \right|^2 \tag{3.33}$$

Using the definition of LFC, &, it is found that

$$\chi^{(3)}(\omega_1, -\omega_1, \omega_2) = \eta\gamma(\omega_1, -\omega_1, \omega_2)\frac{|k_1|^2}{|k_1'|^2} \ . \tag{3.34}$$

Using the expressions for the polarization in the presence of LFC (Eq.(3.32)) and the polarization in the absence of LFC (Eq.(3.26)) and substituting for x*³^ and 7 correspondingly it is seen that they satisfy the Eq.(3.34). The results obtained from perturbation theory satisfy the results of Bloembergen [11] and Mizrahi-Sipe [12].

3.4 Local Field Effect on the Steady State Response

To gauge the effect of local fields on the steady state response of the system the nonlinear coupled equations in Eq.(3.16) are solved numerically by setting the derivative of the

density matrix, p equal to zero (i.e., $p = 0$). The response of the system is studied for various intensities of the external field and a comparison with the behavior in the absence of LFC is done. We specifically present the absorption characteristic of the optical coherence on the transition from $|1 ><-• |2 >$, i.e. $7m(y>_{12})$, the ground state coherence $7ra(/?_23)$ and the behavior of the population of level $|2 >$, $p<n$ as a function of the detuning A_2, for the cases with and without LFC.

We first consider the situation where the fields are weak $(G\,Gi « 71,72)$- For a typical case $6\ = G_2 = 0.1$, $72 = 71 = 1.0$, $Ai = 0$, the behavior of $Im(p_{12})$, $7ra(/>_{23})$ and $P22$ is depicted in Figure 3.1 for the case without LFC (curve with closed circles) along with the case with LFC for two different sets of local field parameters, namely $fa = (3_2 = 0.9$ (dashed curve) and 1.5 (solid curve).

It is observed that at two photon resonance condition. $Ai = A_2$, the coherent dip or electromagnetically induced transparency persists in the absorption characteristic of the fields, $/m(/?i_2)$ shown in Figure 3.1. The inclusion of local field effect does not destroy the trapping condition and inspite of LFC the system evolves to a nonevolving eigenstate of the Hamiltonian. The effect of LFC is prominent for $Ai \wedge A_2$. The Lorentz red shift predicted by Hartmann and coworkers [4], is manifested as an overall shift of the absorption curve. Only at $Aj = A_2$ there is the status quo of the zero absorption minimum.

The ground state coherence behavior represented by $7m(^23)$ corroborates the optical resonance character as shown in the inset of Figure 3.1. LFC do not produce any discernible change. For both the sets of LFC parameters $7ra(/?_{23})$ almost falls on the curve without LFC. As expected the coherence between the states $|2 >$ and $|3 >$ is out of phase with the optical coherences [8]. The imaginary part of $/?_{23}$ shows dispersive behavior, whereas the real part of $/9_{23}$ would show absorptive behavior.

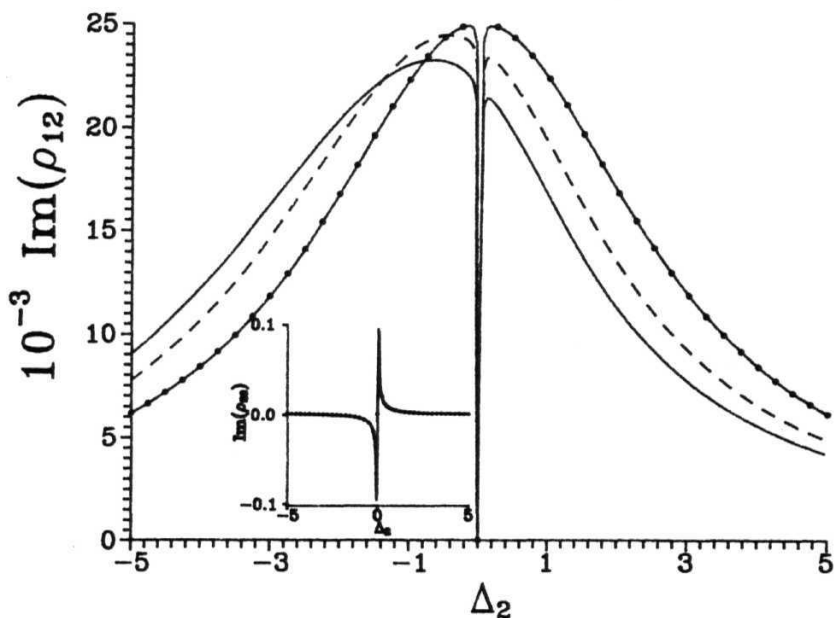The Lorentz shift is demonstrated in the behavior of population of level $|2 >$ in the

Fig. 3.1: *Im(p\2)<>* absorption characteristic of the medium for the transition |1 ⟩⟨• |2 > as a function of the detuning A2; the inset shows the ground state coherence, /m(/>₂3). The parameters are $G_1 = G2 = 0.1$, $A_x = 0.72 = 71 = 1.0$. The curve with closed circles corresponds to the case without LFC. The dashed and solid curves correspond to LFC parameter sets *pi* = /?₂ = 0.9 and 1.5.

Figure 3.2. But at Ai = A₂ the curves corresponding to the two cases of **LFC** (dashed and solid curves) intersect with the curve in the absence of LFC (curve with closed circles). The population of level $|2>$ at Ai = A₂ is \ (CPT condition for symmetric fields). However near the CPT condition a narrow dispersive-like behavior is observed. This unusual phenomenon arises because of the behavior of p_{22} very close to the two photon resonance condition in the absence of LFC. Far from A₂ = 0, the population of level $|2>$ decreases as A₂ -> 0 and it falls below i. But close to the CPT condition, as $A_2 \longrightarrow 0$, *P22* starts increasing till it reaches | at A₂ = 0. This is shown magnified in inset (i) of Figure 3.2, where there is a peak in p_{22} near CPT condition. With the inclusion of LFC this behavior near CPT is affected asymmetrically on either side of zero detuning. This gives rise to the dispersive behavior, shown clearly in inset (ii) of Figure 3.2. Another observation which is clear is that LFC bring about a redistribution of population between the three levels at all Ai ^ A₂. This is responsible for the decrease in absorption with the increase in LFC as depicted in Figure 3.1.

In the previous chapter the occurrence of a sharp dip around the CPT condition in the ground state populations for unequal decay rates was demonstrated. It would be interesting to see how LFC affect the dip. We present the behavior of the population of state $|2>$, *P22* [as a] function of A₂ for the same case as above but with 72 = 2.0 in Figure 3.3. The LFC parameters are also the same as before. As in the previous case at the CPT condition the curves in the presence and absence of LFC intersect. This intersection confirms the independence of CPT on LFC. The dip which arises due to the trapping conditions prevalent persists. But close to the CPT condition **the asymmetric effect of LFC** on either side of zero detuning leads to the shifting of the minimum of the **dip** as shown clearly in the inset of Figure 3.3. This behavior is similar to the dispersive **effect** observed in Figure 3.2.

For the case where the external fields are quite strong (d , *G2* >> 71,72) **it** is observed

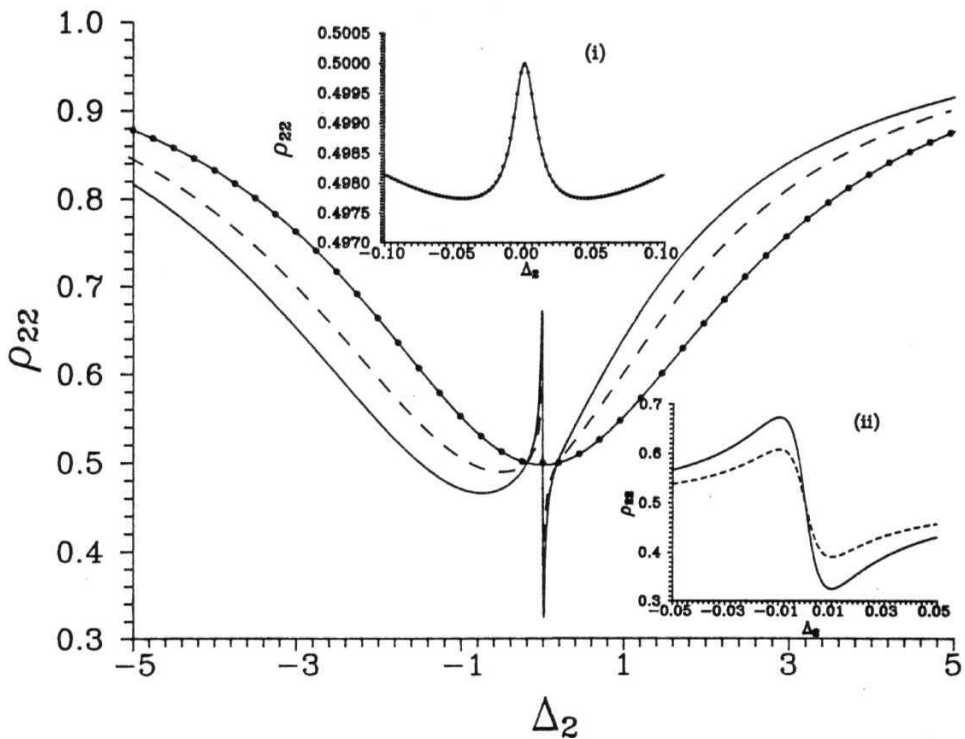**Fig.** 3.2: Population of the level $|2 >$, $\rho 22$ as a function of detuning A_2 **for** same paprameters as in Fig 3.1. Inset(i) [(ii)] gives the behavior of $p_2 2$ near **CPT** condition in the absence [presence] of LFC.
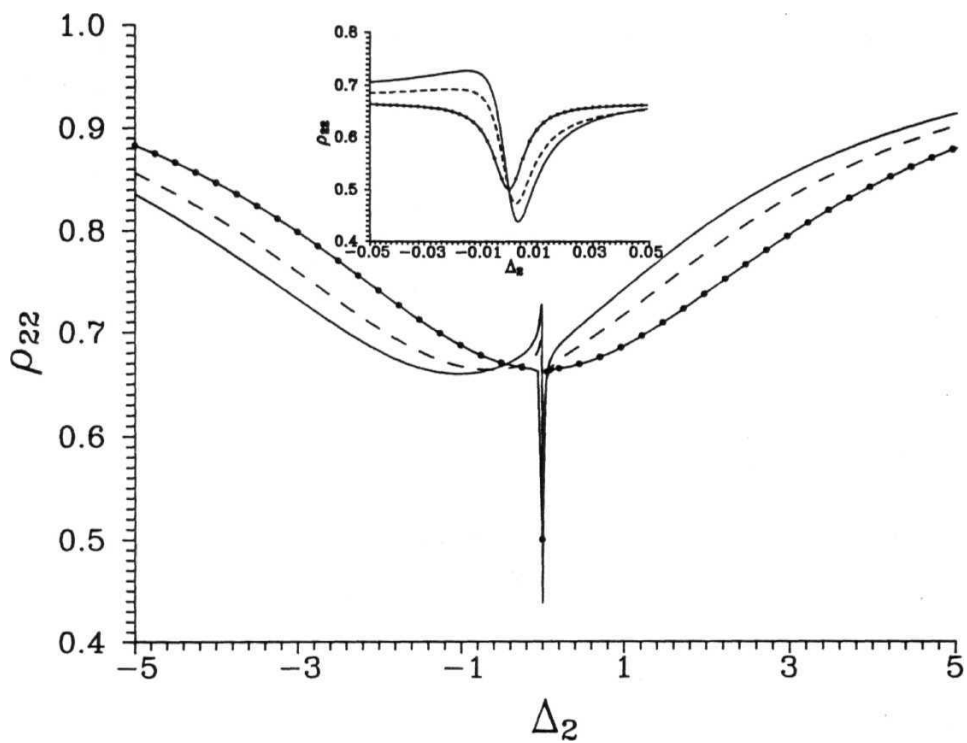
Fig. 3.3: Same as in Fig. 3.2 but with $\gamma_2 = 2.0$ with inset giving the behavior near CPT condition with and without LFC.

that the LFC have to be pretty large for any effect on the medium response. We present the results for $lm(p_{12})$ for a typical case when G\ = 1.0, G_2 = 5.0, 72 = 7! = 1.0, A! = 0 in Figure 3.4. Two different sets of LFC parameters are used, namely & = 0_2 - 1.5 (dashed curve) and 4.0 (solid curve). In the absence of LFC the Autler-Townes splitting [14] is seen.

The Autler-Townes doublet is a result of AC stark splitting. It arises in the response of an atomic system when a weak probe field acts on a transition sharing one common level with a strong field driven transition. The intense pump splits the common level into a closely spaced doublet and the weak field probes the two closely lying levels (also called the dressed states in the dressed atom picture [15] and gives rise to the two peaks in the absorption spectrum.

With the introduction of LFC however, an asymmetric change in the behavior of the absorption is observed on either side of the zero detuning. Along with an overall shift of the absorption curve, on the negative side there is an increase in the maximum absorption while on the positive side there is a. reduction. The CPT persists unhindered. Due to G\ being smaller than G_2, LFC on $G_]$ affect the response of the system more. It is observed that whether fi_2 = 0 or 4 the response $hv(pn)$ is almost the same as in the solid curve. Only /?i affects the response in a marked manner.

Hence, one can conclude that the additional field experienced by the atoms does not change the steady state behavior at exactly the two photon resonance condition. The destructive interference between the two paths to the excited state completely nullifies any possibility of absorption from the field in spite of the LFC. It would now be interesting to study the role of LFC in the dynamical evolution to CPT.
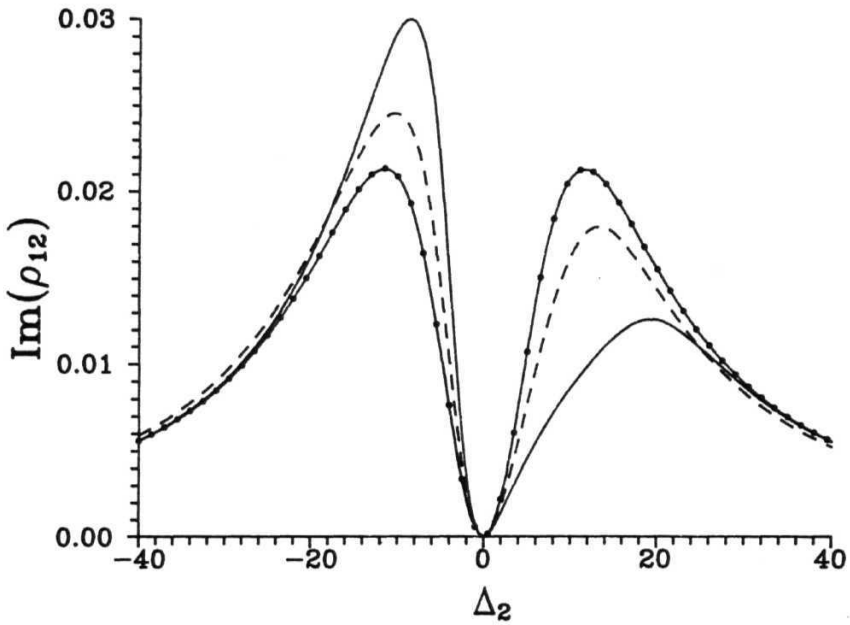
Fig. 3.4: Same as Fig. 3.1 but for strong fields. Parameters are $G\backslash = 1.0$, $(?2 = 5.0$, $Ai = 0.72 = 71 = 1.0$. The curve with closed circles represents the case without LFC. The dashed and solid curves correspond respectively to $fc = p_2 = 1.5$ and 4.0.

3.5 Effect of Local Fields on the Dynamical Evolution to CPT State

Initially, at time $t = 0$, the atom is assumed to be in the ground state. Hence $\rho_{33} = 1$, $\rho_{11} = \rho_{22} = 0$. It is also assumed that there are no coherences *i.e., pi3* $= 0$ where $i \neq j$. To study the evolution of the system to CPT state from the above initial conditions the density matrix equations linear in the absence of LFC (Eq.2.6) and nonlinear in the presence of LFC (Eq.3.16) are numerically integrated using the fourth order Runge-Kutta method at the two photon resonance condition $\Delta_1 = \Delta_2$.

We present the results for the evolution of the optical and ground state coherences, $Im(pi2)$ and $Im.(p_23)$ as a function of time for a. typical case in Figure 3.5. We consider $G_1 = G_2 = 0.1, \gamma_2 = \gamma_1 = 1.0$, $\Delta_1 = \Delta_2 = 0$ and the two sets of LFC parameters used in Section 3.4. The steady state (trapping state) corresponds to the condition $Im(pi_2) = 0$ and $Irn(p22,) = 0$. The time is scaled as γ^{-1}. As illustrated in Figure 3.5a, LFC *delay* the approach to the steady state (CPT) where $Im(p_{12}) = 0$. This delay is reflected in the evolution of $Im(p2z)$ which gets modified by the presence of LFC in the initial times as depicted in Figure 3.5b. The population of level $|2>$, p_22 is not much affected by LFC (figure not shown) and almost exactly follows the same curve as without LFC. For strong fields, LFC have to be quite large to affect the dynamics of the system.

Another observation from Figure 3.5 is that larger the LFC parameters, the longer it takes to reach steady state. This is justified because with the local fields present it takes time for complete destructive interference between the two pathways to the excited state to occur. The direct coupling terms between the coherences, (e.g., in the last equation in Eq.(3.16) the term *ifiipizpm)* are finite at times before steady state $(p_{32} \ / \ 0)$ as depicted in Figure 3.5b and delay the evolution to steady state.
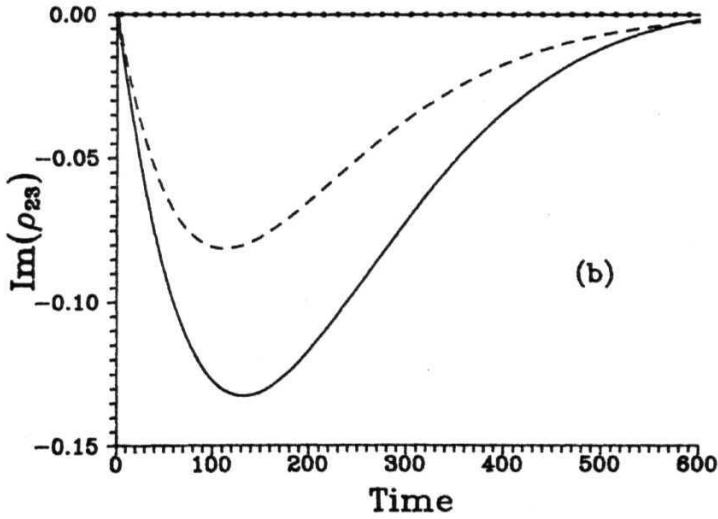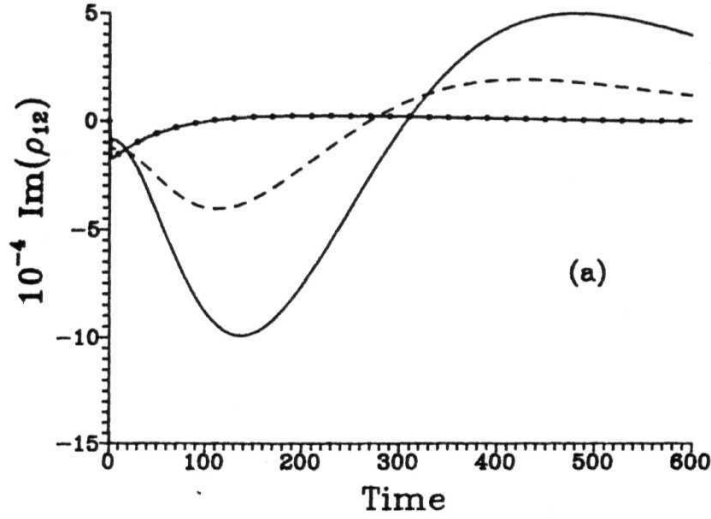
Fig. 3.5: Dynamical evolution of a) $Im(\rho_{12})$ b) $Im(\rho_{23})$ in the presence of LFC. The parameters are $G_1 = G_2 = 0.1$, $A_1 = A_2 = 0,72 = 71 = 1.0$. The curve with closed circles corresponds to the case without LFC; the dashed and solid curves correspond to $fa = fa = 0.9$ and 1.5.

3.6 Lasing Without Inversion in a Dense Medium

The formalism of this chapter is also directly applicable to study **the effect of LFC on** the models of lasing without inversion. Bowden and coworkers **have extended the calculations** of gain in models of lasing without inversion by including **LFC** [6]. For certain values of atomic density they predict an enhancement of inversionless gain and also the absorptionless index of refraction by more than two orders of magnitude.

In this section we introduce the LFC in the lambda system exhibiting gain without population inversion. In this model first proposed by Imamoglu et al [16] there is a strong **pump** field, G2 coupling the state $|2>$ to state $|1>$ and a weak probe field, $G\backslash$ coupling the state $|3>$ to $|1>$ (i. e. for the case $G_2 > G\backslash$ with reference to previous sections). An incoherent pumping rate, 2A, is taken between the states $|1>$ and $|3>$ in addition to the spontaneous decay rate, **2-7l**. Gain in the probe field is indicated by $/ra(/9_{13})$ becoming less than zero. The condition for gain in such a system is $-y_2 > 7i$-

With the presence of A, equations of motion for the density matrix including the **LFC** equations in (3.16) are modified to

$$\dot{\rho}_{11} = -2(\gamma_1 + \gamma_2 + 2\Lambda)\rho_{11} + iG_1\rho_{31} + iG_2\rho_{21} + c.c,$$

$$\dot{\rho}_{12} = -[\gamma_1 + \gamma_2 + \Lambda - i(\Delta_2 + \beta_2(\rho_{22} - \rho_{11})]\rho_{12} + iG_1\rho_{32}$$
$$+iG_2(\rho_{22} - \rho_{11}) + i\beta_1\rho_{13}\rho_{32} \ ,$$

$$\dot{\rho}_{13} = -[\gamma_1 + \gamma_2 + 2\Lambda - i(\Delta_1 + \beta_1(1 - 2\rho_{11} - \rho_{22}))]\rho_{13}$$
$$iG_2\rho_{23} + iG_1(1 - 2\rho_{11} - \rho_{22}) + i\beta_2\rho_{12}\rho_{23} \ ,$$

$$\dot{\rho}_{22} = 2\gamma_2\rho_{11} - iG_2\rho_{21} + c.c \ ,$$

$$\dot{\rho}_{23} = [-\Lambda + i(\Delta_1 - \Delta_2)]\rho_{23} - iG_1\rho_{21} + iG_2^*\rho_{13} + i(\beta_2 - \beta_1)\rho_{13}\rho_{21} \ . \quad (3.35)$$

The equations of motion for the density matrix without LFC are obtained by setting *P's* zero. The modified equations are solved as in the previous sections and the steady

state response of the medium is studied. We take the case $G_t - 0.05$, $G_2 = 5.0$, $7! = 1.0, 72 = 5.0$, $A2 = 0$. We first assume that the incoherent pumping A is absent *(i.e.A = 0)*. We study the absorptive characteristic of the probe held acting on the transition $|1 >+* |3 >$, *Irn(pi3)* as a function of the detuning Aj in the presence of LFC and compare it with the case without LFC [Figure 3.6]. We use two different sets of the local field parameters, namely, $/?j = (3_2 - 6$ and 10. (All quantities are scaled relative to the spontaneous decay rate 7J). In the absence of LFC the usual Autler Townes splitting [14] in the absorption curve is observed. With LFC included asymmetric behavior of the Autler Townes doublet is seen. There is an overall shift, of the two peaks along with the narrowing of the peak on the positive side of the zero detuning and broadening of the peak on the negative side. The maximum value of the absorption on either side is however unaltered. This is in contrast to the behavior of the absorption characteristic of the pump field in Figure 3.4.

We next take the pumping parameter $A = 0.15$. The behavior of *lrn{p\^)* as a function of the detuning Ai for the case above in the absence of LFC (curve with closed circles) and in the presence of LFC (dashed and solid curves correspond to $f3\ = 02 - 6$ and 10 respectively) is depicted in Figure 3.7. As predicted in Ref. [16] with incoherent pumping present there is gain observed in the probe field. At $Ai = 0$, *Im(pi_3)* is -7.07×10^{-4}. With LFC present however there is an enhancement of gain. For the *(3's* value 10, maximum **gain in** the system is -8.58×10^{-4}. With larger values of LFC. more enhancement of gain is observed. For a value of $fii = (3_2 = 40$ enhancement factor of ~ 10 has been noted. These observations are in correspondence with the results in a recent computation [17] **where gain** of the order of 100 times that of the case without LFC has been observed for **very** large *fi's*. However it is not evident how to realize such large local field corrections.

The question which one might ask is whether the same sort of enhancement can be obtained by detuning the field G_2 on the transition $|1 >«+ |2 >$ by the same amount as
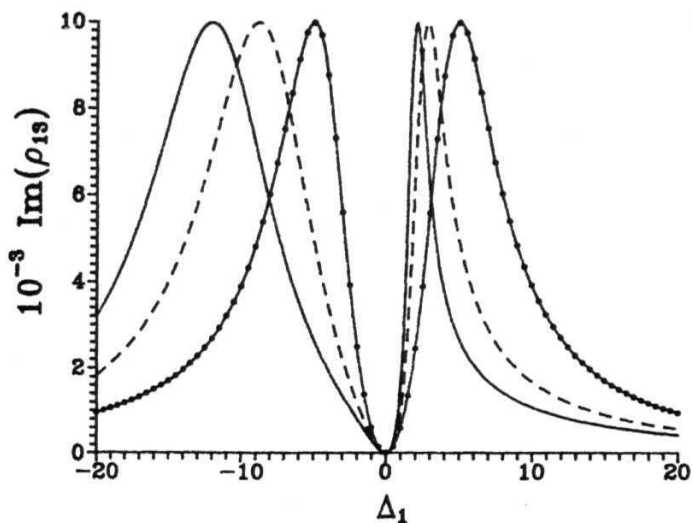
Fig. 3.6: The absorption /m(/9₁₃), of a weak probe in a dense medium as a function of the detuning Ai for parameters $G_x = 0.05$, $G_2 = 5.0$, 71 = 1.0, 72 = 5.0, A2 = 0 and A = 0. The curve with closed circles corresponds to the case without LFC; the dashed and solid curves correspond to (3\ = fa = 6.0 and 10.0.
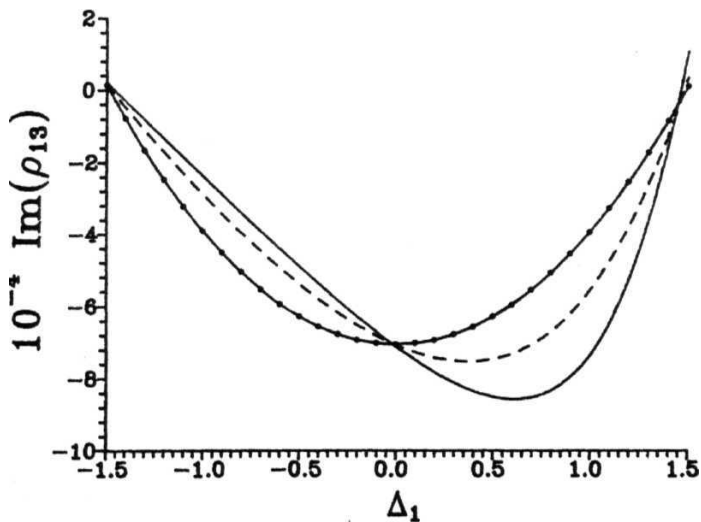

Fig. 3.7: The possibility of lasing without population inversion in a dense medium for parameters same as in Fig3'6 but with A = 0.15.

the detuning on the probe field at maximum gain point. For the above case when *fi's* are equal to 10 maximum gain occurs at Ai = 0.61. By setting A2 = 0.61 the response of the medium was studied but other than a shift in the gain profile there is no enhancement of gain in this situation.

These results indicate that the local field effect is not just a detuning effect but a more complex phenomenon. The complexity seems to arise from the nonlinear couplings involved. More detailed quantitative studies have to be performed to understand the phenomenon underlying the large enhancement of gain.

In conclusion in this chapter we have demonstrated how LFC affect the linear and nonlinear responses of the medium. We calculated the linear and third order susceptibilities of the medium. We have then illustrated how CPT persists undestroyed when local field effects are taken into account in the case of a dense medium of A systems. This behavior is consistent for all ranges of field strengths. In addition to the Lorentz shift in the steady state response we have demonstrated a novel dispersive behavior near the CPT condition for weak fields. A more complex behavior occurs for strong fields which need very large LFC to be present for any discernible change in the response of the medium. We also show that LFC shift the minimum of the sharp dip which was predicted in the previous chapter for unequal decay rates near the CPT condition, without destroying the CPT itself. We have also demonstrated that LFC lengthen the time scale over which evolution to CPT takes place. This is explained by the finiteness of the ground state coherence at times before the steady state. Larger LFC delay the formation of CPT more. Finally, we have demonstrated the enhancement in gain with the inclusion of LFC in a dense medium which exhibits lasing without inversion. We have also shown that the local field effect is not equivalent to a simple detuning effect. A microscopic study of the nonlinear phenomena involved is required to understand the origin of the large gain which should be the aim of future research work.

REFERENCES

1. **H. A.** Lorentz, *The Theory of electrons,* (Dover, New York, 2nd ed., 1952), sections 117-136; M. Born and E. Wolf, *Principles of Optics* 6th ed. (Pergamon, UK, 1980)

2. D. S. Chemla and D. A. B. Miller, Opt. Lett. 11, 522 (1988); K. C. Rustagi and C. Flytzanis, Opt. Lett. 9, 344 (1984).

3. F. A. Hopf, C. M. Bowden and W. H. Louisell, Phys. Rev. A **29,** 2591 (1984).

4. R. Friedberg, S. R. Hartmann and Jamal T. Manassah, Phys. Rev. **A40,** 2446 (1989); *ibid 42,* 494(1990).

5. A. S. Manka, J. P. Dowling and C. M. Bowden, Phys. Rev. Lett. 73, 1789 (1994).

6. J. P. Dowling and C. M. Bowden, Phys. Rev. Lett, **10,** 1421(1993). ,

7. K. Hakuta, L. Marmet, B. P. Stoicheff, Phys. Rev. Lett. 66, 596 (1991).

8. G. Alzetta, A. Gozzini, L. Moi and G. Orriols, Nuovo Cimento, **36B,** 5(1976); G. Alzetta and L. Moi, *ibid.* 52B, 209(1979) ;G. Orriols, Nuovo Cimento **53B,** 1(1979).

9. 0. A. Kocharovskaya, F. Mauri and E. Arimondo, Op. Commun. 84, 393 (1991); O. A.Kocharovskaya, Phys. Rep. **219,** 175 (1992).

10. M. Fleischhauer, C. H. Keital, M. O. Scully, C. Su, B. T. Ulrich and S. Y. Zhu Phys. Rev. A **46,** 1468 (1992).

11. D. Bedeaux and N. Bloembergen, Physica **69,** 57(1973).

12. V. Mizrahi and J. E. Sipe, Phys. Rev. B **34,** 3700 (1986).

13. J. J. Maki, M. S. Malcuit, J. E. Sipe and R. W. Boyd, Phys. **Rev. Lett. 67, 972** (1991).

14. S. H. Autler and C. H. Townes Phys. Rev. **100** 703(1955).

15. C. Cohen-Tannoudji and S. Reynaud, J. Phys. **10,** 345 (1977a); *ibidlO* **2311** (1977).

16. A. Imamoglu, J. E. Field and S. E. Harris, Phys. Rev. Lett. 66, 1154 (1991).

17. S.Singh, C. M. Bowden and J. Rai, to be published.

Chapter 4

PROBING ATOMIC STRUCTURE USING LASER TEMPORAL FLUCTUATIONS

The coherence minimum which occurs when the CPT conditions are satisfied can be utilized in spectroscopic studies. The absorption minimum or the dark resonance is a good indicator of the occurrence of a particular transition and hence a pinpointer to the presence of an atomic level. However CPT needs two laser fields to act simultaneously on adjacent transitions. One is the pump laser run at a fixed detuning from precise resonance and the other is the probe laser which is scanned across the transition. Keeping in view the experimental conditions, it would be advantageous to have a single field which can provide complete information of the atomic system under consideration. One such recent idea in which researchers have evinced interest is the use of laser temporal fluctuations in other words, noise, to probe atomic structure.

A lot of study of atomic interactions with noisy fields has been done in the past [1-5]. Renewed interest in noise spectroscopy has been stimulated by some recent work. Most of the earlier works dealt with stochastic (noisy) processes to either compare the behavior of atoms in fluctuating fields with that in monochromatic fields or to use the sensitivity of atomic response to fields with different statistics as an indicator of the field statistics itself as done by Zoller, Cooper and coworkers [3]. However in a recent paper Yabuzaki, Mitsui and Tanaka [6] demonstrated that stochastic fluctuations in the radiation from a diode laser can be used to derive spectroscopic data on an atom. These authors used

the technique on Cs transitions, where the intensity fluctuations on a diode laser beam transmitted through an atomic sample were spectrally analyzed to reveal the atomic level structure information. The method used appears to be an important spectroscopic technique, where the fluctuations in the radiation from a laser are utilized to get useful information. Related experiments have also been performed by McLean, Hannaford and Fairchild [7] to probe atmospheric oxygen, and by Mclntyre, et. al. [8], where the diode laser field, modeled as a phase-diffusing field, was used to probe rubidium. Diode lasers have large phase fluctuations but a stable amplitude. Hence the frequency fluctuates at random i. e. with a very short correlation time which results in a broad spectral line. The half - width being in tens of MHz but the wing extending upto several Ghz from the line center. There is sufficient spectral density in the tails of the spectrum to resonantly excite an atomic transition if the laser is tuned approximately in the vicinity of the atomic transition.

The fact that laser field fluctuations can be used for spectroscopy is quite contrary to the rather accepted notion that fluctuations should be avoided. Previous theoretical studies [4,5] to understand the issue of laser noise in spectroscopy have usually relied on the solution of some form of the optical Bloch equations with the noise incorporated into the equations. In this chapter we present a very simple but general theoretical framework for extracting spectroscopic data on an atom via stochastic probing with a fluctuating laser source.

Generally in light scattering experiments [9] the medium is fluctuating with the incident field being a coherent one. The output field is fluctuating as the medium is characterized by a fluctuating response. However in our case the incident field is fluctuating and the medium is characterized by the average response. In Section 4.1 we describe briefly the optical mixing techniques with an introduction to correlation functions. In Section 4.2 we introduce the general technique of extracting spectroscopic information

applicable to any atomic system and calculate the intensity-intensity correlation func-
tion and the power spectrum of the intensity-intensity correlations. In Section 4.3 we use
the three-level V-system to demonstrate how the spectroscopic information about atom-
ic transition frequencies is deduced from the power spectrum of the intensity-intensity
correlations.

4.1 Time Correlation Functions **and** Optical Mixing Techniques

Time correlation functions express the degree to which two dynamical properties are cor-
related over a period of time. If a property $A(t)$ fluctuates in time then the measurement
of the bulk property of the system is just the time average of the property given as

$$\bar{A}(t_0, T) = \frac{1}{T} \int_{t_0}^{t_0+T} A(t)dt \qquad (4.1)$$

where t_0 is the initial time of measurement and T is the interval over which the property
is averaged. A must be averaged over an infinite time T and if it is independent of the
initial time t_0, A is said to be a stationary property. Hence it can be expressed as

$$\langle A \rangle = \lim_{T \to \infty} \frac{1}{T} \int_{0}^{T} A(t)dt. \qquad \textbf{(4.2)}$$

The property A at two times t and $/ + r$ can have different values so that $A(t + r)$ ^
$A(t)$. However if r is small compared to the fluctuation period then $A(t + r)$ deviates from
$A(t)$. Then $A(t$ -f r) can be said to be correlated to $A(t)$ when r is small. A measure of
the correlation of the property of a medium at two different times is the auto-correlation
function of the property A defined as

$$\langle A(t)A(t + \tau) \rangle = \lim_{T \to \infty} \frac{1}{T} \int_{0}^{T} A(t)A(t + \tau)dt. \qquad \textbf{(4.3)}$$

For time-invariant random processes the correlation function (4.d) is independent of time
t i.e. $\langle A(t)A(t + \tau) \rangle = \langle A(0)A(\tau) \rangle$.

In most scattering experiments what is measured usually is the **spectral density or power spectrum** of the correlation function defined as

$$P_A(\omega) = \frac{1}{2\pi} \int_{-\infty}^{\infty} \langle A^*(t)A(t+\tau)\rangle e^{i\omega t} dt. \tag{4.4}$$

where A is the complex conjugate of A. The power spectrum and auto-correlation function are Fourier transforms of one another and experimental determination of one as a function of its arguments is sufficient for the determination of the other. The quantity $PA(U))CLJ$ is the amount of $|A|^2$ in the frequency interval $(\omega, \omega \pm d\omega)$.

The optical mixing techniques are the most common ways of study of correlation functions. Here the scattered light impinges directly on the photomultiplier tube. One of the methods is the heterodyne where the scattered light is mixed with a local oscillator **and** then impinged on the photomultipler. Another way is the homodyne method where the local oscillator is of the same frequency as the scattered beam (i.e. it is a small portion of the incident electric field). A schematic of the homodyne technique is shown in Figure 4.1.

In general homodyne and heterodyne experiments yield different information about the system. However under the Gaussian assumption where the property is a stochastic variable same information is found to be contained in both the experiments. A Gaussian stochastic variable is distributed according to a Gaussian distribution **which** is completely characterized by its first and second moments. All higher order moments **of this distribution** are factorizable into the first two moments. The Gaussian moment theorem is a consequence of this property. If $E(t)$ is a Gaussian variable then an example of the factorizabilty is

$$\langle E(t_1)E^*(t_2)E(t_3)E^*(t_4)\rangle = \langle E(t_1)E^*(t_2)\rangle\langle E(t_3)E^*(t_4)\rangle$$
$$+\langle E(t_1)E^*(t_4)\rangle\langle E(t_3)E^*(t_2)\rangle \tag{4.5}$$

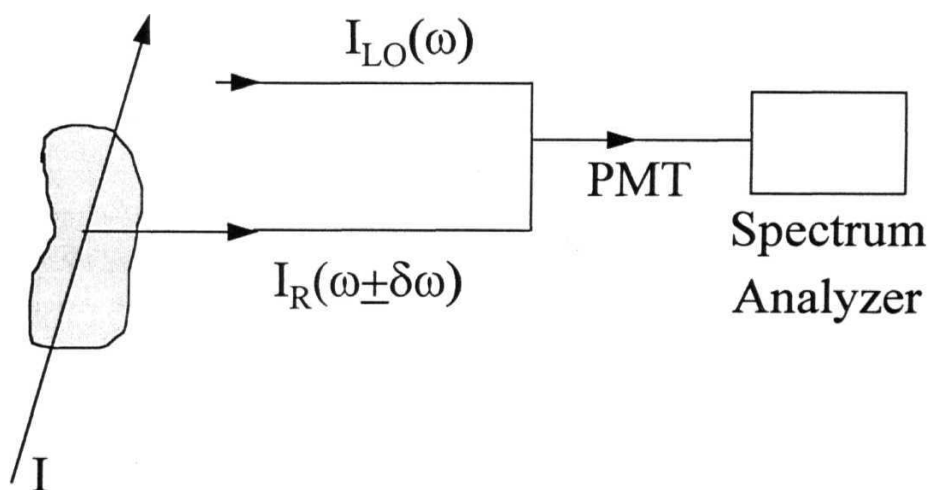provided that $\langle E(t_1)E(t_3)\rangle = 0$

Fig. 4.1: The Homodyne method of optical mixing. I_{L0C} and I_R are the local oscillator and the radiated beam intensities.

4.2 **The** Spectroscopic Technique

Consider a sample of an atomic medium irradiated by a field whose amplitude, phase, frequency or some combination of these fluctuate. Here we present a very simple and yet general enough argument to decode the spectroscopic information contained in the intensity-intensity correlations of the laser beam transmitted through the atomic sample. The fluctuating laser field produces a fluctuating polarization in the medium which we denote by P(r,a;). This induced polarization can be written as

$$\vec{P}(r,\omega) = \vec{\chi}(\omega).\vec{E}(r,\omega), \tag{4.6}$$

where x(<^) is the linear response of the medium at the applied frequency. We will assume that the incident field is weak so that it is sufficient to work with the results of the linear response theory. The induced polarization radiates a field which can be obtained from Maxwell's equations. In the far zone, this radiated field [10] is given by

$$\vec{E}_R(\vec{r},\omega) \sim -\frac{e^{i\frac{\omega}{c}r}}{r}\frac{\omega^2}{c^2}\vec{n} \times \vec{n} \times \int_V \vec{P}(r',\omega)e^{-i\frac{\omega}{c}\vec{n}.\vec{r}'}d^3r', \tag{4.7}$$

where *n* is the unit vector in the direction of observation, and the integral in Eq. (4.7) extends over the volume of the medium. On combining Eq. (4.6) and Eq. (4.7) we get,

$$\vec{E}_R(\vec{r},\omega) \sim -\frac{e^{i\frac{\omega}{c}r}}{r}\frac{\omega^2}{c^2}\vec{n} \times \vec{n} \times \vec{\chi}(\omega)\int_V \vec{E}(r',\omega)e^{-i\frac{\omega}{c}\vec{n}.\vec{r}'}d^3r', \tag{4.8}$$

which for a plane wave in the direction *q*

$$\vec{E}(\vec{r},\omega) = e^{i\frac{\omega}{c}\vec{q}.\vec{r}}\vec{E}(\omega), \tag{4.9}$$

becomes

$$\vec{E}_R(\vec{r},\omega) \sim -\frac{e^{i\frac{\omega}{c}r}}{r}V\frac{\omega^2}{c^2}\vec{n} \times \vec{n} \times \vec{\chi}(\omega).\vec{E}(\omega)\Delta_\omega(\vec{n},\vec{q}), \tag{4.10}$$

where

$$\Delta_\omega(\vec{n},\vec{q}) = \frac{1}{V}\int_V e^{i\frac{\omega}{c}(-\vec{n}+\vec{q}).\vec{r}}d^3r. \tag{4.11}$$

Thus, the positive frequency part of the radiated field at the frequency $u>$ can be written in the form

$$E_R(\omega) \sim f_\omega \chi(\omega) E(\omega), \tag{4.12}$$

where for simplicity we have dropped the tensor and vector character of $X(UJ)$ and E. The field E(t) is centered around the frequency ui with a slowly varying envelope $e(t)$. The radiated field is also expected to be a slowly varying function around the central frequency ui. We thus approximate Eq. (4,12) by

$$E_R(\omega' + \omega_L) \sim f_{\omega_L} \chi(\omega' + \omega_L) E(\omega' + \omega_L). \tag{4.13}$$

We rewrite Eq. (4.13) in terms of the Fourier transforms $e(iv)$ of the envelopes $e(t)$

$$\varepsilon_R(\omega') \sim f\chi(\omega' + \omega_L)\varepsilon(\omega'), \tag{4.14}$$

which when transformed to the time domain reads as $(\varepsilon(t) = \int_{-\infty}^{\infty} \varepsilon(\omega)e^{-i\omega t}d\omega)$

$$\varepsilon_R(t) \sim \frac{f}{2\pi} \int_{-\infty}^{\infty} X(t-t')\varepsilon(t')dt'. \tag{4.15}$$

Here X(t) is the Fourier transform of

$$\Psi(\omega') \equiv \chi(\omega' + \omega_L). \tag{4.16}$$

We next consider the detection of the radiated field by homodyning it **with the incident field.** The instantaneous intensity at the detector will be

$$\begin{aligned} I(t) &= |\varepsilon(t)e^{i\theta} + \varepsilon_R(t)|^2 \\ &= |\varepsilon(t)|^2 + \frac{f}{2\pi} \int_{-\infty}^{\infty} X(t-t')\varepsilon^*(t)\varepsilon(t')e^{-i\theta}dt' \end{aligned}$$

$$(4.17)$$

Here we have included an extra phase factor in the homodyning process. That is, a phase-shifter is introduced in one of the arms of the detection apparatus. This would enable us to discriminate between different contributions to the observed signal. Since the field $e(t)$ is fluctuating, the intensity becomes a stochastic variable. As discussed in Section 4.1 the quantity of interest is the intensity-intensity correlation which is obtained from the definition of correlation function as

$$C_I(\tau) = \langle I(t+\tau)I(t) \rangle. \tag{4.18}$$

The correlation $C_I(\tau)$ has the significant property of being real and even, i.e. $C_I^*(\tau) = C_I(\tau)$ and $C_I(-\tau) = C_I(\tau)$. Using Eq. (4.17) we get,

$$C_I(\tau) = \langle |\varepsilon(t)|^2 |\varepsilon(t+\tau)|^2 \rangle + C_L(\tau) + C_Q^{(1)}(\tau) + C_Q^{(2)}(\tau) + \ldots \tag{4.19}$$

where,

$$
\begin{aligned}
C_L(\tau) &= \langle |\varepsilon(t)|^2 \{ \int_{-\infty}^{\infty} \frac{f}{2\pi} X(t+\tau-t')\varepsilon^*(t+\tau)\varepsilon(t')e^{-i\theta}dt' \\
&\quad + \int_{-\infty}^{\infty} \frac{f^*}{2\pi} X^*(t+\tau-t'')\varepsilon(t+\tau)\varepsilon^*(t'')e^{i\theta}dt'' \} \rangle \\
&\quad + \text{terms with } t \text{ and } (t+\tau) \text{ interchanged,} \tag{4.20}
\end{aligned}
$$

$$
\begin{aligned}
C_Q^{(1)}(\tau) &= \int_{-\infty}^{\infty} \int_{-\infty}^{\infty} \frac{f^2}{4\pi^2} \langle \varepsilon^*(t+\tau)\varepsilon^*(t)X(t-t')X(t+\tau-t'')\varepsilon(t')\varepsilon(t'') \rangle e^{-2i\theta}dt'dt'' \\
&\quad + \int_{-\infty}^{\infty} \int_{-\infty}^{\infty} \frac{|f|^2}{4\pi^2} \langle \varepsilon^*(t'')\varepsilon^*(t)X(t-t')X^*(t+\tau-t'')\varepsilon(t')\varepsilon(t+\tau) \rangle dt'dt'' \\
&\quad + \text{ c. c,} \tag{4.21}
\end{aligned}
$$

and,

$$C_Q^{(2)}(\tau) = \langle |\varepsilon(t)|^2 |\varepsilon_R(t+\tau)|^2 \rangle + \langle |\varepsilon(t+\tau)|^2 |\varepsilon_R(t)|^2 \rangle. \tag{4.22}$$

Here *CL* and *CQ* are respectively linear and quadratic in the scattered field. The dots in Eq. (4.19) give terms of higher order in the scattered field. We will ignore such higher order contributions. Note that by choosing $0 = 0$ and x [relative to the phase of /] and by adding or subtracting the two measurements, we can study separately the linear and quadratic terms. This is reminiscent of what one does in the context of balanced detection [11]. Thus in what follows we will study the behavior of linear and quadratic terms separately. Since the two contributions are studied separately we drop the scale factor.

The power spectrum of the intensity-intensity correlations is defined from Eq.(4.4) as

$$P(\omega) = \frac{1}{2\pi} \int_{-\infty}^{\infty} C_I(\tau) e^{i\omega\tau} d\tau. \tag{4.23}$$

Replacing r by — r in Eq. (4.23) and using the evenness of *CJ(T)* we get

$$P(\omega) = \frac{1}{2\pi} \int_{-\infty}^{\infty} C_I(\tau) e^{-i\omega\tau} d\tau. \tag{4.24}$$

From Eq. (4.23) and Eq. (4.24), it's evident that

$$P(\omega) = \frac{1}{2\pi} \int_{-\infty}^{\infty} C_I(\tau) Cos(\omega\tau) d\tau. \tag{4.25}$$

To simplify Eq. (4.19) we adopt a simple model for the amplitude *e(t)* and assume that it is a Gaussian stochastic process. Needless to say, other models of stochastic noise can also be dealt with, within the framework described here. In what follows we will drop from the spectrum the dc terms along with the peak at $u = 0$. We first analyze the linear terms *CL(T)*- Using the moment theorem for Gaussian random processes Explained by Eq.(4.5), Eq.(4.20) reduces to

$$C_L(\tau) = \frac{1}{2\pi} \int_{-\infty}^{\infty} \langle |\varepsilon(t)|^2 \rangle \langle \varepsilon^*(t+\tau)\varepsilon(t') \rangle X(t+\tau-t') e^{-i\theta} dt' +$$

$$\frac{1}{2\pi} \int_{-\infty}^{\infty} \langle \varepsilon(t)\varepsilon^*(t+\tau) \rangle \langle \varepsilon^*(t)\varepsilon(t') \rangle X(t+\tau-t')e^{-i\theta}dt'$$

$$+c.c + \text{terms with } t \text{ and } (t+\tau) \text{ interchanged.} \qquad (4.26)$$

Note that the first term in Eq. (4.26) corresponds to the dc term[12] and can be dropped. We next introduce the second order correlation function F(r) for the field and its fourier transform,

$$\Gamma(\tau) = \langle \varepsilon^*(t)\varepsilon(t+\tau) \rangle, \qquad (4.27)$$

and

$$\Gamma(\omega) = \frac{1}{2\pi} \int_{-\infty}^{\infty} \Gamma(\tau)e^{i\omega\tau}d\tau, \qquad (4.28)$$

as well as the fourier transform of X(t)

$$X(t) = \int_{-\infty}^{\infty} \Psi(\omega)e^{-i\omega t}d\omega. \qquad (4.29)$$

Using Eq.(4.27), Eq. (4.26) reduces to

$$C_L(\tau) = \frac{1}{2\pi} \int_{-\infty}^{\infty} \Gamma(t-(t+\tau))\Gamma(t-t')X(t+\tau-t')e^{-i\theta}dt'$$

$$+c.c + \text{terms with } t \text{ and } (t+\tau) \text{ interchanged.}$$

$$(4.30)$$

On substituting Eq.(4.29) in Eq. (4.30) and using Eqs. (4.25) and (4.28), algebraic calculations lead to the following contribution to the spectrum

$$P_L(\omega) = 2 \int_{-\infty}^{\infty} \Gamma(\omega')\{\Gamma(\omega'+\omega) + \Gamma(\omega'-\omega)\} Re[\Psi(\omega')]d\omega'. \qquad 4.31$$

We next simplify the quadratic contributions to $P(\omega)$. We examine the two quadratic contributions separately. On using the moment theorem $C_Q^{(1)}(\tau)$ can be written as

$$C_Q^{(1)}(\tau) = \frac{1}{4\pi^2} \int_{-\infty}^{\infty}\int_{-\infty}^{\infty} \Gamma(-t'-\tau)\Gamma(\tau-t'')X(t')X(t'')dt'dt'' +$$

$$\frac{1}{4\pi^2} \int_{-\infty}^{\infty}\int_{-\infty}^{\infty} \Gamma(-t'-\tau+t'')\Gamma(\tau)X(t')X^*(t'')dt'dt'' + c.c. \qquad (4.32)$$

which on using Eqs. (4.28) and (4.29) simplifies to

$$
\begin{aligned}
C_Q^{(1)}(\tau) &= \int_{-\infty}^{\infty}\int_{-\infty}^{\infty} \Psi(\omega')\Psi(\omega'')\Gamma(\omega')\Gamma(\omega'')e^{i(\omega'-\omega'')\tau}d\omega'd\omega'' + \\
&\quad \int_{-\infty}^{\infty}\int_{-\infty}^{\infty} |\Psi(\omega')|^2\Gamma(\omega')\Gamma(\omega'')e^{i(\omega'-\omega'')\tau}d\omega'd\omega'' + c.c.
\end{aligned} \tag{4.33}
$$

Assuming that *T(LJ)* is real and using the real nature of C//(r) we can write Eq. (4.33) as

$$
\begin{aligned}
C_Q^{(1)}(\tau) &= \{\int_{-\infty}^{\infty}\int_{-\infty}^{\infty} \Psi(\omega')\Psi(\omega'')\Gamma(\omega')\Gamma(\omega'')Cos(\omega'-\omega'')\tau d\omega'd\omega'' + c.c\} \\
&\quad + 2\int_{-\infty}^{\infty}\int_{-\infty}^{\infty} |\Psi(\omega')|^2\Gamma(\omega')\Gamma(\omega'')Cos(\omega'-\omega'')\tau d\omega'd\omega''.
\end{aligned} \tag{4.34}
$$

Using the relation, $\int_{-\infty}^{\infty} Cos(\omega'-\omega'')\tau Cos(\omega\tau)d\tau = \pi[\delta(\omega'-\omega''+\omega) + \delta(\omega'-\omega''-\omega)]$, and substituting for $C_Q^{(1)}(\tau)$ from Eq. (4.34) into Eq. (4.25), we get

$$
\begin{aligned}
P_Q^{(1)}(\omega) &= \{\frac{1}{2}\int_{-\infty}^{\infty} \Psi(\omega')\Psi(\omega'+\omega)\Gamma(\omega')\Gamma(\omega'+\omega)d\omega' + \\
&\quad \frac{1}{2}\int_{-\infty}^{\infty} \Psi(\omega')\Psi(\omega'-\omega)\Gamma(\omega')\Gamma(\omega'-\omega)d\omega' + c.c\} + \\
&\quad \int_{-\infty}^{\infty} |\Psi(\omega')|^2\Gamma(\omega')\{\Gamma(\omega'+\omega) + \Gamma(\omega'-\omega)\}d\omega'.
\end{aligned} \tag{4.35}
$$

The calculation of the contribution $P_Q^{(2)}(\omega)$ proceeds along similar lines and we quote the final result,

$$
\begin{aligned}
P_Q^{(2)}(\omega) &= \int_{-\infty}^{\infty} \Gamma(\omega'+\omega)\Gamma(\omega')\Psi^*(\omega'+\omega)\Psi(\omega')d\omega' + \\
&\quad \int_{-\infty}^{\infty} \Gamma(\omega'-\omega)\Gamma(\omega')\Psi^*(\omega'-\omega)\Psi(\omega')d\omega'.
\end{aligned} \tag{4.36}
$$

The complete quadratic contribution is obtained by adding (4.35) and (4.36). The information coded in Eqs. (4.31), (4.35) and (4.36) has to be understood next.

4.3 Derivation of Spectroscopic Information of a V-System

We consider the simple V-system shown in Figure 4.2, i.e. a three-level **atom with** ground state |3) and two closely spaced excited levels |1) and |2). The spontaneous decay rates from |1) —• |3) and |2) -+ |3) are denoted by 2713 and 2723 respectively. A fluctuating driving field centered at frequency $U>L$ drives the atom and couples the two transitions |1) •-• |3) and |2) ⇔ |3). The total Hamiltonian of the system is written as

$$H = \hbar\omega_{13}|1\rangle\langle 1| + \hbar\omega_{23}|2\rangle\langle 2| - \hbar G_1 \exp\left(-i\omega_L t\right)|1\rangle\langle 3|$$

$$-\hbar G_2 \exp\left(-i\omega_L t\right)|2\rangle\langle 3| + h.c. \quad . \tag{4.37}$$

where $G_1 = \frac{\vec{d}_{13}\cdot\vec{E}_1}{\hbar}$ and $G_2 = \frac{\vec{d}_{23}\cdot\vec{E}_1}{\hbar}$ and $\vec{E}_1$ is the electric field amplitude.

The linear susceptibility is found using the density matrix formalism. As elucidated in Chapter 2 the evolution of the reduced density matrix, p for the atomic system is governed by the Liouville equation, modified to include the spontaneous decays. The equations of motion for the components of the density matrix in a frame rotating at the fast optical frequency w_i can be written as

$$\dot{\rho}_{11} = -2\gamma_{13}\rho_{11} + iG_1\rho_{31} + c.c,$$

$$\dot{\rho}_{12} = -[(\gamma_{13} + \gamma_{23}) + i(\omega_{13} - \omega_{23})]\rho_{12} + iG_1\rho_{32} - iG_2^*\rho_{13},$$

$$\dot{\rho}_{13} = -[\gamma_{13} + i(\omega_{13} - \omega_L)]\rho_{13} - iG_2\rho_{12} + iG_1(\rho_{33} - \rho_{11}),$$

$$\dot{\rho}_{22} = 2\gamma_{23}\rho_{22} + iG_2\rho_{32} + c.c.,$$

$$\dot{\rho}_{23} = -[\gamma_{23} + i(\omega_{23} - \omega_L)]\rho_{23} + iG_2(\rho_{33} - \rho_{22}) - iG_1^*\rho_{21} . \tag{4.38}$$

The linear susceptibility is obtained from optical coherence contributions **which are** first order in the field. The first order contribution to the coherence /)$_{13}$ is given by
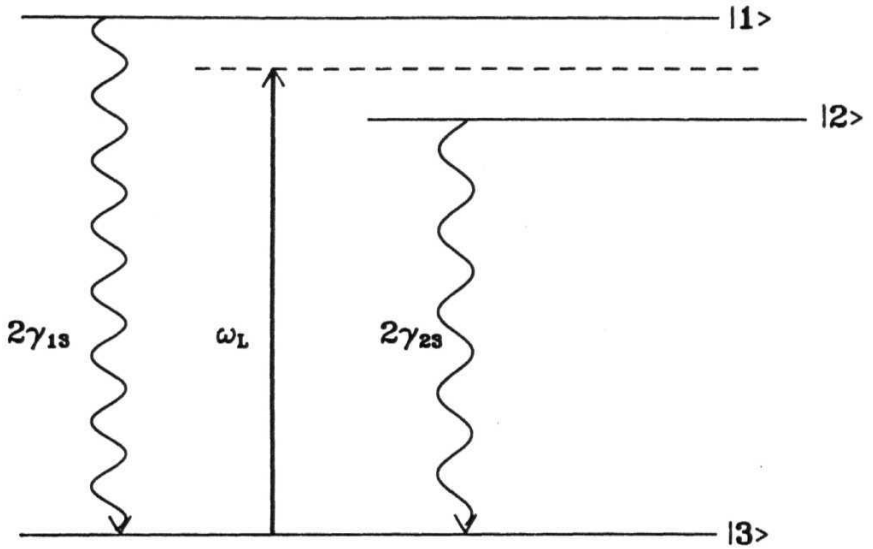
Fig. 4.2: Schematic representation of a three level V-system with ground state
|3⟩ and two excited states |1⟩ and |2⟩. The spontaneous decay rates from |1⟩
to |3⟩ and |2⟩ to |3⟩ are $2\gamma_{13}$ and $2\gamma_{23}$ respectively. The transition from |1⟩
to |2⟩ is not allowed. ω_L is the central frequency of the exciting field.

$$\rho_{13}^{(1)} = \frac{iG_1\rho_{33}^{(0)}}{\gamma_{13} + i(\omega_{13} - \omega_L)}. \tag{4.39}$$

Similarly

$$\rho_{23}^{(1)} = \frac{iG_1\rho_{33}^{(0)}}{\gamma_{23} + i(\omega_{23} - \omega_L)}. \tag{4.40}$$

Now $p\pounds = 1$. The total linear suceptibility is the sum of the susceptibilties corresponding to the two transitions. Hence using the relation in Eq. (4.16) the linear susceptibility of the atomic medium is found to be

$$\Psi(\omega) = [\frac{i\chi_1}{\gamma_{13} + i(\omega_{13} - \omega - \omega_L)} + \frac{i\chi_2}{\gamma_{23} + i(\omega_{23} - \omega - \omega_L)}]. \tag{4.41}$$

The constants x» ^{a}re related to the densities and oscillator strengths of the transitions. A Lorentzian profile centered at zero is chosen for the spectrum of the envelope, $\pounds(\pounds)$, of the exciting field, and is given by

$$\Gamma(\omega) = \frac{\gamma_c/\pi}{\gamma_c^2 + \omega^2}, \tag{4.42}$$

where 7_C is the spectral width of the incident beam.

   Substituting from Eq. (4.41) and Eq. (4.42) into Eqs (4.31),(4.35) and (4.36), *P(u)* is calculated analytically. A typical term involves calculation of an integral of the type

$$\int_{-\infty}^{\infty} [\; (\omega' + i\gamma_c)(\omega' - i\gamma_c)[\omega' - (-\omega - i\gamma_c)] \\ \times [\omega' - (-\omega + i\gamma_c)][\omega' - (\omega_{13} - \omega_L - i\gamma_{13})] \\ \times [\omega' - (\omega_{23} - \omega_L - \omega + i\gamma_{23})]]^{-1}d\omega', \tag{4.43}$$

which is evaluated using contour integration. The resulting analytical expressions representing various contributions to the power spectrum are

$$P_o(\omega) = \frac{2\gamma_c/\pi}{\omega^2 + 4\gamma_c^2}$$

$$
\begin{aligned}
P_L(\omega) \;=\;& \frac{4\gamma_C^2 i}{\pi}\,[2i\gamma_c\omega(\omega+2i\gamma_c)]^{-1}\,\{(\omega_A-i\gamma_c)\,[\omega_A-i(\gamma_c+\gamma_{13})]^{-1} \\
\times\;& [\omega_A-i(\gamma_c-\gamma_{13})]^{-1}+(\omega_B-i\gamma_c)\,[\omega_B-i(\gamma_c+\gamma_{23})]^{-1} \\
\times\;& [\omega_B-i(\gamma_c-\gamma_{23})]^{-1}\} \\
+\;& [2i\gamma_c\omega(\omega-2i\gamma_c)]^{-1}\,\big\{(\omega_A+\omega-i\gamma_c)\,[\omega+\omega_A-i(\gamma_c+\gamma_{13})]^{-1} \\
\times\;& [\omega+\omega_A-i(\gamma_c-\gamma_{13})]^{-1} \\
+\;& (\omega_B+\omega-i\gamma_c)\,[\omega+\omega_B-i(\gamma_c+\gamma_{23})]^{-1}\,[\omega+\omega_B-i(\gamma_c-\gamma_{23})]^{-1}\big\} \\
-\;& \frac{1}{2}\big\{[\omega_A+i(\gamma_c+\gamma_{13})]^{-1}\,[\omega_A-i(\gamma_c-\gamma_{13})]^{-1} \\
\times\;& [\omega+\omega_A+i(\gamma_c+i\gamma_{13})]^{-1}\,[\omega+\omega_A-i(\gamma_c-\gamma_{13})]^{-1} \\
+\;& [\omega_B+i(\gamma_c+\gamma_{23})]^{-1}\,[\omega_B-i(\gamma_c-\gamma_{23})]^{-1} \\
\times\;& [\omega+\omega_B+i(\gamma_c+\gamma_{23})]^{-1}\,[\omega+\omega_B-i(\gamma_c-\gamma_{23})]^{-1}\big\} \\
+\;& (\text{terms with } \omega \longrightarrow -\omega)\;.
\end{aligned}
$$

$$
\begin{aligned}
P_Q^{(1)}(\omega) \;=\;& \frac{2\gamma_c^2 i}{\pi}\,[2i\gamma_c\omega(\omega+2i\gamma_c)]^{-1}\,\big([\omega_A-i(\gamma_c+\gamma_{13})]^{-1} \\
+\;& [\omega_B-i(\gamma_c+\gamma_{23})]^{-1}\big)\,\big([\omega_A-i(\gamma_c-\gamma_{13})]^{-1} \\
+\;& [\omega_B-i(\gamma_c-\gamma_{23})]^{-1}\big)+[2i\gamma_c\omega(\omega-2i\gamma_c)]^{-1} \\
\times\;& \big([\omega+\omega_A-i(\gamma_c+\gamma_{13})]^{-1}+[\omega+\omega_B-i(\gamma_c+\gamma_{23})]^{-1}\big) \\
\times\;& \big([\omega+\omega_A-i(\gamma_c-\gamma_{13})]^{-1}+[\omega+\omega_B-i(\gamma_c-\gamma_{23})]^{-1}\big) \\
+\;& [\omega_A+i(\gamma_c+\gamma_{13})]^{-1}\,[\omega_A-i(\gamma_c-\gamma_{13})]^{-1} \\
\times\;& [\omega+\omega_A+i(\gamma_c+\gamma_{13})]^{-1}\,[\omega+\omega_A-i(\gamma_c-\gamma_{13})]^{-1} \\
\times\;& \big([2i\gamma_{13}]^{-1}+[\omega_A-\omega_B+i(\gamma_{23}+\gamma_{13})]^{-1}\big) \\
+\;& [\omega_B+i(\gamma_c+\gamma_{23})]^{-1}\,[\omega_B-i(\gamma_c-\gamma_{23})] \\
\times\;& [\omega+\omega_B+i(\gamma_c+\gamma_{23})]^{-1}\,[\omega+\omega_B-i(\gamma_c-\gamma_{23})]^{-1}
\end{aligned}
$$

$$\times \ \left([2i\gamma_{23}]^{-1} + [\omega_B - \omega_A + i(\gamma_{23} + \gamma_{13})]^{-1}\right) + \text{terms with } \omega \longrightarrow -\omega\bigg]$$

$$- \ \frac{4\gamma_c^2 i}{\pi} Re\bigg[[2i\gamma_c\omega(\omega + 2i\gamma_c)]^{-1}\left([\omega_A - i(\gamma_c + \gamma_{13})]^{-1}\right.$$

$$+ \ [\omega_B - i(\gamma_c + \gamma_{23})]^{-1}\Big)\left([\omega - \omega_A + i(\gamma_c + \gamma_{13})]^{-1}\right.$$

$$\times \ [\omega - \omega_B + i(\gamma_c + \gamma_{23})]^{-1}\Big) + \text{terms with } \omega \longrightarrow -\omega\bigg]$$

$$P_Q^{(2)}(\omega) \ = \ \frac{2\gamma_c^2 i}{\pi}\bigg[-[2i\gamma_c\omega(\omega + 2i\gamma_c)]^{-1}\left([\omega_A - i(\gamma_c + \gamma_{13})]^{-1}\right.$$

$$+ \ [\omega_B - i(\gamma_c + \gamma_{23})]^{-1}\Big)\left([\omega - \omega_A + i(\gamma_c - \gamma_{13})]^{-1}\right.$$

$$+ \ [\omega - \omega_B + i(\gamma_c - \gamma_{23})]^{-1}\Big) + [2i\gamma_c\omega(\omega - 2i\gamma_c)]^{-1}$$

$$\times \ \left([\omega_A - i(\gamma_c - \gamma_{13})]^{-1} + [\omega_B - i(\gamma_c - \gamma_{23})]^{-1}\right)$$

$$\times \ \left([\omega + \omega_A - i(\gamma_c + \gamma_{13})]^{-1} + [\omega + \omega_B - i(\gamma_c + \gamma_{23})]^{-1}\right)$$

$$+ \ [\omega - \omega_A - i(\gamma_c + \gamma_{13})]^{-1} \, [\omega - \omega_A + i(\gamma_c - \gamma_{13})]^{-1}$$

$$\times \ [\omega_A - i(\gamma_c - \gamma_{13})]^{-1} + [\omega_A + i(\gamma_c + \gamma_{13})]^{-1}$$

$$\times \ \left([-\omega + 2i\gamma_{13}]^{-1} + [\omega_A - \omega_B - \omega + i(\gamma_{23} + \gamma_{13})]^{-1}\right)$$

$$+ \ [\omega - \omega_B - i(\gamma_c + \gamma_{23})]^{-1} \, [\omega - \omega_B + i(\gamma_c - \gamma_{23})]^{-1}$$

$$\times \ [\omega_B - i(\gamma_c - \gamma_{23})]^{-1} \, [\omega_B + i(\gamma_c + \gamma_{23})]^{-1}$$

$$\times \ \left([-\omega + 2i\gamma_{23}]^{-1} + [\omega - \omega_A - \omega + i(\gamma_{23} + \gamma_{13})]^{-1}\right)\bigg]$$

where $\omega_A = \omega_{13} - \omega_L$, $\omega_B = \omega_{23} - \omega_L$ and $P_o(\omega)$ is the zeroth order contribution which can be dropped. The terms with difference of decays can be shown to cancel out in each contribution.

The numerical behavior of $P(u>)$ is studied as a function of frequency for different values of 7_C as shown in Figures 4.3 and 4.4. There are two peaks in the susceptibility behavior corresponding to the two transitions from |1) ⟺ |3) and |2) ⟷ |3) in the atom.
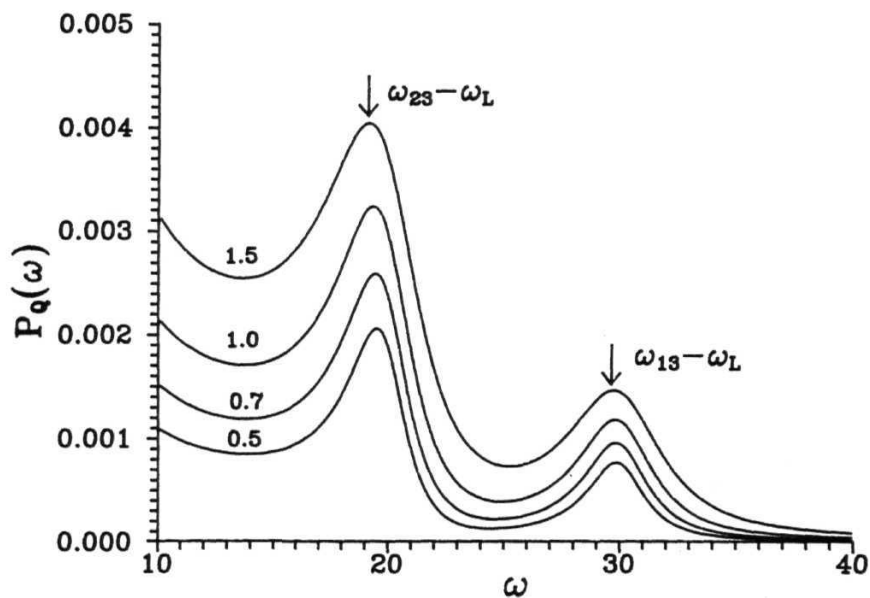
Fig. 4.3: The quadratic contribution $PQ(UJ)$ (in arbitrary units) to the power spectrum of the intensity - intensity correlations is plotted as a function of frequency, ω, for values of y_c of 0.5, 0.7, 1 and 1.5. The other parameters are xi = $X2$, $^13 - ^L = 30$ and $\omega_{23} — L = 20$. All frequencies and widths are in units of $713 = 723$.
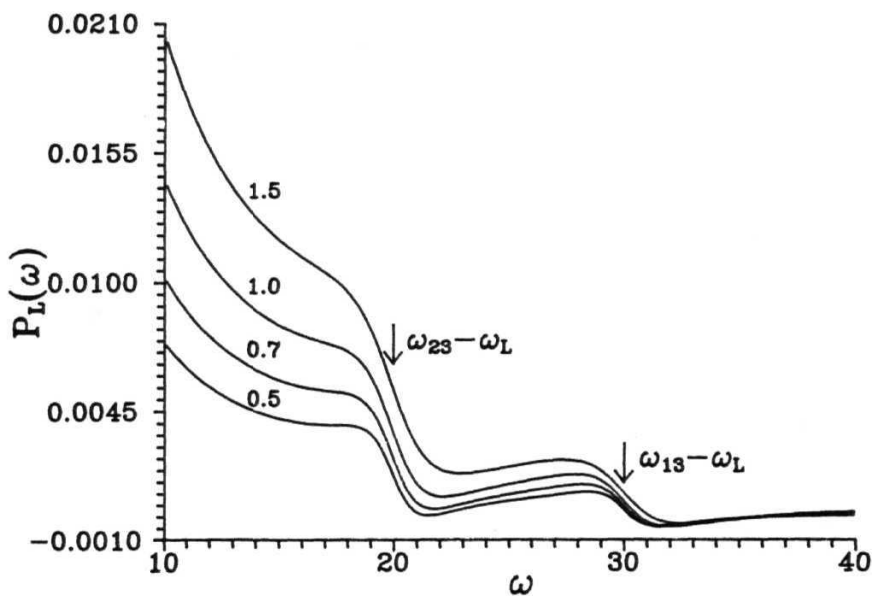
Fig. 4.4: The linear contribution $PL(U)$ to the power spectrum of the intensity - intensity correlations for the same parameters as in Fig.4.3.

Both these resonances are observed in P(u>), at *u> = U>\3-U>L* and *U>23-WL.* It should be noted that the resonances in the linear term *PL(U)* have dispersive character.

Hence, the intensity fluctuations provide spectroscopic information of the atomic system. We emphasize here that the merits of the arguments presented here are the simplicity of the approach and its general applicability. Our scheme exploits the fact that the linear susceptibility has all the atomic level information built into it, and that a single fluctuating laser source can be used to extract that information. The analysis presented here is extendable to other complicated atomic/molecular systems and shows that contrary to the usual belief, laser noise can be used for doing spectroscopy. Also related, earlier works [13] have utilized laser noise to determine atomic dephasing times in the context of four-wave mixing schemes.

Recently this work was extended to include additional aspects of diode laser based fluctuation spectroscopy. Vasavada, Vemuri and Agarwal [14] presented a general model where the diode laser radiation was treated as a phase - diffusing field and used Monte-Carlo methods in density matrix formalism for a wide range of field strengths and band widths. In addition to contributions to the signal that are linear and quadratic in the electric field the fourth order contribution was also analyzed. The homodyne method used in the work in this chapter could identify only the dipole-allowed transitions but not the dipole-forbidden. In this recent work a direct detection scheme was also adopted which displayed the crossover transitions too. The fourth order contributions are the ones measured in this direct detection.

As a conclusion, it should be emphasized that contrary to traditional belief that noise should be avoided, the present trend of research seems to pave the way to a novel **way** of utilizing noise for useful ends.

REFERENCES

1. G. S. Agarwal Phys. Rev. Lett. 37, 1383 (1976); J. H. Eberly, Phys. Rev. Lett. 37, 1387 (1976); H. J. Kimble and L. Mandel Phys. Rev. A 15, 689 (1977).

2. A. T. Georges, P. Lambropoulos and P. Zoller, Phys. Rev. Lett. 42, 1609 (1979); A. T. Georges Phys. Rev. A 21, 2034 (1980).

3. M. W. Hamilton, D. S. Elliott, S. J. Smith, M. Dziemballa and P. Zoller Phys. Rev. AS 36, 178 (1987); D. S. Elliott, M. W. Hamilton, K.Arnett and S. J. Smith, Phys. Rev. A 32, 887 (1985); Phys. Rev. Lett. 53, 439 (1984); M. H. Anderson, G. Vemuri, J. Cooper, P.Zoller and S. J. Smith, Phys. Rev. A 47, 3202 (11993).

4. Th. Haslwanter, H. Ritsch, J. Cooper and P. Zoller, Phys. Rev. A 38, 5652 (1988); H. Ritsch, P. Zoller and J. Cooper, Phys. Rev. A 41, 2653 (1990), R.Walser **and** P. Zoller, Phys. Rev. A 49, 5067(1994).

5. G. Vemuri and G. S. Agarwal, Phys. Rev. A 42, 1687 (1990); G. Vemuri Phys. Rev. A 48, 3256 (1993).

6. T. Yabuzaki, T. Mitsui and U. Tanaka, Phys. Rev. Lett. 67, 2453 (1991).

7. R.J. McLean, P. Hannaford and C.E. Fairchild, Opt. Lett. **18, 1675 (1993).**

8. **D.H.** Mclntyre, C.E. Fairchild, J. Cooper and R. Walser, Opt. Lett. 18, 1816 (1993).

9. B. Chu, *Laser light scattering,* (Academic, New York, 1974).

10. J. D. Jackson, *Classical Electrodynamics,* (Wiley, New York, 1975), 2nd ed., Chap. 9.

11. H. P. Yuen and W. S. Chan, Opt. Lett, g, 177 (1983).

12. For the phase diffusion model the linear contribution leads only to a dc term in *CI(T)* and thus carries no information.

13. G.S. Agarwal and C.V. Kunasz, Phys. Rev. **A37,** 996 (1983); G. Vemuri, G.S. Agarwal, R. Roy, M.H. Anderson, J. Cooper and S.J. Smith, Phys. Rev. **A44,** 6009 (1991).

14. K. V. Vasavada, G. Vemuri, G. S. Agarwal, to be published in Phys. Rev. A

Chapter 5

THE JAYNES-CUMMINGS MODEL WITH CONTINUOUS EXTERNAL PUMPING

In the standard JCM [1] the atom and the field in the cavity get so entangled as to form a single entity. This is revealed in the vacuum field Rabi splitting [2] which has been observed by Thompson et al [3]. An external probe is necessary to get information about the system in the cavity. One of the ways would be to use a strong laser pump externally which would drive the atom in the cavity. Alsing et al [4] studied the driven JCM and obtained the steady state solution of it where they investigate the effect of field strengths on the dynamic Stark splitting induced. They solved the eigenvalue problem and found the dressed states of the driven system. They studied two situations. In the first one, the external field pumps the cavity mode which corresponds to the experiment of Thompson et al. In the second situation the field drives the atom directly. In this chapter we study the dynamics of the latter system numerically and analytically illustrate the model's correspondence with the standard JCM where the coherent field enters via the initial conditions. Our model is a simple example of the two-channel JCM [5] with the external laser making the second channel between the two states of the atom.

In Section 5.1 we present a brief mathematical review of the standard JCM demonstrating the sinusoidal Rabi oscillations and the periodic collapse and revivals for different initial field states. In Section 5.2 we present the state vector approach to the JCM with

continuous pumping. Numerical results for various coherent **field amplitudes are** pre-
sented. Large coherent amplitudes are shown to demonstrate collapse and revivals as
in the standard JCM. In Section 5.3 the origin of this phenomenon is understood using
a simple analytic technique making use of unitary transformations. In Section 5.4 the
continuously pumped JCM is studied when the external field is detuned from the atom
and the cavity.

5.1 The Standard Jaynes - Cummings Model

The fully quantized model of a single atom interacting with a single cavity mode con-
stitutes the standard JCM. A lot of study has been done on this fundamental model in
radiation-matter interaction. For a detailed description of the JCM and its numerous
extensions see the reviews by Haroche and Raimond [6], Yoo and Eberly [7], Barnett et
al [8], Meystre and Sargent [9], Meystre [10] and Shore and Knight [11].

The interaction of a single atom of transition frequency u_o with a single mode of the
radiation field of frequency a; in a cavity in the dipole and rotating wave approximations
is described by the Jaynes-Cummings Model Hamiltonian [1]

$$H = \hbar\omega_o S^z + \hbar\omega b^\dagger b + \hbar g(S^+ b + S^- b^\dagger) \tag{5.1}$$

which is derived from the general Hamiltonian in Eq.(1.44) in the introductory Chapter
1. Here g is the strength of the coupling between the radiation mode and the atom,
which contains the transition dipole moment matrix element. Now S*, S* are the atomic
spin | operators and 6,6* are the bosonic ladder operators.

The interaction part of the Hamiltonian indicates the single photon processes that
the atom undergoes. The $S^+ b$ term describes the excitation of the atom from the ground
state to the excited state with the absorption of a photon from the cavity mode. The

$S''b$ term describes the de-excitation of the atom from excited state to the ground state with the emission of a photon into the cavity mode.

Let $|e\rangle$ and $|g\rangle$ be the eigenstates of the S^z operator with eigenvalues $\frac{1}{2}$ and $-\frac{1}{2}$ where $|e\rangle$ and $|g\rangle$ represent the excited and ground states of the atom. From the structure of the Hamiltonian we observe two conservation laws. One is

$$\langle S^z\rangle^2 + \langle S^x\rangle^2 + \langle S^y\rangle^2 = \frac{3}{4} \tag{5.2}$$

and another which conserves total excitation in the field-atom system

$$\langle S^z\rangle + \langle b^\dagger b\rangle = \text{ constant} . \tag{5.3}$$

The atomic state vector at time t is

$$|\psi_A(t)\rangle = C^e|e\rangle + C^g|g\rangle . \tag{5.4}$$

The field state vector at time t is expressed in terms of the complete set of Fock states as

$$|\psi_F(t)\rangle = \sum_{n=0}^{\infty} C_n|n\rangle . \tag{5.5}$$

The state vector for the system of atom and the field mode is a direct product of the atom and field state vectors and is given by

$$\begin{aligned}|\psi(t)\rangle &= |\psi_A(t)\rangle \otimes |\psi_F(t)\rangle \\ &= \sum_{n=o}^{\infty} C_n^e|n,e\rangle + C_n^g|n,g\rangle .\end{aligned} \tag{5.6}$$

In Eqs.(5.4), (5.5) and (5.6) C's are the complex amplitudes.

Due to the conservation laws (5.2) and (5.3) the JCM which is infinite dimensional reduces to a two dimensional problem. The Hamiltonian matrix has a block diagonal form consisting of many (2 x 2) matrices along the main diagonal. Hence there are an

infinite set of uncoupled two state Schrodinger equations, each pair identified by the number of photons in the ground state. For a fixed n the state vector is given by

$$|\psi(t)\rangle = C_n^e|n, e\rangle + C_{n+1}^g|n + 1, g\rangle \quad . \tag{5.7}$$

The Hamiltonian matrix for the pair of basis vectors is

$$\begin{pmatrix} (n + 1)\hbar\omega - \hbar\omega_o/2 & \hbar g\sqrt{n + 1} \\ \hbar g\sqrt{n + 1} & n\hbar\omega + \hbar\omega_o/2 \end{pmatrix} \quad . \tag{5.8}$$

From the diagonalization of H the whole dynamics of JCM is studied. The eigenvalues and eigenfunctions of H, given by $H|\psi_n^\pm\rangle = \hbar\omega_n^\pm|\psi_n^\pm\rangle$ are defined from

$$H|\psi_n^\pm\rangle = \left[\left(n + \frac{1}{2}\right)\hbar\omega \pm \frac{\hbar\Omega_{n\Delta}}{2}\right]|\psi_n^\pm\rangle \tag{5.9}$$

where

$$\Omega_{n\Delta}^2 = 4g^2(n + 1) + \Delta^2 \quad \text{and} \quad \Delta = \omega_o - \omega \quad . \tag{5.10}$$

and

$$|\psi_n^\pm\rangle = \begin{pmatrix} \cos\theta_n \\ -\sin\theta_n \end{pmatrix}|n + 1, g\rangle + \begin{pmatrix} \sin\theta_n \\ \cos\theta_n \end{pmatrix}|n, e\rangle \tag{5.11}$$

where $n = 0, 1, 2, \cdots$ and θ_n is defined from

$$\tan\theta_n = \frac{2g\sqrt{(n + 1)}}{(\Omega_{n\Delta} - \Delta)} \quad . \tag{5.12}$$

At exact resonance, when the transition frequency is equal to the frequency of the radiation mode, i.e., A = 0 and at $n = 0$, $H_nA = 2g$, the Rabi splitting frequency. Here $2g$ is called the single photon Rabi frequency and $Q_n\&$ is called the generalized Rabi frequency. The evolution operator is found to be

$$\exp[-\frac{iHt}{\hbar}] = \exp[-it\frac{(\omega - \omega_o)}{2}]|0, g\rangle\langle 0, g| + \sum_{n=0}^{\infty} \exp(-i\omega_n^+ t)|\psi_n^+\rangle\langle\psi_n^+|$$
$$+ \sum_{n=0}^{\infty} \exp(-i\omega_n^- t)|\psi_n^-\rangle\langle\psi_n^-| \quad . \tag{5-13}$$

If the atom is initially in the excited state and the radiation field is in the Fock state, with n photons then the state of the system at any time t is given by

$$|\psi(t)\rangle = \exp\left[-\frac{iHt}{\hbar}\right]|n, e\rangle$$
$$= A_{n,e}|n, e\rangle + B_{n,e}|n + 1, g\rangle \tag{5.14}$$

where

$$A_{n,e} = \sin^2\theta_n \exp\left(-i\omega_n^+ t\right) + \cos^2\theta_n \exp\left(-i\omega_n^- t\right)$$
$$B_{n,e} = \cos\theta_n \sin\theta_n[\exp\left(-i\omega_n^+ t\right) - \exp\left(-i\omega_n^- t\right)] \ . \tag{5.15}$$

The probability that the atom emits a photon into the cavity mode and goes to the ground state is

$$P_g(t) = P_{n,e} \rightarrow P_{n+1,g} = \frac{4g^2(n+1)}{\Omega_{n,\Delta}^2}\sin^2\frac{\Omega_{n,\Delta}t}{2} \ .$$

Eq.(5.16) predicts sinusoidal Rabi oscillations much like the classical case. However, even when the field is initially in vacuum state, i.e., $n = 0$, the probability exists. This is a purely quantum feature of periodic reversible spontaneous emission. (Probability would be zero for zero classical field amplitude). The vacuum fluctuations stimulate spontaneous emission from the atom which is followed by reabsorption and so on.

If the radiation mode is intially in a coherent state the inversion of the atom is given **by**

$$\langle S^z \rangle = \sum_{n=0}^{\infty} \frac{e^{(-\bar{n}^n)}\bar{n}^n}{n!}\cos 2g\sqrt{n}t \ . \tag{5.17}$$

Numerical evaluation of the infinite sum leads to the collapse and revival phenomena. If **the** atom is in the ground state and the field is coherent initially, then the expectation **value** of the energy of the atom oscillates sinusoidally initially and **then decays rapidly** to a constant value even though the Hamiltonian describing the system is **Hermitian (no damping).** Following the decay are periodic revivals to large amplitudes on a much

larger time scale. On a still larger time scale neighbouring revivals begin to overlap **and** the regions of overlap gradually include more distant revivals causing the envelope of atomic inversion signal to appear irregular and noisy. Narozhny et al [12,13] gave analytic formulas for the collapse function, the revival period and the amplitude of the revival envelope. Recently with the success of the one-atom maser the collapse and revival phenomenon has been observed [14].

5.2   The Jaynes - **Cummings Model with Continuous Pumping**

In this model in addition to the atom interacting with a single cavity mode, it is driven continuously by an external field of frequency $U>L$ as shown in Figure 5.1. There are two processes connecting the two states of the atom. One is the single photon process occurring due to the interaction with the cavity mode. The other is the direct coherent excitation by the external field. The total Hamiltonian for this system can be written as

$$H = hu>_o S^z \text{ -f } hutfb + hg(S^+ b + S \sim tf) + ha(S^+ \exp(-iu>_L t) \text{ -f } S \sim \exp(iu>_L t)) \quad . \quad (5.18)$$

where a is the Rabi frequency of the external pumping field and g is the single photon Rabi frequency.

Let $|<t>)$ be the state of the system at time t. The dynamics of the system is governed by the Schrodinger equation

$$i\hbar \frac{\partial |\phi\rangle}{\partial t} = H|\phi\rangle \tag{5.19}$$

To get rid of the optical frequency in the Hamiltonian in Eq.(5.18) we go to a frame rotating with the frequency $U>L$ by the unitary transformation.

$$|\psi\rangle = U^\dagger |\phi\rangle \quad , \tag{5.20}$$

where

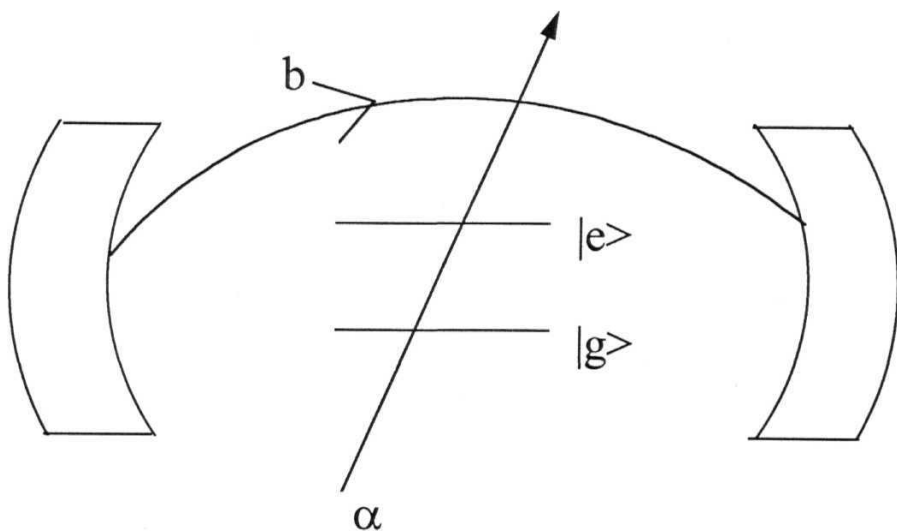$$U^\dagger = \exp(i\omega_L(S^z + b^\dagger b)t) \quad . \tag{5.21}$$

Fig. 5.1: A two-level atom in a cavity which supports a quantized mode 6, as welj as being pumped by an external field a.

Differentiating Eq.(5.20) w.r.t. time we get

$$\frac{\partial|\psi\rangle}{\partial t} = \frac{\partial U^\dagger}{\partial t}|\phi> +U^\dagger\frac{\partial|\phi\rangle}{\partial t} \quad . \tag{5.22}$$

Using Eqs. (5.19) and (5.21) in above equation

$$\frac{\partial|\psi\rangle}{\partial t} = i\omega_L(S^z + b^\dagger b)U^\dagger|\phi\rangle - \frac{iU^\dagger H|\phi\rangle}{\hbar} \quad . \tag{5.23}$$

Using the unitarity property $UW = 1$ in Eq. (5.23),

$$\frac{\partial|\psi\rangle}{\partial t} = i\omega_L(S^z + b^\dagger b)|\psi\rangle - \frac{iU^\dagger HU}{\hbar}|\psi\rangle \quad . \tag{5.24}$$

The second term in Eq.(5.24) is evaluated as follows.

$$
\begin{aligned}
U^\dagger HU &= \hbar\omega_o S^z + \hbar\omega b^\dagger b + \exp\left(i\omega_L(S^z + b^\dagger b)t\right)\\
&\quad \times \left[\hbar g(S^+ b + S^- b^\dagger) + \hbar\alpha(S^+ \exp\left(-i\omega_L t\right) + S^- \exp\left(i\omega_L t\right))\right]\\
&\quad \times \exp\left(-i\omega_L(S^z + b^\dagger b)t\right) \quad .
\end{aligned}
\tag{5.25}
$$

Using the bosonic and atomic commutation relations Eq.(5.25) reduces to

$$U^\dagger HU = \hbar\omega_o S^z + \hbar\omega b^\dagger b + \hbar g[S^+ b + S^- b^\dagger] + \hbar\alpha[S^+ + S^-]. \tag{5.26}$$

Substituting (5.26) in Eq.(5.24) Schrodinger equation in the rotating frame is obtained as

$$i\hbar\frac{\partial|\psi\rangle}{\partial t} = \mathcal{H}|\psi\rangle \tag{5.27}$$

where the effective Hamiltonian in the rotating frame is given by

$$\mathcal{H} = \hbar(\omega_o - \omega_L)S^z + \hbar(\omega - \omega_L)b^\dagger b + 2\hbar\alpha S^x + g\hbar(S^+ b + S^- b^\dagger). \tag{5.28}$$

In order to understand the basic features of the JCM with continuous pumping, we first consider the case of exact resonance $u_o = u > i = u$. The Hamiltonian (5.28) reduces to

$$\mathcal{H} = 2\hbar\alpha S^x + g\hbar(S^+ b + S^- b^\dagger). \tag{5.29}$$

Because of the structure of the term corresponding to the coherent pump it is useful to work in a representation in which S^x is diagonal. Let $|\pm)$ be the eigenstates of the S^x operator with eigenvalues $\pm\rangle$. The two sets of eigenstates are related by

$$|+\rangle = \frac{|e\rangle + |g\rangle}{\sqrt{2}} , \; |-\rangle = \frac{|e\rangle - |g\rangle}{\sqrt{2}}; \; S^x|\pm\rangle = \pm\frac{1}{2}|\pm\rangle. \tag{5.30}$$

The state vector at time t can be expressed in terms of the complete set of states as

$$|\psi(t)\rangle = \sum_{n=0}^{\infty} C_n^-|-,n\rangle + \sum_{n=0}^{\infty} C_n^+|+,n\rangle \tag{5.31}$$

where C's are the complex amplitudes. Using the Schrodinger equation in (5.27),

$$i\left[\sum_{n=0}^{\infty} \dot{C}_n^-|-,n\rangle + \sum_{n=0}^{\infty} \dot{C}_n^+|+,n\rangle\right] = -\alpha\left[\sum_{n=0}^{\infty} C_n^-|-,n\rangle - \sum_{n=0}^{\infty} C_n^+|+,n\rangle\right]$$
$$- \frac{g}{2}\left[\sum_{n=0}^{\infty} C_n^- \sqrt{n} - \sum_{n=0}^{\infty} C_n^+ \sqrt{n}\right][|-,n-1\rangle + |+,n-1\rangle]$$
$$- \frac{g}{2}\left[\sum_{n=0}^{\infty} C_n^- \sqrt{n+1} + \sum_{n=0}^{\infty} C_n^+ \sqrt{n+1}\right][|-,n+1\rangle - |+,n+1\rangle]$$
$$\tag{5.32}$$

Taking the scalar product with $(-,p|$ and $(+,p|$ on both sides Eq. (5.32), the equation of motion for the coefficients C's are found to be

$$i\dot{C}_p^- = -\alpha C_p^- - \frac{g}{2}(C_{p-1}^- + C_{p-1}^+)\sqrt{p} + \frac{g}{2}(C_{p+1}^+ - C_{p+1}^-)\sqrt{p+1}$$
$$i\dot{C}_p^+ = \alpha C_p^+ + \frac{g}{2}(C_{p-1}^- + C_{p-1}^+)\sqrt{p} + \frac{g}{2}(C_{p+1}^+ - C_{p+1}^-)\sqrt{p+1} \tag{5.33}$$

where $p = 0,1,2, \bullet \bullet \bullet \, \infty$.

Unlike the standard JCM where the cavity mode is prepared in a coherent state initially, in our model we assume the cavity field to be in vacuum. The atom is assumed to be in the ground state $|2\rangle$. The initial values of the C's are deduced as follows:

Initially, at time $t = 0$ the state of the system is

$$|\psi(0)\rangle = C_o^-|-,0\rangle + C_o^+|+,0\rangle \; . \tag{5.34}$$

The probability of the system to be in the ground state $|2,0\rangle$ initially is equal to 1. Taking scalar product $\langle 2,0|$ on both sides of Eq.(5.34),

$$Ct - C; = \sqrt{2} \quad . \tag{5.35}$$

Similarly from the stipulation that probability of the system to be in the excited state initially is zero, we get

$$C+ + C; = 0 \quad . \tag{5.36}$$

Solving the simultaneous equations (5.35) and (5.36) the initial conditions on C's are found to be $C^* = 4\text{-}$, $C\sim - -A^{\wedge}$ with all other C's zero. The coupled equations are solved using the Fehlberg's Runge Kutta method [15] for various values of the external field amplitudes, a, relative to the atom-field mode coupling.

The infinite number of photons present in the sum in Eq.(5.31) indicates that the convergence of the equations in (5.33) has to be tested for each a. Convergence is indicated by stable, unchanging values of the coefficients C's. The number of photons needed in the infinite sum in Eq.(5.31) for convergence is roughly estimated from the photon number distribution of the coherent external held. The coherent state has a Poissonian distribution with Poisson coefficients $^{\wedge}$—. For small n values a^n dominates over $\sqrt{n!}$, till the mean photon number $n = |a|^2$, where the distribution increases to a maximum. After the mean photon number is reached, the factorial in the denominator starts influencing the coefficient $-j\sim$ and the distribution falls off till any increase in n does not influence it. The photon number n around this point is the convergency limit. **For** example for $a = 3.0$, n is taken from 0 to $\sim 12 - 15$ for convergence.

We **study** the dynamics of the photon statistics of the cavity mode and the atomic excitation as in the standard JCM. We specifically present results for the evolution of the photon number (6t&) and the atomic population $P_c(t)$, *(the* probability that the atom is

in the excited state). In terms of the complex C's defined in Eq.(5.31) these are

$$\langle b^\dagger b \rangle = \sum_{n=o}^{\infty} n \left\{ \left| C_n^-(t) \right|^2 + \left| C_n^+(t) \right|^2 \right\}$$

$$P_e(t) = \frac{1}{2} \sum_{n=0}^{\infty} \left| C_n^+(t) + C_n^-(t) \right|^2 \quad . \tag{5.37}$$

The behavior of (bH) and $P_e(t)$ for the values $a = 1.0$ and $a = 3.0$ when $g = 1.0$ (this implies that time is scaled as gt) is shown in Figures. 5.2(a), (b) and 5.3(a), (b). For $a = 1.0$, there are no pronounced collapse and revivals. There are modulated sinusoidal oscillations. For the larger value of $a = 3.0$, $P_e(t)$ exhibits collapses and revivals like in the standard JCM where for increasing a the Rabi oscillations are affected by the Poisson distribution of photon numbers. Eventhough the cavity mode was initially in vacuum state, the atomic excitation probability exhibits the collapse and revival phenomena. The field mode initially with zero photons gains energy, becomes finite and oscillates with time even as the atom also exhibits modulated Rabi oscillations. The transfer of energy between the coherent laser field and the cavity mode is mediated by the atom due to simultaneous excitation pathways of the two fields. A pictorial comparison of the standard JCM with the JCM with external pumping is given in Figure 5.4. In the next section we explain the origin of such collapses and revivals in the continuously pumped model. Another interesting feature is that the number of photons in the cavity increases as the intensity of the pump increases.

Note that the usual JCM is characterized by the Hamiltonian H obtained from (5.29) by setting $a = 0$

$$\tilde{\mathcal{H}} = \hbar g (S^+ b + S^- b^\dagger). \tag{5.38}$$

The initial conditions are now different. The atom may be in any state but the field is say in a coherent state $| /?\rangle$. Thus the initial state for the atom-field system is

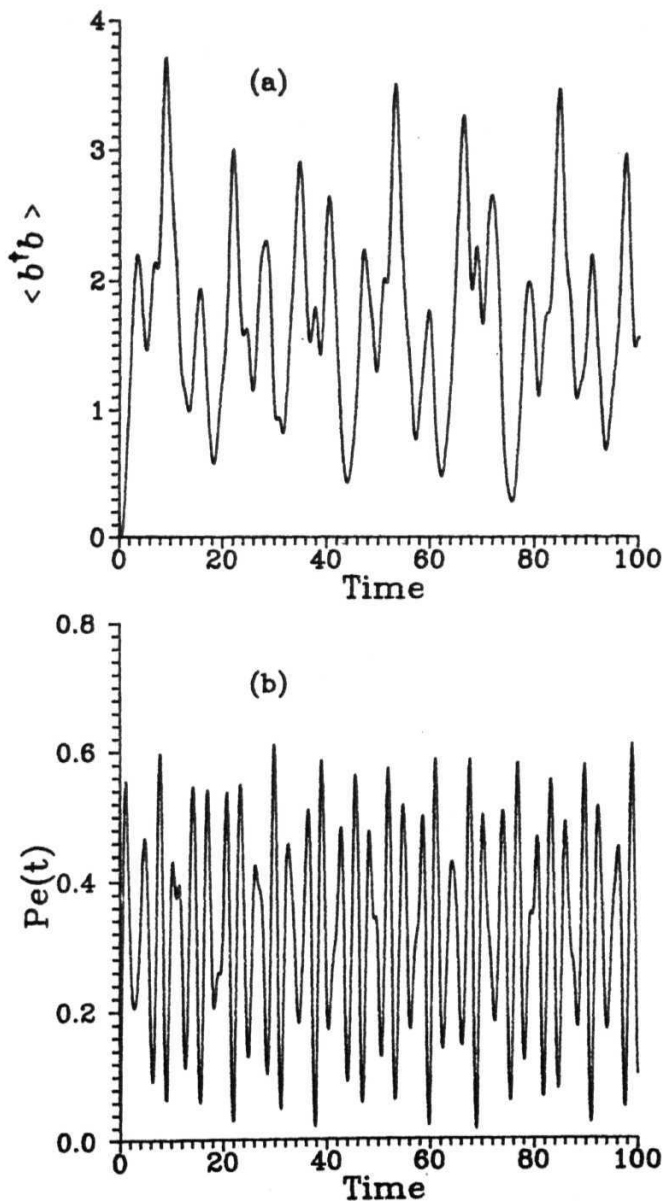$$|\psi(0)\rangle = |\psi_A(0)\rangle |\beta\rangle \tag{5.39}$$

Fig. 5.2: Dynamical results for the JCM with continuous pumping for a = 1.0
a) Mean number of photons in the cavity mode, *(bh)* as a function of time
b) $P_e(t)$ (Probability that the atom is in the excited state) as a function of
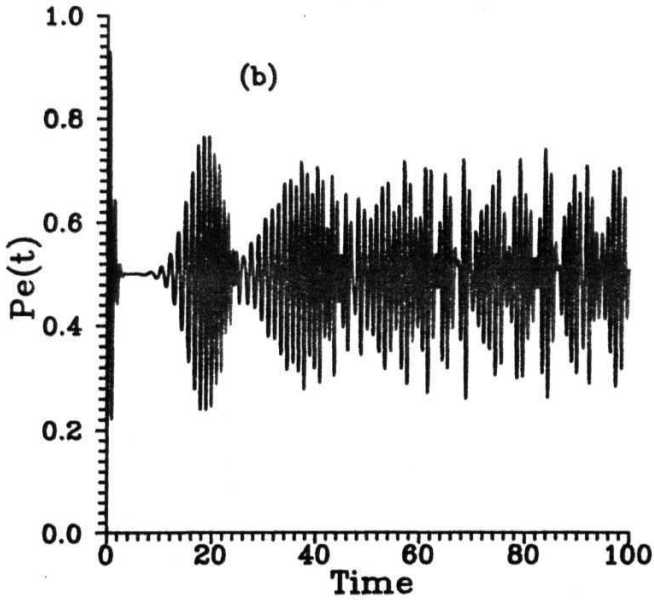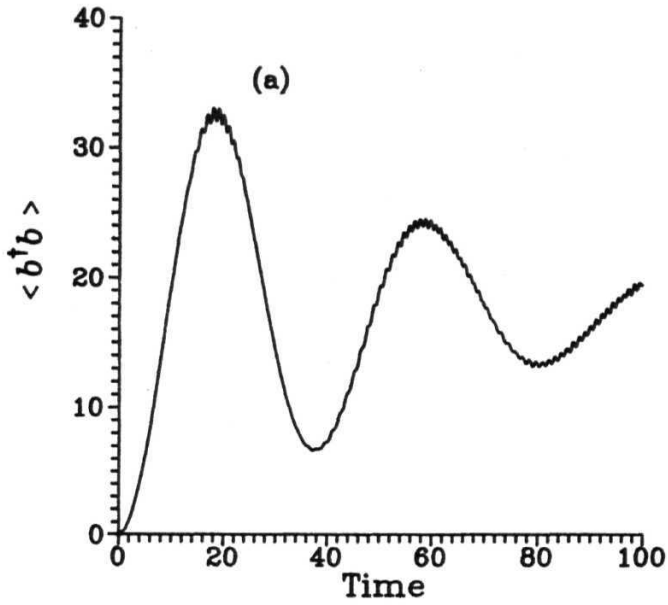a time.

Fig. 5.3: Dynamical results for the JCM with continuous pumping for a 3.0a)Same as in Fig. 5.2(a). b) Same as in Fig. 5.2(b).
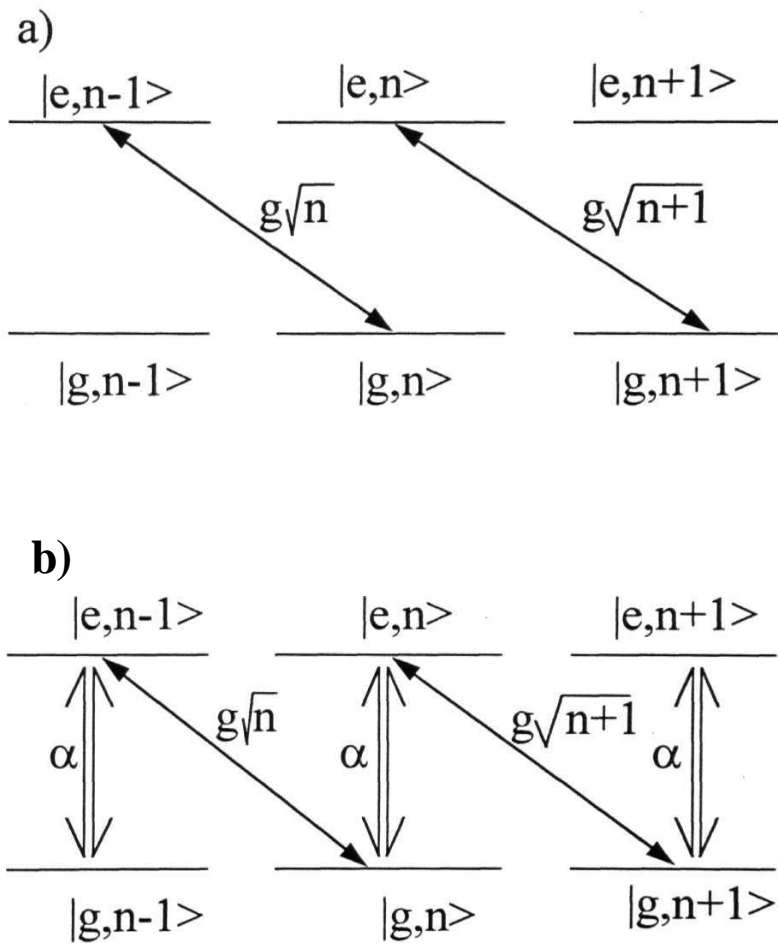
Fig. 5.4: The eigenstates of the standard JCM and the JCM with external pump-
ing are depicted in a) and b) respectively

and the time dependent wave function is

$$|\psi(t)\rangle = \exp\left(\frac{-it\tilde{\mathcal{H}}}{\hbar}\right)|\psi_A(0)\rangle|\beta\rangle. \tag{5.40}$$

5.3 Analytical Results

In this section we use unitary transformations to obtain some analytical results. We rewrite the Hamiltonian (5.29) in the form

$$\mathcal{H} = \hbar g\left[S^+\left(b + \frac{\alpha}{g}\right) + S^-\left(b^\dagger + \frac{\alpha^*}{g}\right)\right]. \tag{5.41}$$

Introducing the displacement operator $D(0)$ defined by $D\{0) = \exp(/96^f - /3*b)$, $D\sqrt{3})bD(j3) = 6 + /?$, the Hamiltonian (5.41) reduces to

$$\mathcal{H} = \hbar g D^\dagger(\beta)(S^+ b + S^- b^\dagger)D(\beta) \ , \quad \beta = \frac{\alpha}{a} \ . \tag{5.42}$$

The time evolution of the wave function is then given by

$$\begin{aligned}
|\psi(t)\rangle &= \exp\left(\frac{-i\mathcal{H}t}{\hbar}\right)|\psi(0)\rangle \\
&= \exp\left(\frac{-it}{\hbar}D^\dagger(\beta)\tilde{\mathcal{H}}D(\beta)\right)|\psi(0)\rangle
\end{aligned} \tag{5.43}$$

where we have used (5.38).

Expanding the exponential in (5.43) gives

$$|\psi(t)\rangle = \left[1 - \frac{it}{\hbar}D^\dagger(\beta)\tilde{\mathcal{H}}D(\beta) + \left(\frac{-it}{\hbar}\right)^2(D^\dagger(\beta)\tilde{\mathcal{H}}D(\beta))^2 + \cdots\right]|\psi(0)\rangle. \tag{5.44}$$

Using the unitary property of displacement operator i.e., $D^\dagger(\beta)D(\beta) = 1$, Eq.(5.44) becomes

$$|\psi(t)\rangle = D^\dagger(\beta)\left[1 - \frac{it}{\hbar}\tilde{\mathcal{H}} + \left(\frac{it}{\hbar}\right)^2\tilde{\mathcal{H}}^2 + \cdots\right]D(\beta)|\psi(0)\rangle \ . \tag{5.45}$$

Hence

$$|\psi(t)\rangle = D^\dagger(\beta)\exp\left(\frac{-it\tilde{\mathcal{H}}}{\hbar}\right)D(\beta)|\psi(0)\rangle \ . \tag{5.46}$$

We write the initial condition in the form

$$|\psi(0)\rangle = |\psi_A(0)\rangle|0\rangle \quad . \tag{5.47}$$

Here $|0\rangle$ is the vacuum state of the field and $|I/M(0)\rangle$ is the initial state of the atom. Note that the displacement operator acting on the vacuum yields the coherent state $|/?\rangle$ of the field i.e.,

$$D(\beta)|0\rangle = |\beta\rangle \quad . \tag{5.48}$$

Thus (5.46) becomes

$$|\psi(t)\rangle = D^\dagger(\beta)\exp\left(\frac{-it\tilde{\mathcal{H}}}{\hbar}\right)|\psi_A(0)\rangle|\beta\rangle \quad . \tag{5.49}$$

To understand the dynamics of the system we use the density operator formalism. The state vector in Eq.(5.49) completely describes the state of the system of the interacting atom and cavity mode. Such a state is called a pure state. The density operator, p, for such a pure state is defined as

$$/\!\!\ast = W\,)\,)\,W\,)\,I \quad \bullet \qquad - \tag{5-50}$$

Substituting the state vector from Eq.(5.49) the density operator of the coupled system of the atom and the radiation field is given by

$$\rho = D^\dagger(\beta)\exp\left(\frac{-it\mathcal{H}}{\hbar}\right)|\psi_A(0)\rangle|\beta\rangle\langle\beta|\langle\psi_A(0)|\exp\left(\frac{it\mathcal{H}}{\hbar}\right)D(\beta) \tag{5.51}$$

The reduced density matrix DA for the atom is obtained by taking a trace over the field variables as

$$\begin{aligned}
\rho_A(t) &= Tr_F D^\dagger(\beta)\exp\left(\frac{-it\tilde{\mathcal{H}}}{\hbar}\right)|\psi_A(0)\rangle|\beta\rangle\langle\beta|\langle\psi_A(0)|\exp\left(\frac{it\tilde{\mathcal{H}}}{\hbar}\right)D(\beta) \\
&= Tr_F \exp\left(\frac{-it\tilde{\mathcal{H}}}{\hbar}\right)|\psi_A(0)\rangle|\beta\rangle\langle\beta|\langle\psi_A(0)|\exp\left(\frac{it\tilde{\mathcal{H}}}{\hbar}\right) \quad . \tag{5.52}
\end{aligned}$$

In obtaining Eq.(5.52) we used the cyclic property of the trace which states that $Tr[ABC] = Tr[BCA]$ where A, B, C are represented as matrices in matrix notation and

the unitary property of displacement operator. Note that the right hand side of (5.52) is nothing but the solution (5.40) for the standard JCM. Thus we have shown that

$$p_A(t) = PA(t) \qquad . \qquad (5.53)$$

i.e., the dynamical properties of the atomic system for a continuously pumped JCM are identical to the dynamical properties of the atomic system for the standard JCM in which the coherent field appears in the initial conditions. This explicit connection explains the existence of the collapse and revival of the Rabi oscillations in Figure 5.3.

We next examine the reduced density matrix *pr* for the field mode which is obtained by tracing over the atomic variables in Eq.(5.51) as

$$
\begin{aligned}
\rho_F(t) &= Tr_A D^\dagger(\beta) \exp\left(\frac{-it\mathcal{H}}{\hbar}\right) |\psi_A(0)\rangle |\beta\rangle \langle\beta| \langle\psi_A(0)| \exp\left(\frac{it\mathcal{H}}{\hbar}\right) D(\beta) \\
&= D^\dagger(\beta) Tr_A \left[\exp\left(\frac{-it\tilde{\mathcal{H}}}{\hbar}\right) |\psi_A(0)\rangle |\beta\rangle \langle\beta| \langle\psi_A(0)| \exp\left(\frac{it\tilde{\mathcal{H}}}{\hbar}\right) \right] D(\beta) \ .
\end{aligned}
$$
$$(5.54)$$

Note further that the term in the square bracket in (5.54) is just the field density matrix for the standard JCM and hence

$$\rho_F(t) = D^\dagger(\beta)\tilde{\rho}_F(t)D(\beta) \qquad . \qquad 5.55$$

This relation indicates that the moments of the field variables are very simply related. For example the mean photon number of the cavity mode is calculated. In the density matrix formalism the expectation value of an operator is defined as *(A) = TrpA* . Using Eq.(5.55) the mean number of photons in cavity mode is found to be

$$
\begin{aligned}
\langle b^\dagger(t)b(t)\rangle &= Tr D^\dagger(\beta)\tilde{\rho}_F(t)D(\beta)b^\dagger b \\
&= Tr \tilde{\rho}_F(t)D(\beta)b^\dagger b D^\dagger(\beta) \\
&= Tr \tilde{\rho}_F(b^\dagger - \beta^*)(b - \beta) \\
&= \langle (b^\dagger - \beta^*)(b - \beta)\rangle \qquad . \qquad (5.56)
\end{aligned}
$$

The results obtained by using the solution of the standard JCM model and the equations (5.53) and (5.56) agree with the ones calculated in Section 5.2 from the direct numerical integration of the Schrodinger equation.

Hence results in Eq. (5.53) and Eq.(5.56) indicate that in the cavity QED experiments which need the cavity mode to be in the coherent state initially, could use an external coherent laser field to prepare the cavity mode which initially is in a vacuum state, to be in a coherent state. The situation would be not very different from the case where the cavity mode was initially in a coherent state which is a difficult proposition. The atomic properties will be identical at all times whereas field properties will be related in a simple manner. Our model can also be viewed as an exactly soluble example of the two-channel JCM.

5.4   Non-zero Detuning

In this section we consider the effect of detuning the cavity and the external field from the atomic resonance i.e., $U?L \wedge u>o / v \bullet$ We find that the results proved in the Section 5.3 also hold if the external field is on resonance with the cavity field i.e., when $LJ = u^\wedge$.

We define Ai as the detuning between the atom and the external pump i.e., Ai = $u\triangleright o$ — LJL and A2 as the detuning between the cavity and the external pump i.e. A2 = w — UJI. The general Hamiltonian (5.28) is thus rewritten as

$$\mathcal{H} = \hbar\Delta_1 S^z + \hbar\Delta_2 b^\dagger b + 2\hbar\alpha S^x + \hbar g(S^+ b + S^- b^\dagger) \ . \tag{5.57}$$

Working in the S^x basis as before, the state vector at time t can be expressed in terms of the complete set of states as

$$|\psi(t)\rangle = \sum_{n=o}^{\infty} D_n^- |-,n\rangle + \sum_{n=o}^{\infty} D_n^+ |+,n\rangle \tag{5.58}$$

where the complex coefficients D's are determined from the Schrodinger equation (5.19).

The equations of motion for the coefficients D's are found to be

$$i\dot{D}_p^- = \frac{1}{2}\Delta_1 D_p^+ + (p\Delta_2 - \alpha)\Delta_p^- - \frac{g}{2}(D_{p-1}^- + D_{p-1}^+)\sqrt{p} + \frac{g}{2}(D_{p+1}^+ - D_{p+1}^-)\sqrt{p+1}$$
$$i\dot{D}_p^+ = \frac{1}{2}\Delta_1 D_p^- + (p\Delta_2 + \alpha)\Delta_p^+ + \frac{g}{2}(D_{p-1}^- + D_{p-1}^+)\sqrt{p} + \frac{g}{2}(D_{p+1}^+ - D_{p+1}^-)\sqrt{p+1}$$

$$(5.59)$$

where $p = 0,1,2 \dots \infty$.

As before assuming the atom to be in the ground state |2) and the cavity field to be in vacuum, the initial conditions on Vs are $D+ = 4^\wedge$, $D\sim = -4$- with all other D's zero. The coupled equations are solved using Fehlberg's Runge Kutta method. The dynamics of the system is studied for different values of the external field and different detunings relative to the atom field coupling $(g = 1.0)$. As before we present the results for the evolution of the photon number $(b*b)$ and $P_e(t)$(the probability that the atom is in the excited state).

It is observed that A2, the detuning between the cavity and the external field alone affects the behavior of (6^f6) and $P_e(t)$. For instance, for $A_2 = 0.2$,(6+6) and $P_e(t)$ behave identically for any value of Ai like 0.1, 0.2, 0.3 *etc.* For the case where a = 3.0 the behavior of $(6*6)$ and $P_e(t)$ is shown in Figure 5.5 for the representative set of the detunings i.e., Ai= 0.0, A2 = 0.2. The mean photon number (6*6) reaches a maximum 18.63 which is very much less than the maximum of the exact resonance case. Thus the amount by which the field is detuned from the cavity affects the dynamics of the system in a quantitative way. In Figure 5.6 we give the dynamical behavior of the field and the atom when both the external field and the cavity field are detuned from the atomic transition.

In conclusion we have studied the dynamical properties of an example of the two-channel JCM where the atom is driven continuously by an external laser field in addition
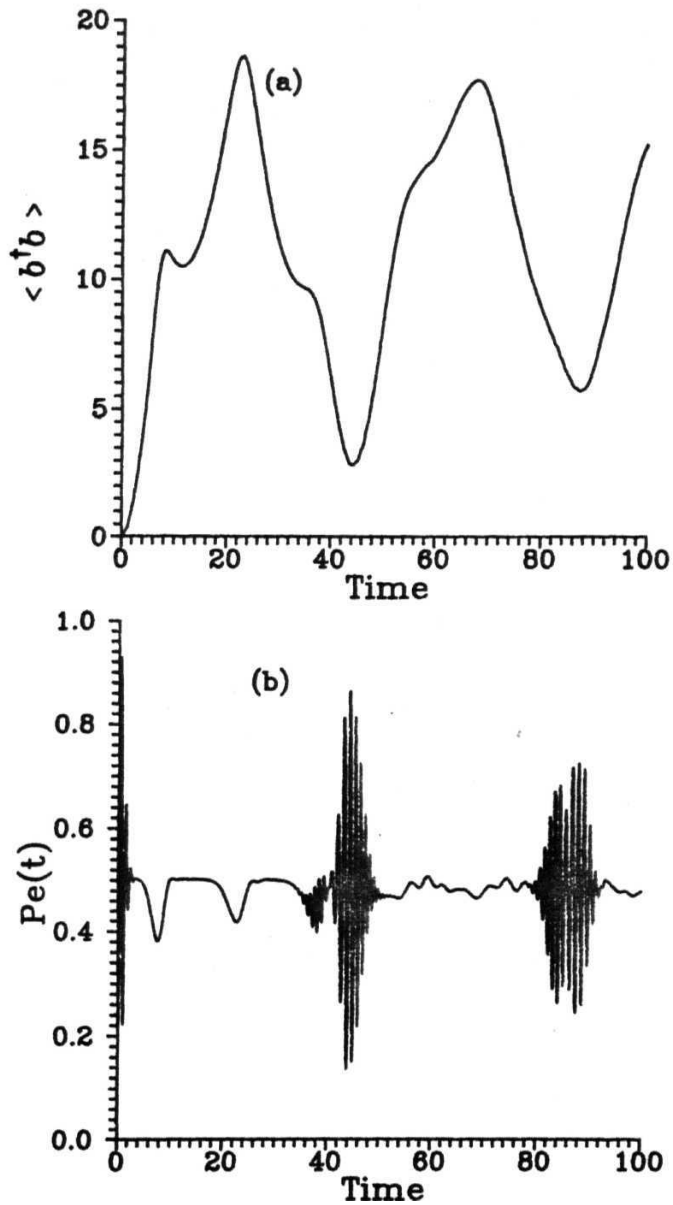
Fig. 5.5: Dynamical results for the JCM with continuous pumping for $a = 3.0$. Now the the external field is detuned A2 = u - $u>i$ = 0.2, Ai = u_o — UJI = 0.0 a) Mean number of photons in the cavity mode, (6^6) as a function of time 6)$P_e(<)$(Probability that the atom is in the excited state) as a function of time.
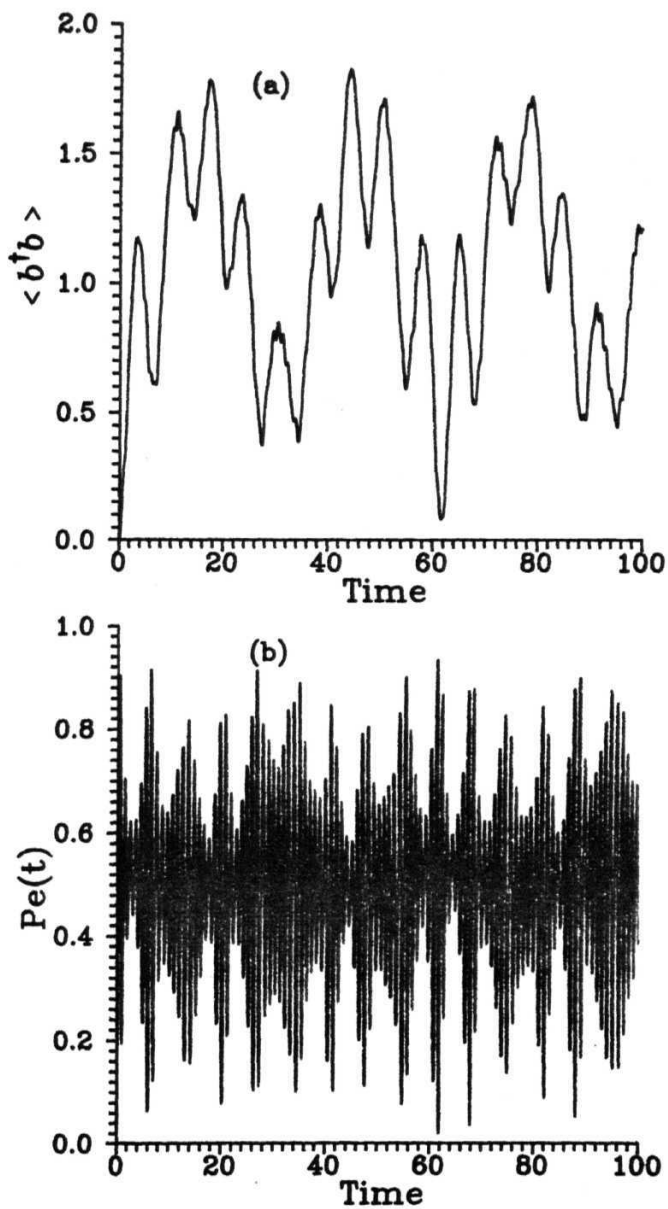
Fig. 5.6: Same as in Fig. 5.5 but now all transition frequencies are different i.e. *UL ^ u>o £* w. Aj = 1.0, A_2 = 1.0

to being coupled to a cavity mode. We compare the standard JCM with our model in the resonance case and establish a one to one correspondence between the results for the JCM with continuous pumping and the standard JCM where the field enters via the initial conditions. The situation however becomes more complex if the external field is detuned from the cavity field.

In a recent work P. L. Knight and coworkers [16] discussed the dynamics of the JCM with external pumping but with the cavity mode initially in a coherent state and the atom in the excited state. They discover collapse and revivals ("super revivals") which appear at time scales larger than their counterparts in the standard JCM. They also report sub-Poissonian statistics for certain interaction times of the external field and the atoms.

Our model dispels the difficulty of the micromaser experiments involved in studying the fundamental atom and field interaction. There need be no ambiguity in the photon statistics of the cavity mode. In the way suggested by our model the external pump can prepare the cavity mode initially in vacuum state, to be in the coherent state. The complexity of the external field entering into the cavity can be dealt with as in Kimble's experiment [3] which uses an extra field to study the JCM.

REFERENCES

1. E. T. Jaynes and F. W. Cummings, Proc. IEEE 1, 89 (1963).

2. G. S. Agarwal, Phys. Rev. Lett. 53, 1732 (1984); J. Op. Soc. Am. B 2, 480 (1985); Phys. Rev. A 43, 2595 (1991).

3. M. G. Raizen, R. J. Thompson, R. J. Brecha, H. J. Kimble and H. J. Carmichael, Phys. Rev. Lett., 63, 240 (1989); R. J. Thompson, G. Rempe and H. J. Kimble, Phys. Rev. Lett. 68, 1132 (1992).

4. P. Alsing, D. S. Guo, H. J. Carmichael, Phys. Rev. A 45, 5135 (1992).

5. L. Wang, R. R. Puri and J. H. Eberly, Phys. Rev A 46, 7192 (1992).

6. S. Haroche and J. M. Raymond, in *Advances in Atomic and Molecular Physics,* Vol. 20 (eds D. Bates and B. Bederson, Orlando: Academic, 1985, Pg 350).

7. H. I. Yoo and J. H. Eberly Phys. Rep. **118,** 239 (1985).

8. S. M. Barnett and P. L. Knight, Opt. Acta 31, 435 (1984); P. L. Knight, Physica Scripta **T12,** 51 (1986), S. M. Barnett and P. L. Knight, Phys. Rev. **A33,** 2433 (1986), S. M. Barnett, P. Filipowicz, J. Javaninen et al in *Frontiers in Quantum Optics* ed. by E. R. Pike and S. Sarkar, Adam-Hilger. (1986).

9. P. Meystre and M. Sargent **III,** *Elements of Quantum Optics,* (New York; Springer Verlag) 1990.

10. P. Meystre, Phys. Rep. **219,** 243-262 (1992).

11. B. W. Shore and P. L. Knight, J. Mod. Optics **40,** 1195-1238, 1993.

12. F. W. Cummings, Phys. Rev. A **140,** 1051 (1965).

13. J. H. Eberly, N. B. Narozhny and J. J. Sanchez Mondragon, Phys. Rev. Lett. 44, 1323 (1980); N. B. Narozhny, J. J. Sanchez-Mondragon and J. H. Eberly, Phys. Rev. A3, 236 (1981).

14. D. Meschede, H. Walther and G. Muller Phys. Rev. Lett. 54, 551 (1990); G. Rempe, H. Walther and N. Klein, Phys. Rev. Lett. 58, 353 (1987).

15. **J.M.A.** Danby, *Computing applications to differential equations* Reston Publishing Company. (1985). Pg. 32 - 48.

16. S. M. Dutra, P. L. Knight and H. Moya - Cessa, Phys. Rev. A 49, 1993 (1994).

Chapter 6

COMPETING THREE PHOTON AND ONE PHOTON TRANSITIONS IN CAVITY QUANTUM ELECTRODYNAMICS

The experimental realization of the ideal JCM [1] has been made possible by the one-atom maser [2]. The purely quantum mechanical phenomenon of collapse and revivals of the atomic inversion predicted by JCM [3] has been demonstrated for the first time [4]. Nonclassical effects like sub-Poissonian photon statistics [5] and antibunching [6] predicted in the JCM have been observed in the microwave cavities. Recently the direct spectroscopic measurement of vacuum field Rabi-splitting [7] has been observed in the optical domain [8].

All these experimental successes in realizing ideal simplified, purely quantum systems has led to a surge of interest in the study of a little more complicated, generalized systems in the purview of JCM in cavity QED. Several reviews of cavity QED [9] and JCM [10] have appeared which give a summary of the recent developments in the generalization of JCM. One of the natural extensions is the two channel fully quantized cavity QED model. Here a two-level atom couples to a multimode quantized field with two channels that independently connect the two states of the atom. This leads to interesting competing effects. In Chapter 5 we had considered a very simplified version of the two channel model where one of the channels has a classical field.

In nonlinear optics, competing nonlinear processes have attracted considerable atten-tion due to the novel interference effects which came to be discovered. One such discovery was by Aron and Johnson [11] of the absence of an expected three photon resonance en-hancement of a five photon multiphoton ionization process in Xenon at vapour pressures greater than 1 Torr. Miller et al [12] subsequently discovered that the disappearance of the resonantly enhanced signal was proportional to the appearance of a generated signal at third harmonic frequency. Many other examples are known in nonlinear optics. In amplified spontaneous emission it was experimentally discovered that the absorption of two photons at a fundamental frequency is cancelled in the presence of generated pho-tons at intermediate frequencies [13]. Another such an example of competing effects is the competition between Stokes and anti-Stokes processes [14]. The cause of such competitive effects has been shown to be due to the destructive interference between simultaneously present pathways of multiphoton excitation of resonance media. Multi-photon excitation induces nonlinear polarization and generates new fields which create the second excitation pathway to a resonant intermediate level. A simple illustration is given here. Consider a system interacting with an electromagnetic field of frequency *u*. The system can generate radiation of frequency 3ω. Once the radiation at 3ω is gener-ated, the system interacts with both fields at *u* and at *ZUJ*. The generation of radiation at 3a; is a coherent process and carries information on the phase of the radiation at *u*>. Consider now the three photon excitation of this system. The effective field leading to three photon excitation turns out to be zero [15] in the steady state and in the limit of long sample lengths. Thus there is a type of destructive interference which originates be-tween the two pathways and prohibits the excitation itself. That two processes interfere destructively follows from the principle of nonlinear optical balance (NLOB) proposed by Wynne [15] which actually originates from Maxwell's theory of minimum dissipation [16]. The mechanism underlying is that the amplitudes and phases of waves propagating

through a nonlinear medium are developed in such a way as to minimize the dissipative losses or absorption. However, the semiclassical approach followed by **Wynne and** other does not give any information on the quantum dynamics of the competing processes. It would be desirable to examine how the fields build up and how these finally lead to destructive interference. One should thus consider not only steady state dynamics but also transient dynamics. In addition one should also consider fields quantum mechanically. This would be important in understanding -

  i) the build up of the field at 3a;,

 ii) the coherence characteristics of the field at 3a; and consequently the competition between one photon and three photon processes at QED level,

iii) the quantum correlation between two modes and the possibility of the entangled states of fields at u and 3a;.

The nonlinear optical balance has been studied in the quantum mechanical context by Agarwal [17], Baker [18] and others who studied the general structure of quantum field states and discovered a new class of coherent states which show rich quantum features. Recently an exactly soluble coupled channel cavity QED model in the Stokes and anti-Stokes case was studied by Eberly et al [19]. They use a Raman like configuration to include three cavity modes and two independent channels and give a closed form solution to the eigenvalues and eigenstates. The eigenstates have a 'chain' character of being linked together by the interaction Hamiltonian. The dimension of **the** chain is limited **only** by the initial choice.

    In this chapter we examine a model of two channel cavity QED consisting of three photon and one photon transitions i.e., we present a lossless cavity **QED** version of a nonlinear optical balance. The alternate pathways which exist between **the two** levels

of **the** atom create quantum interferences which are studied in detail. We study the competition between the two processes by introducing different initial conditions for the system. In Section 6.1 we study the simplest case of competition in which the fundamental mode is assumed to have three photons, the minimum number to trigger a three photon process. A detailed study of mode mixing and entanglement of states is made. In Section 6.2 we study the dynamics when the fundamental field is in an arbitrary Fock state. We present details of field and atomic dynamics. In Section 6.3 we take the coherent state as the initial state for the fundamental mode. We compare the results obtained with the corresponding results when the fundamental mode was in the Fock state. In Section 6.4 we study the two channel model in the semiclassica:l domain. It is observed that the variables execute a periodic behavior. We derive the conservation laws existing in the two channel model which clarify the periodicity. We also demonstrate the steady state NLOB condition when decays are taken into account for the atomic system. We also compare these results with the corresponding ones obtained in the quantum domain. Finally we study the case when one of the modes is prescribed i.e., when the field in one of the channels is treated classically, similar to the problem studied in Chapter 5 and compare the results with the fully quantum two-channel model.

6.1 **The Model Hamiltonian and** Exchange **of Energy between Atom and** **Fields**

Consider the interaction of a two-level atom with states $| e)$ and $| g)$ separated by the frequency ɯ$>_o$, with two modes of the cavity radiation field of frequencies, u_a and av We assume that one of the modes, a interacts with the atom through a three photon process **and the** other mode, b interacts via a single photon process. For simplicity we further assume **that** the two cavity modes are in perfect resonance with the atomic transition

i.e. $u)_o = Suj_a =$ WE a is the fundamental mode and b is the third harmonic of it. [Figure 6.1].

As in the previous chapter the two-level atom is characterized by the spin — ~ angular momentum operators $5^{\pm}$, S^c. In the rotating wave approximation the interaction Hamiltonian for the two-level system interacting with two fields via two competing processes is given by

$$H_{ef} = k(KS^{+}a^{3} + K^{m}S{\sim}a^{\wedge 3}) + h({}_9S^{+}b + g^{m}S{\sim}tf) \quad . \tag{6.1}$$

The field modes a and 6 are described by the annihilation and creation operators a, a' and 6,6' respectively. Furthermore K is the coupling strength containing the transition element for the three photon process; g is the coupling strength containing the transition dipole moment matrix element for the single photon process. These are evaluated using perturbation theory to the first arid third order in the field amplitude [20]. The single photon Rabi frequency is given by

$$g = \sqrt{\frac{2\pi\omega_a}{V\hbar}}\, d_{ge} \quad , \tag{6_2}$$

where g and c are the relevant levels separated by frequency u_a. From the third order perturbation theory the three photon Rabi frequency is given by

$$\kappa = -\left(\frac{2\pi\omega_a}{V\hbar}\right)^{3/2} \frac{d_{ej}d_{jl}d_{lg}}{(\omega_g - \omega_j + 2\omega_a)(\omega_g - \omega_l + \omega_a)} \tag{6 3}$$

where g is the initial state, e is the final state and l,j are the intermediate states. Here g, l,j, e are equally spaced with frequency difference $u>_a$. The levels have energies as *tuvj* corresponding to the jth level etc. Here V is the cavity volume. The $d's$ are the dipole matrix elements corresponding to the respective transitions.

The $S^{+}a^{3}$ term in Eq. (6.1) describes the excitation of the atom from the ground state by absorbing three photons from the a-mode while the $5^{+}6$ term leads to the excitation
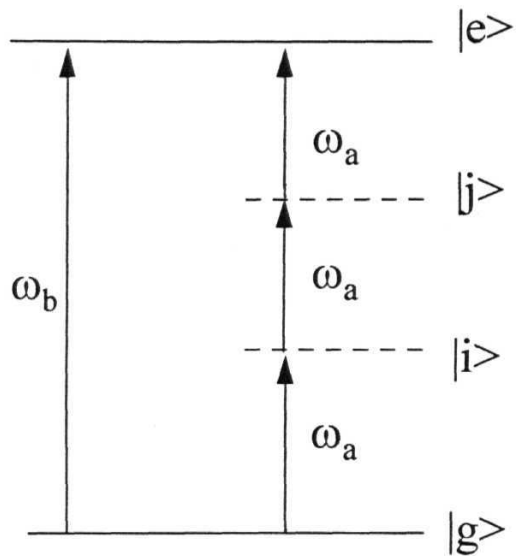
Fig. 6.1: Schematic illustration of the three photon and one photon processes in a two-level atom.

of the atom by absorbing one photon from the 6-mode.

In order to understand the basic behavior of the system we first consider a simple case. We assume that initially, at time $t = 0$, only the fundamental mode, a- mode exists and it is in a Fock state with just three photons which is the minimum number of photons required for the three photon absorption. We also assume that the third harmonic mode, 6-mode is not yet generated and hence is in the vacuum state and the atom is in the ground state $\g)$. Thus the initial state of the system is the direct product of the states of the two modes and the atom and is given by $|3,0,^\wedge)$.

$$| \mathcal{H}(\!\!) > = C_i(t) \text{ I } 0,0, e) + C_,(t) \mid 0,1,g) + C_3(t) \mid 3,0,*),\qquad(6\text{-}4)$$

where the Cs are the complex probability amplitudes determined using the Schrodinger equation. The equations of motion of the complex amplitudes are

$$\dot{C}_1 = -iC_2 g - i\kappa\sqrt{6}C_3 ,\qquad(6.5a)$$

$$\dot{C}_2 = -ig^*C_1 ,\qquad(6.56)$$

$$\dot{C}_3 = -i\kappa^*\sqrt{6}C_1 \quad .\qquad(6.5c)$$

Differentiating the equation (6.5a) we get

$$\ddot{C}_1 = -ig\dot{C}_2 - i\kappa\sqrt{6}\dot{C}_3.\qquad(6.6)$$

Substituting equations (6.5b) and (6.5c) in (6.6),

$$\ddot{C}_1 = -|\Omega|^2 C_1\qquad(6.7)$$

where

$$|\Omega|^2 = | g |^2 + 6 | \kappa |^2 .\qquad\textbf{(6.8)}$$

The second order differential equation in Eq. (6.7) is the simple harmonic oscillator equation of motion and gives a hint about the periodicity to be expected in the observed variables. At time $t = 0$, the complex amplitudes are given by $C_1 = 0, C_2 = 0, C_3 = 1$. Using these initial conditions solution of the differential equation is found to be

$$C_1(t) = \frac{-i\kappa\sqrt{6}}{|\Omega|} \sin |\Omega| t \tag{6.9}$$

Using Eq.(6.9) the solutions of Eq.(6.5b) and Eq.(6.5c) are found to be

$$C_2(t) = \frac{-2g^*\kappa\sqrt{6}}{|\Omega|^2} \sin^2 \frac{|\Omega| t}{2} \tag{6.10}$$

and

$$C_3(t) = 1 - \frac{12|\kappa|^2}{|\Omega|^2} \sin^2 \frac{|\Omega| t}{2} . \tag{6.11}$$

We now study the dynamical behavior of the atom and the field variables which can be described in terms of the complex amplitudes. Here we specifically present the results for the evolution of the atomic population $P_e(t)$, (the probability that the atom is in the excited state) and the average number of photons in the a-mode and the fr-mode, (a'a) and (6 • 6) respectively. These quantities are expressed in terms of the complex amplitudes as $P_e(t) =| d(t) |^2, (<*M = 3$ I $C_3(t) |^2$ and $(bH) =| C_2(t) |^2$. Substituting for the C's given in Eqs. (6.9),(6.10) and (6.11)

$$P_e(t) = \frac{3|\kappa|^2}{|\Omega|^2}(1 - \cos 2|\Omega| t), \tag{6.12}$$

$$\langle a^\dagger a \rangle = 3\left(1 - \frac{6|\kappa|^2}{|\Omega|^2}(1 - \cos |\Omega| t)\right)^2 , \tag{6.13}$$

$$\langle b^\dagger b \rangle = \frac{6|g|^2|\kappa|^2}{|\Omega|^4}(1 - \cos |\Omega| t)^2 . \tag{6.14}$$

The dynamics of the system can be studied for different values of the coupling constants. The three photon coupling is usually much weaker in comparison with the one

photon coupling. However Rydberg atoms can be used for multiphoton transition stud-
ies. The Rydberg atoms have a very large dipole moment which is proportional to the
square of the principal quantum number, n, of the spectroscopic states. Using spectro-
scopic states of sufficiently high principal quantum number *n* so that the dipole matrix
elements are very high and also adjusting the detuning appearing in the denominator
of Eq. (6.3) suitably the three photon Rabi frequency can be made sufficiently high
enough to be comparable to the single photon Rabi frequency. In the case of two-photon
micromaser Haroche and Raimond [21] showed that the two-photon Rabi frequency can
be quite large for Rydberg states of principal quantum number *n* of the order of 40.

In this simplest case we choose $n/g = 0.1$. As observed from the form of the above
solutions the system executes sinusoidal oscillations as shown in Figure 6.2. There is a
periodic exchange of energy between the two modes with the atom acting as an interme-
diary. The oscillation frequency of $P_e(t)$ is twice that of the field modes. This is because
the atom goes to the ground state twice. Once when the atom emits three photons into
the a-mode i.e. *(a^a)* reaches the maximum value of 3.0 and again when the atom emits
one photon into the *b*-mode *i.e.* (6*6) reaches the maximum value of 0.21.

If the single photon process were non-existent *[g = 0*; this is the analog of vacuum
field Rabi-oscillations for the usual Jaynes-Cummings model], we find that

$$P_e(t) = \sin^2 |n|* \qquad (6.15)$$

$$(a^a) = 3\cos^2|0|tf. \qquad (6.16)$$

The oscillation frequency of $P_e(t)$ is the same as the oscillation frequency of *(a^a).* This
is because the atom comes back to the ground state only when it emits three photons to
the a-mode. Clearly the interference between the two pathways $| 0,0, e) \longrightarrow\rangle 3,0,g)$ and
$| 0,0, e) \longrightarrow 0,1,\langle7)$ leads to this difference (as also $n <C g)$ in the dynamical behavior. It
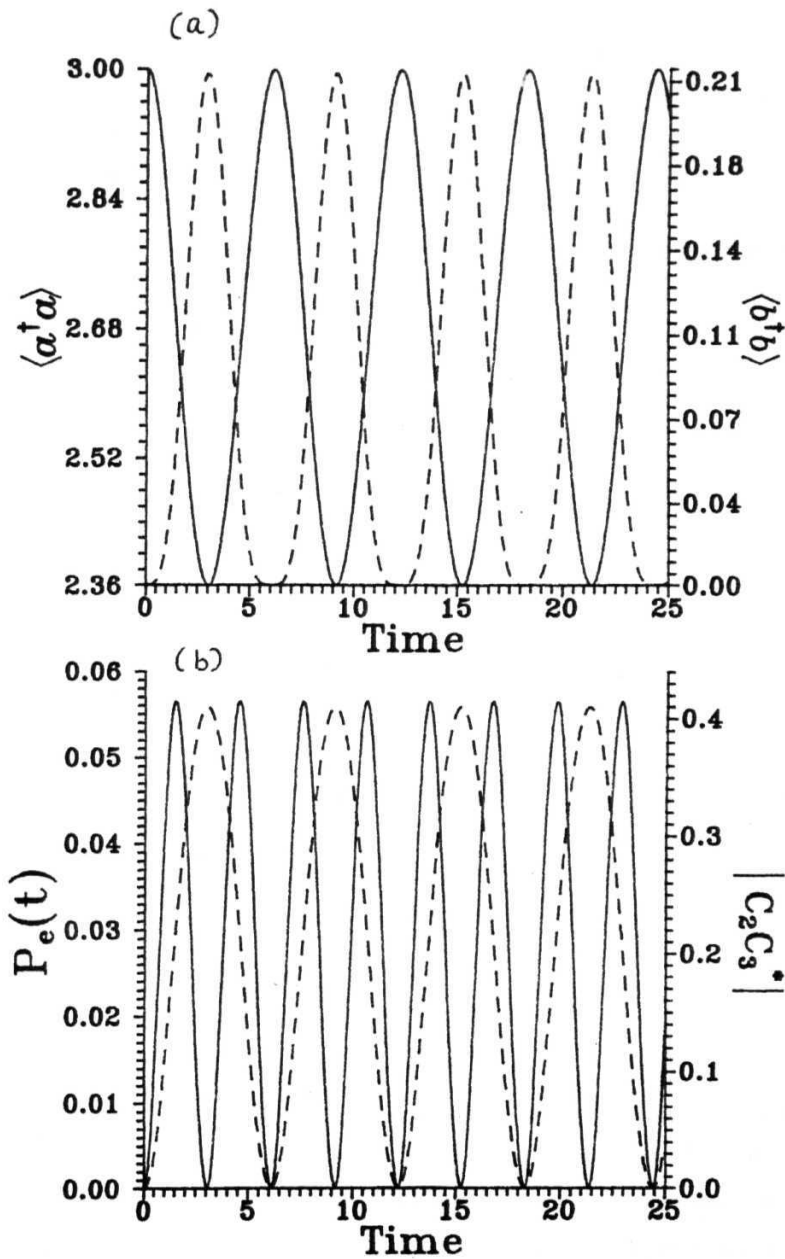is a manifestation of the mode-mixing property of the model where the atom acts as a

Fig. 6.2: The time dependence of (a) the number of photons in mode a (solid curve) and mode b (dashed curve), (b) the probability $P_e(t)$, that the atom is in the excited state (solid curve) and the entanglement | C2C3 | of the two field modes a and 6(dashed curve). The time is in units of g and $K/J = 0.1$

catalyst and brings about a redistribution of photons among the two modes *a* and *b* of the cavity.

Another consequence of the two competing processes in a cavity is the appearance of strong entanglement between the two modes. To see this we calculate the density matrix, *p*. As the state vector in Eq.(6.4) completely describes the system of atom and two field modes, $|\psi(t)\rangle$ is a pure state. The density matrix, corresponding to the pure state $|\psi\rangle(0)$ is given by the bilinear product of the state as

$$\rho = |\psi(t)\rangle\langle\psi(t)|$$
$$= (C_1 |0,0,e\rangle + C_2 |3,0,g\rangle + C_3 |0,1,g\rangle)$$
$$\times (C_1^* \langle 0,0,e| + C_2^* \langle 3,0,g| + C_3^* \langle 0,1,g|) \quad . \quad (6.17)$$

We get an idea about the entanglement between the modes by studying the density matrix corresponding to just the field variables. The reduced density matrix of the field is obtained by taking a trace over the atomic variables. It is given by

$$\rho_F = Tr_A |\psi(t)\rangle\langle\psi(t)|$$
$$= |C_1|^2 |0,0\rangle\langle 0,0| + C_2 C_3^* |3,0\rangle\langle 0,1|$$
$$+ C_3 C_2^* |0,1\rangle\langle 3,0| + \ldots \quad (6.18)$$

The quantity $|C_2 C_3|$ is a measure of the entanglement of the field modes and is shown in Figure 6.2b. Initially at time $t = 0$ the two modes are disentangled. However the interaction with the atom produces correlation between the two modes. The entanglement vanishes whenever either Cv or $C3$ is zero. Even this simplest case of simultaneously present pathways exhibits interference consequences.

6.2 Numerical Results for Dynamics of the Fundamental Field in a Fock State

We next consider the more general case with *3n* photons in the a-mode where *n* can take any value greater than one. As before we assume that at time $t = 0$, the 6-mode is in vacuum state and the atom is in the ground state, $\mid g)$. Thus the initial state of the atom-field system is given by $\mid 0(0)) =\mid 3n,0,p)$. The state vector for each value of *n* is a linear combination of all the possible states the system can exist in. For the case $n — 1$, there are the three states mentioned in Section 6.1. For the case $n = 2$, there are five possible states the system can exist in by virtue of the two channel interaction Hamiltonian(6.1). These are $|6,0,p)$, $|3,0,e)$, $|3,1,\#)$, $|0,1,e)$ and $|0,2,\#)$. By induction we find that the number of such states for a particular *n* value is $2n + 1$. These are akin to the 'chain' of states linked by the two processes occurring in the medium mentioned in Ref. [19]. To write the state vector of the system for a general 'n' value, we observe that there is a chain of states as depicted below:

$$|3(n-1),0,e\rangle \qquad |3(n-2),1,e\rangle$$

$$|3n,0,g\rangle \qquad\qquad |3(n-1),1,g\rangle \qquad\qquad |3(n-2),2,g\rangle \qquad \ldots\ldots$$
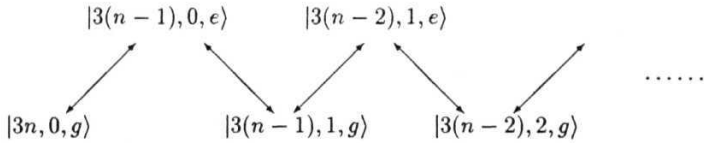
Here the chain ends whenever the number of photons in 6-mode is equal to n. Denoting the number of photons in &-mode by *m* and summing over the complete set of states the state vector of the system at time *t* for a particular n is given by

$$| \psi(t)\rangle = \sum_{m=o}^{n} A_m(t) \mid 3(n-m),m,g\rangle + \sum_{m=1}^{n} B_m(t) \mid 3(n-m),m-1,e\rangle, \qquad (6.19)$$

where the complex amplitudes are determined from the Schrodinger equation. The equations of motion for the complex amplitudes are

$$\dot{A}_p = -i\kappa^* B_{p+1}\sqrt{3(n-p)(3(n-p)-1)(3(n-p)-2)} - ig^* B_p\sqrt{p} \ ,$$

$$\dot{B}_p = -igA_p\sqrt{p} - i\kappa A_{p-1}\sqrt{(3(n-p)+1)(3(n-p)+2)(3(n-p)+3)} \ ,$$

$$(6.20)$$

where p varies from 0 to n. At time $t - 0$, corresponding to the initial state $|3,0,<7)$, the complex amplitude $A_o = 1$ and $B_o = 0$. Other amplitudes for $p > 0$ are all zeros i.e., $A_p = 0$ and $B_p = 0$, where $p = 1,2,... n$. Using the initial conditions the coupled equations (6.20) are solved using Fehlberg's Fourth order Runge-Kutta method [22]. The dynamical behavior of the atom and the field variables is studied. We calculate $<P_e(<)$, $(a^\wedge a)$ and $(6^* 6)$ in terms of the complex coefficients as

$$P_e(t) = \sum_{m=1}^{n} |B_m(t)|^2,$$

$$\langle a^\dagger a \rangle = \sum_{m=0}^{n-1} 3(n-m)|A_m(t)|^2 + \sum_{m=1}^{n-1} 3(n-m)|B_m(t)|^2,$$

$$\langle b^\dagger b \rangle = \sum_{m=1}^{n} m|A_m(t)|^2 + \sum_{m=2}^{n} (m-1)|B_m(t)|^2 \ . \qquad \mathbf{(6.21)}$$

The dynamics of the system is studied for j = 0.01, which appears to be reasonable for Rydberg atoms. A representative value of $n - 33$ is taken so that **the** initial state is $|99,0,</)$. The number of basis states involved is $2n - f 1 = 67$. The number of coupled complex equations is 67. By converting the equations into equations **for all real quantities there** are 2x67=134 coupled equations. The fourth order Runge Kutta method solves the **134** coupled differential equations and the behavior of the above variables in Eq.(6.21) is shown in Figure 6.3. In the absence of mode competition $(g = 0)$ the atomic and field
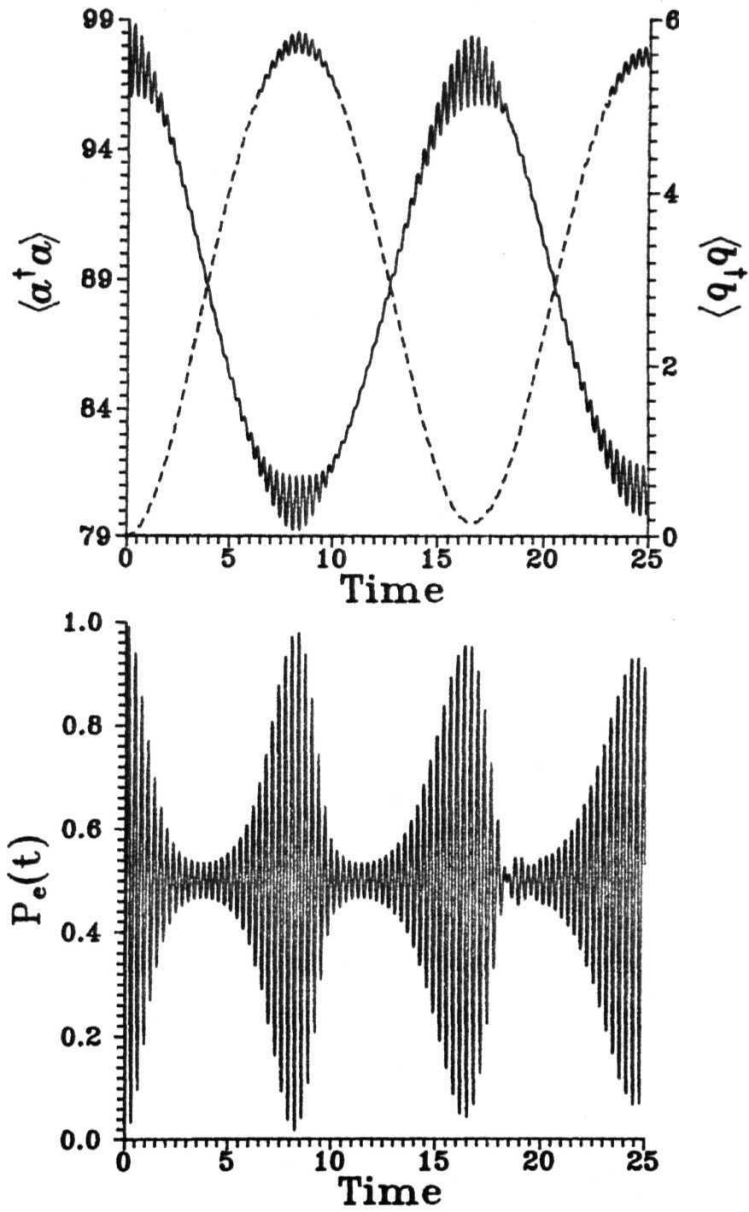
Fig. 6.3: Same as in Fig. 6.2 but now the fundamental field is in a Fock state | 99) and $n/g = 0.01$.

variables would exhibit simple sinusoidal behavior characteristic of Rabi oscillations. There are only two states of consequence in this case, |99,0,p) **and** |96,0, e) as the single photon absorption and emission processes no longer exist. The state vector of the system oscillates sinusoidally between these two states and consequently the system variables perform Rabi oscillations. The mode competition changes the almost sinusoidal behavior of say (a'a) to quite a complex behavior (Figure 6.3a) exhibiting different scales of oscillations. The mode competition leads to coupling between 67 states instead of just two states in the absence of mode coupling. The presence of a large number of photons in the Fock state of the a-mode leads to an interference of a number of sinusoidally oscillating contributions and hence the complex collapse and revivals arise. Also the mean photon number of generated third harmonic field 6-mode photon number, (6» 6) which is zero initially, oscillates to a maximum of about 6.8.

One should bear in mind that the initial choice 3rc, of the number of photons in the a-mode is not necessary. Initial states having the structure | *3n + l,0,g)* and | 3n-f2,0,#) would each belong to its own complete set of basis states. But, qualitatively they will exhibit the same kind of dynamics as described earlier.

6.3 Mode Competition with the Fundamental Mode **Initially in a Coherent State**

In this section we take the a-mode in a coherent state $| a \rangle$ at $t = 0$

$$| \alpha \rangle = \sum_{n=o}^{\infty} \frac{\alpha^n}{\sqrt{n!}} \exp\left\{ -\frac{| \alpha |^2}{2} \right\} | n \rangle \ , \tag{6.22}$$

where a is the complex amplitude of the coherent state. As in the previous cases, $t = 0$ the atom is assumed to be in the ground state and the 6-mode to be **in** the vacuum state. The coherent state has a Poissonian distribution over an infinite number of photons. The

infinite number of photons can be divided into three parts with 3n, 3n 4- 1 and 3n -f 2 photons respectively with n varying from 0 to oc, in each **part. At** time $t = 0$, **the initial** state is hence written as

$$|\psi(0)\rangle = \sum_{n=0}^{\infty} \frac{\alpha^{3n} e^{-|\alpha|^2/2}}{\sqrt{3n!}} |3n, 0, g\rangle + \sum_{n=0}^{\infty} \frac{\alpha^{3n+1} e^{-|\alpha|^2/2}}{\sqrt{(3n+1)!}} |3n + 1, 0, g\rangle$$

$$+ \sum_{n=0}^{\infty} \frac{\alpha^{3n+2} e^{-|\alpha|^2/2}}{\sqrt{(3n+2)!}} |3n + 2, 0, g\rangle \ . \qquad (6.23)$$

Within each of the three parts, corresponding to each n there is a chain of basis states linked together by the interaction Hamiltonian and the state vector corresponding to that particular n in each of these parts with (3n, $3n + 1$,3n -f 2) photons would be represented by a combination like Eq.(6.19). The state vector at time / is thus a linear combination of the basis vectors for the 3n, 3n + 1 and $3n$ -f 2 photon states. Corresponding to each n would be the coherent state Poissonian weightage factor for the state vector. The state vector is written as

$$|\psi(t)\rangle = \sum_{n=o}^{\infty} \frac{\alpha^{3n} e^{-|\alpha|^2/2}}{\sqrt{3n!}} \left[\sum_{m=o}^{n} A_m^n(t) \,|\, 3(n-m), m, g\rangle \right.$$

$$\left. + \sum_{m=1}^{n} B_m^n(t) \,|\, 3(n-m), m-1, e\rangle \right]$$

$$+ \sum_{n=o}^{\infty} \frac{\alpha^{3n+1} e^{-|\alpha|^2/2}}{\sqrt{(3n+1)!}} \left[\sum_{m=o}^{n} C_m^n(t) \,|\, 3(n-m) + 1, m, g\rangle \right.$$

$$\left. + \sum_{m=1}^{n} D_m^n(t) \,|\, 3(n-m) + 1, m-1, e\rangle \right]$$

$$+ \sum_{n=o}^{\infty} \frac{\alpha^{3n+2} e^{-|\alpha|^2/2}}{\sqrt{(3n+2)!}} \left[\sum_{m=o}^{n} E_m^n(t) \,|\, 3(n-m) + 2, m, g\rangle \right.$$

$$\left. + \sum_{m=1}^{n} F_m^n(t) \,|\, 3(n-m) + 2, m-1, e\rangle \right] \qquad (6.24)$$

where $A,B,\_\_\_F$ are the complex amplitudes. Here the evolution of 3n + 1 **and** $Sn + 2$ states is similar to the 3n case.

As in the previous section equations of motion for the complex coefficients axe derived using the Schrodinger equation. At time $t = 0, v4'' = 1, E\% = 1, F_o{}^n = 1$ and the rest of the coefficients are zero. As discussed in Chapter 5 the convergence of the equations has to be tested. In the two channel model, if convergence occurs for $n \sim N$ the total number of photons actually taken into account in the coherent state is $\sim 37V$. Now in each of the three sums in Eq.(6.23) n runs from 0 to N. Corresponding to each n there are (2n -f 1) complex coupled equations in each part. For one part of the state vector basis the total number of equations is given by

$$\sum_{n=0}^{N}(2n + 1) = (N + 1)^2 \quad . \tag{6.25}$$

Corresponding to the total state vector basis there are $3(N \text{ -f } I)^2$ complex coupled equations to be solved. For the representative value $a = 10$, convergence is found to occur at $n = 62$, or the actual number of photons taken is 3 x 62 = 186. The number of equations involved is $3(62 \text{ -f } I)^2 = 11,907$ complex coupled differential equations. When converted into real equations there are 23,814 coupled real differential equations which are solved efficiently using the Fehlberg's Runge Kutta method. We specifically present the results for the evolution of $P_e(t)$, (a^*a) and (b^*b) for the coherent amplitude $a — 10.0$ and $- = 0.01$ in Figure 6.4. The atomic excitation probability shows the familiar collapse and revival and the photon statistics show modulated Rabi oscillations. These must be compared with the corresponding results in Figure 6.3 for the case when the a-mode is initially in a Fock state with the same number of photons. Clearly the photon distribution of the input field changes the dynamics considerably. The symmetric Poisson distribution of photons in the coherent state leads to the dephasing of oscillations and the collapse and then due to the quantum nature of the field the oscillations reconstruct. to give the revival. In the Fock state case, incomplete collapse and revivals occur due to the absence of any symmetry in the photon distribution.
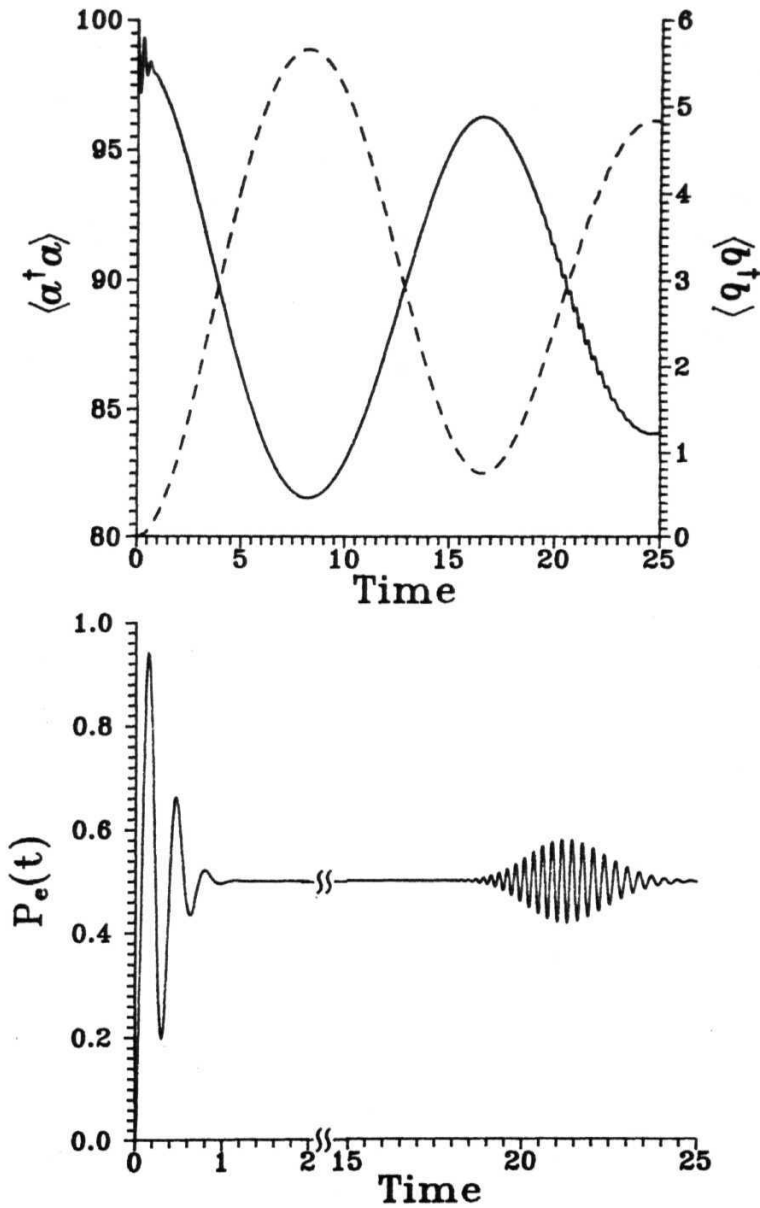
Fig. 6.4: Dynamical results for the fundamental field initially in a coherent state, a = 10.; */g = 0.01.

In Figure 6.5 we show the results for the atomic population and the mean number of photons in a-mode by ignoring the mode competition *i.e.* by setting <7=0. A comparison of the two Figures 6.4 and 6.5 is quite revealing. For example in Figure (6.4a) *(a*a)* oscillates around 90 whereas in Figure (6.5a) it oscillates around 98.6. Also the qualitative behavior of the curves in the two cases is different. The collapse and revival phenomenon observed in the time scales shown for *(a^a)* in the case of no mode competition is absent in Figure 6.4 where there is mode competition.

6.4 Comparison of Quantum Treatment with Semiclassical Treatment

It would be interesting to compare and contrast the predictions of the quantum theory with the results obtained using semiclassical approximation, where the fields evolve according to classical dynamics. In general,the Heisenberg equation of motion gives the equations for the mean values of the operators:

$$\langle \dot{X} \rangle = \frac{-i}{\hbar} \langle [X, H] \rangle. \tag{6.26}$$

Using the interaction Hamiltonian (6.1) the equations of motion for the atom and field operators are obtained. In the semiclassical approximation one ignores the quantum correlations between the field and atomic variables. The average of the product of operators is written as the products of their averages. For example $(S \sim a^{\wedge 3}) = (S \sim)(a*)^3$. Using this procedure we obtain

$$\langle \dot{a} \rangle = -3i\kappa^* \langle S^- \rangle \langle a^\dagger \rangle^2 \tag{6.27a}$$

$$\langle \dot{b} \rangle = -ig^* \langle S^- \rangle \tag{6.276}$$

$$\langle \dot{S}^+ \rangle = -2i\kappa^* \langle S^z \rangle \langle a^\dagger \rangle^3 - 2ig^* \langle S^z \rangle \langle b^\dagger \rangle \tag{6.27c}$$

$$\langle \dot{S}^z \rangle = -i\kappa \langle S^+ \rangle \langle a \rangle^3 - ig \langle S^+ \rangle \langle b \rangle + i\kappa^* \langle S^- \rangle \langle a^\dagger \rangle^3 + ig^* \langle S^- \rangle \langle b^\dagger \rangle \tag{6.27a^1}$$
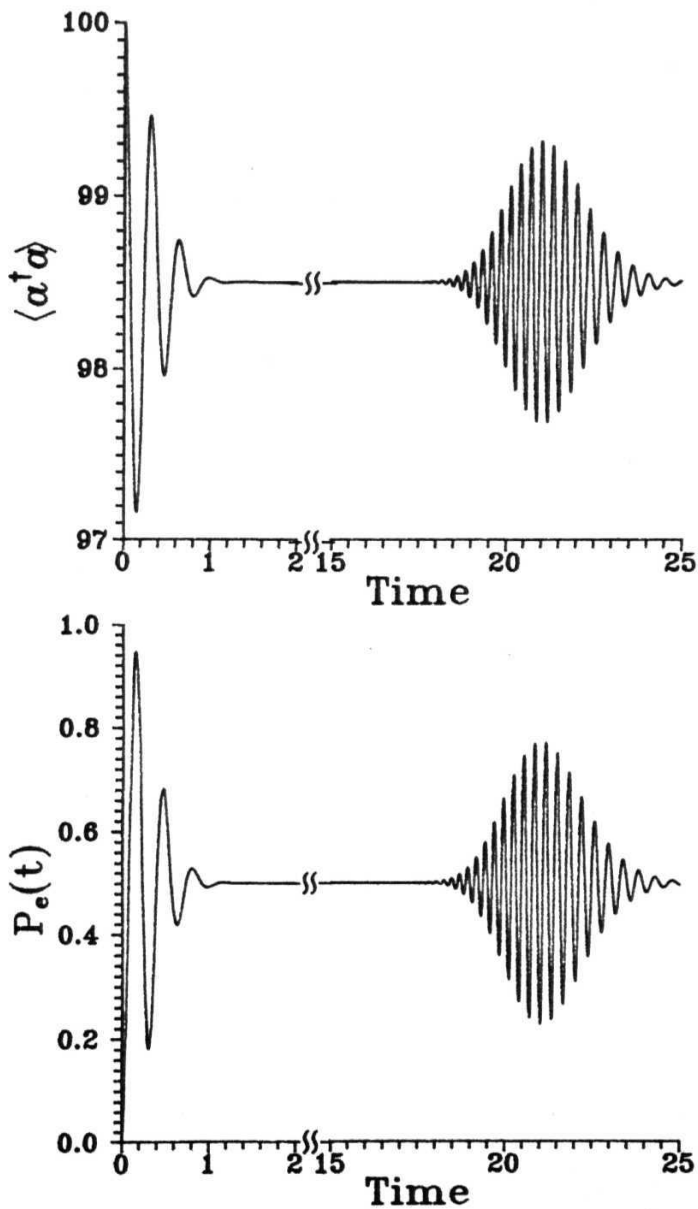
Fig. 6.5: Dynamical results in the absence of mode competition *(g = 0)* for the fundamental field initially in a coherent state a = 10.0. The scale on the x-axis corresponds to 100 *nt*.

Initially the atom is in the ground state, 6-mode is in vacuum and a-mode is in a coherent state, a = 10. (S^z) is the energy of the atom. If the atom is in the ground (excited) state (S^z) = -5(5). Hence using the initial conditions $|(a)| = 10, |(6)| = 0$ and $(S^z) = -\backslash$ the equations (6.27) are solved numerically using the Fehlberg's Runge-Kutta method. The dynamical behavior of $P_e(t)$ which is equal to (S^z) -f | and the average number of photons in the *a* and 6 modes | (a) |² and | (6) |² is observed (inset of Figure 6.6) to be periodic which is in complete contrast with the predictions of quantum theory (Figure 6.4). The sinusoidal oscillations are the semiclassical Rabi oscillations of the atom which get modulated once the quantum nature of the field modes is taken into account. Semiclassical results are similar to the semiclassical results for the case of the single photon JCM [1].

To understand the periodicity in the semiclassical model a simple exercise is now performed. Rewriting the complex quantites in Eqs. (6.27) as follows:

$$\langle a \rangle = |\langle a \rangle| e^{i\theta_a}$$
$$\langle b \rangle = |\langle b \rangle| e^{i\theta_b}$$
$$\langle S^- \rangle = |\langle S^- \rangle| e^{i\chi} \tag{6.28}$$

Substituting these into Eqs.(6.27) gives

$$|\langle \dot{a} \rangle| = -3i\kappa \langle S^- \rangle ||\langle a \rangle|^2 e^{i\phi_a}$$
$$|\langle \dot{b} \rangle| = -ig\langle S^- \rangle| e^{i\phi_b}$$
$$|\langle \dot{S}^- \rangle| = 2i\kappa \langle S^z \rangle e^{-i\phi_a} + 2ig\langle S^z \rangle |\langle b \rangle| e^{-i\phi_b}$$
$$\langle \dot{S}^z \rangle = i\kappa \langle S^- \rangle ||\langle a \rangle|^2 e^{i\phi_a} + ig\langle S^- \rangle ||\langle b \rangle| e^{i\phi_b} \tag{6.29}$$

where $<f>_a$ — $X \sim\sim 3\#_0$ and $<j>_b = \backslash\sim$ ^6. If^{tne} phases are chosen as $<j>_a = fo = |$ Eqs. (6.29) reduce to

$$|\langle \dot{a} \rangle| = 3\kappa |\langle S^- \rangle| |\langle a \rangle|^2 \tag{6.30a}$$
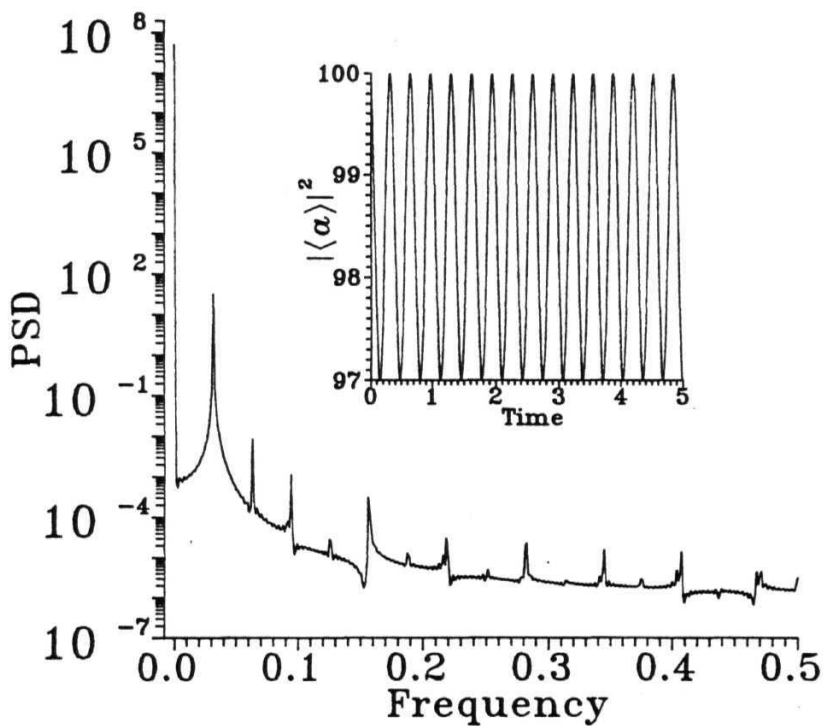
Fig. 6.6: Power spectral density (PSD) corresponding to the dynamical behavior of number of photons in a-mode in the semiclassical case. The inset shows the behavior in time domain. Frequency is in units of the time interval between consecutive points in time domain.

$$|\langle \dot{b} \rangle| = g|\langle S^- \rangle| \tag{6.306}$$

$$|\langle \dot{S}^- \rangle| = 2\kappa|\langle S^z \rangle||\langle a \rangle|^3 + 2g\langle S^z \rangle|\langle b \rangle| \tag{6.30c}$$

$$\langle \dot{S}^z \rangle = -2\kappa|\langle S^- \rangle||\langle a \rangle|^3 - 2g|\langle S^- \rangle||\langle b \rangle| \tag{6.30J}$$

One obvious conservation law is the conservation of the energy of the system given as

$$\langle S^z \rangle + |\langle b \rangle|^2 + \frac{1}{3}|\langle a \rangle|^2 = \text{constant} \ . \tag{6.31}$$

By inspection of Eqs.(6.30c) and (6.30d) we find that

$$\frac{\langle \dot{S}^z \rangle}{|\langle S^- \rangle|} - \frac{|\langle \dot{S}^- \rangle|}{\langle S^z \rangle} = 0 \tag{6.32}$$

which implies that

$$\langle S^z \rangle^2 + |\langle S^- \rangle|^2 = \text{constant} \ . \tag{6.33}$$

Dividing Eq.(6.30a) by 3Ac|⟨a⟩|² and multiplying it with *g* we find that

$$\frac{g|\langle \dot{a} \rangle|}{3\kappa|\langle a \rangle|^2} = |\langle \dot{b} \rangle| \ . \tag{6.34}$$

Integrating w.r.t. time on both sides the third conservation law is obtained as

$$3\kappa|\langle b \rangle| + \frac{g}{|\langle a \rangle|} = \text{constant} \ . \tag{6.35}$$

In the light of the conservation laws (6.31, 6.33, 6.35) and the phase relations we effectively have two independent variables coupled nonlinearly. This would lead to some kind of elliptic integrals whose solutions are periodic. This property along with the fact that the system is described by a Hamiltonian enables us to understand the periodicity of the dynamical behavior.

The periodicity is demonstrated rather clearly by numerically estimating the power spectral density (PSD) corresponding to the dynamical behavior of the number of photons in a-mode. PSD indicates the dominant frequencies present in a frequency interval and

gives a relative estimate of their power in the frequency spectrum. It has finite values at all frequencies except where the function in the time domain has a sine wave component of finite amplitude. At these frequencies PSD becomes a delta function i. e. a sharp spike. The PSD is shown in Figure 6.6 as a function of frequency which is scaled in units of the interval between consecutive points in time domain. There are harmonics of decreasing intensity with the odd harmonics being less prominent than the even ones. The separation between two neighbouring harmonics is 0.03 which is in agreement with the time period of the inset in Figure 6.6. The dynamics of $| (a) |^2$ is hence governed by a series of sinusoids of frequencies which are multiples of the fundamental.

For systems with small life time of the excited state the steady state characteristics are important. We now demonstrate the formation of the nonlinear optical balance as first conceived by Wynne [15]. Decays are introduced into the atomic equations. The dipole moment can always decay separately from the population inversion in the atomic system due to the elastic collisions which may disturb the dipole oscillation of the atom without disturbing its energy. We introduce the longitudinal decay $7\|$ in the inversion equation and the transverse decay 7_X in the dipole moment equations in the nomenclature of magnetic resonance. In laser physics the longitudinal decay rate is twice the transverse decay i.e., $7\| = 2y\pm,$

The atomic equations in (6.27c,d) get modified when the decays are added phenomenologically as

$$\langle \dot{S}^+ \rangle = -\gamma_\perp \langle S^+ \rangle - 2i\kappa^* \langle S^z \rangle \langle a^\dagger \rangle^3 - 2ig^* \langle S^z \rangle \langle b^\dagger \rangle$$

$$\langle \dot{S}^z \rangle = -\gamma_\| \langle S^z - \eta \rangle - i\kappa \langle S^+ \rangle \langle a \rangle^3 - ig \langle S^+ \rangle \langle b \rangle + i\kappa^* \langle S^- \rangle \langle a^\dagger \rangle^3$$
$$+ ig^* \langle S^- \rangle \langle b^\dagger \rangle \qquad (6.36)$$

where rj is the equilibrium value. When the laser fields are switched off the inversion (S^z) can relax to an equilibrium value, $r) = ~\backslash$ which corresponds to the atom being in

the ground state.

Considering the case with the initial condition $|\langle a \rangle| = 3$, $|(6)| = 0$, $(S^z) = -|$ the Eqs.(6.36) along with field equations in (6.27) are integrated using the Runge-kutta method. With these parameters the dynamics of the system is easier to study than **the** previous values where the coherent field had a larger field strength ($\sim$ 10) and hence needs very large decay rates to reach steady state in an observable manner. In this case we take $71 = 0.1$. The dynamical behavior of $P_e(t)$ and average number of photons in a and b modes $|(a)|^2$ and $|(b)|^2$ is depicted in Figure 6.7, where each of the variables decays to a steady state value. At long enough time (scaled as gt) the system reaches a steady state where the atom is in the ground state, $P_e(t) = 0$ and $|(a)|^2 = 3.5$, $|(6)|^2 = 0.44$. The steady state corresponds to the NLOB condition [15] satisfying **the** relation

$$K(a)^3 + g(b) = 0 \quad . \tag{6.37}$$

It has been shown by Wynne that NLOB occurs whenever there is multiphoton excitation in a system. This excitation induces a nonlinear polarization and generates new fields which create a second excitation pathway between the atomic levels. The three photon process in our system generates the third harmonic field which initiates a single photon process in the system. The two processes interfere destructively according to the NLOB condition which stipulates that the amplitudes and phases of waves propagating through the medium develop in such a way as to minimize the dissipation. Then there is no further change in the intensities of the generated signal nor the **fundamental input** frequency signal as depicted in Figure 6.7.

We now deal with one more case which would explicitly underline **the** differences of **the** semiclassical **and** quantum theories. The mode a is treated as prescribed i. e. **the** operator a is replaced with a complex number a in the Hamiltonian **(6.1) which** gives

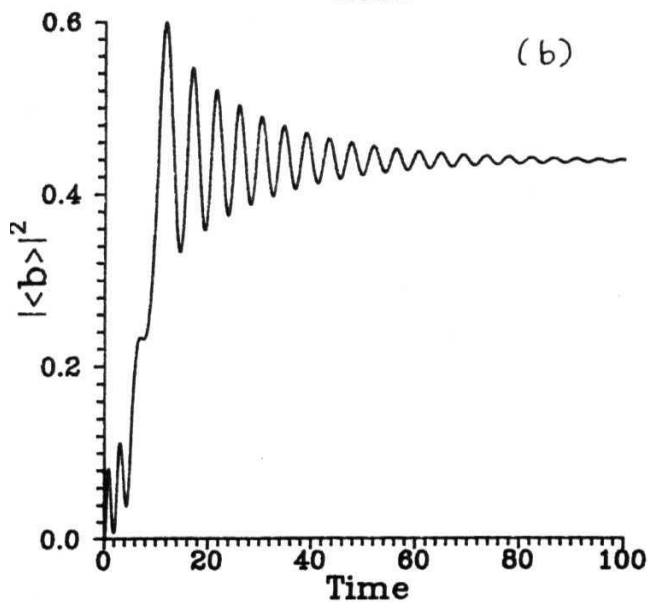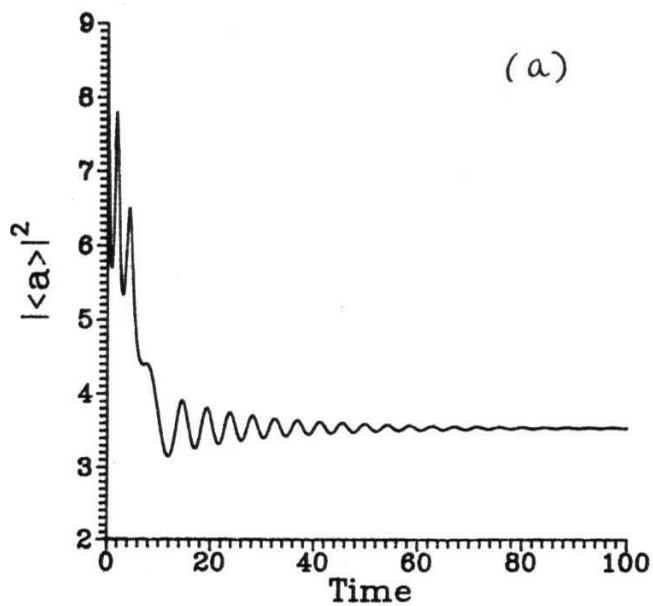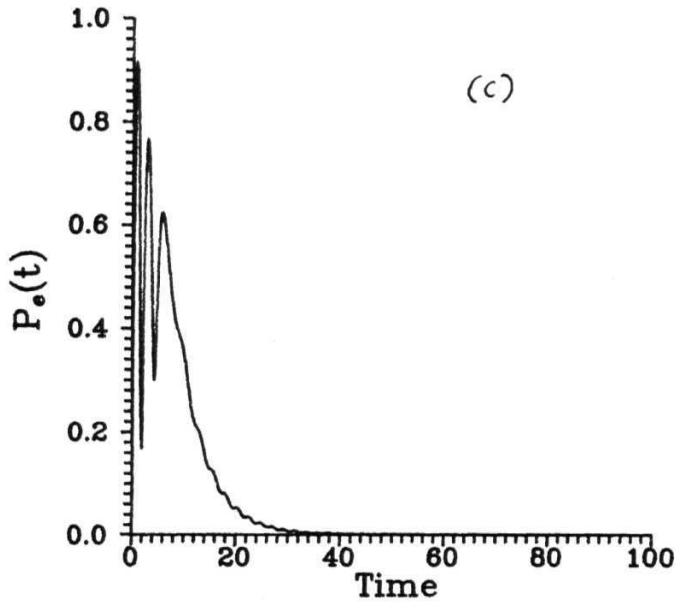$$H_{eff} = \hbar(\kappa S^+ \alpha^3 + \kappa S^- \alpha^{*3}) + \hbar(g S^+ b + g^* S^- b^\dagger) \tag{6.38}$$

Fig. 6.7: Dynamical results in the semiclassical case with the decays included. Parameters used are $\langle a \rangle = 3.0$, $|(6)| = 0$, and $(S^z) = -\langle$ and $7_X = 0.1$. The mean number of photons in a) *a* mode and b) *b* mode.

Fig. 6.7: Dynamical results in the semiclassical case with the decays included. Parameters used are \(a)\ = 3.0, |(6)| = 0, and (S²) = -\ and -)₊ = 0.1. c) Probability of the atom being in the excited state.

Taking /c,p and a to be real by choosing the phase relations appropriately Eq.(6.38) reduces to

$$H_{eff} = 2hna^3 S^x + hg(S+b + 5"6^f) \tag{6.39}$$

which is equivalent to the Hamiltonian for the JCM with an external pump (Eq. 5.29) dealt with in Chapter 5 where KQ^3 is equal to the coherent amplitude a of the external pump. In this case 6-mode evolves quantum mechanically but the a-mode remains fixed. Choosing a = 10 and n/g — 0.01, gives $\sqrt{na^3} = 10$ which is consistent with the mean number of photons chosen in the *a* -mode throughout the chapter. We depict $P_e(t)$ and *(tfb)* in Figure 6.8. On comparison with Figure 6.4 we see the significant differences between the full quantum calculation and the approach in which a-mode is treated as a prescribed field. The mean number of photons going into the 6-mode from the coherent a-mode field is very much higher (~400) than the quantum case where *(tfb)* goes to a maximum of ~6 photons. The behavior in Figure 6.8 is also quite unlike the periodicity predicted by the semiclassical approach above. The collapse and revivals in Figure 6.8 arise from the discrete nature of the levels associated with the 6-mode.

In conclusion we have demonstrated the presence of strong quantum mechanical interference effects in a cavity QED model involving three photon and one photon absorption processes. We have also shown how the quantum results differ from the different types of semiclassical theories. The two channel cavity QED model exhibits rich quantum features like mode mixing, and mode entanglement even in simplest cases. Having a classical field in one of the channels differs considerably from having two fully quantized fields in the two channels. The periodic behavior in the semiclassical approximation is radically different from the fully quantized two channel model as well as the single quantized channel model both of which show collapse and revivals indicating that the quantum effects are rather dominant.
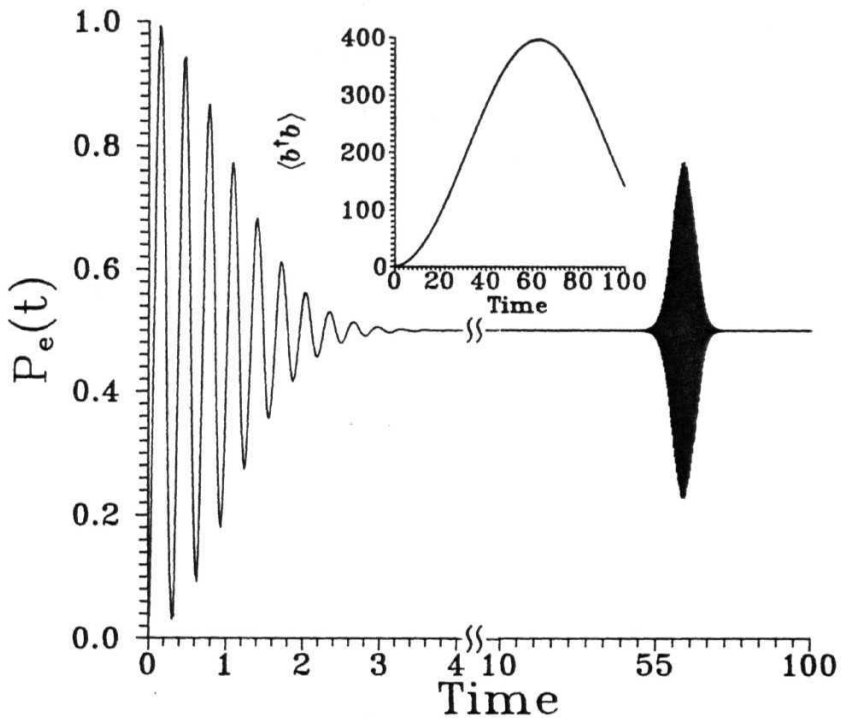
Fig. 6.8: Dynamics in the case where the mode a is prescribed. Parameters used are a = 10.0, AC/#=0.01.

REFERENCES

1. E. T. Jaynes and F. W. Cummings, Proc. IEEE 51, 89 (1963) .

2. D. Meschede, H. Walther and G. Muller, Phys. Rev. Lett. 54, 551 (1985).

3. J. H. Eberly, N. B. Narozhny and J. J. Sanchez Mondragon, Phys. Rev. Lett. 44, 1323 (1980), N. B. Narozhny, J. J. Sanchez-Mondragon and J. H. Eberly, Phys. Rev A23, 238 1981; L. Filipowicz, J. Phys. **A79,** 3785 (1986).

4. G. Rempe, H. Walther and N. Klein, Phys. Rev. Lett., 58, 353 (1987).

5. G. Rempe, F. Schmidt-Kaler and H. Walther, Phys. Rev. Lett. 64, 2783 (1990).

6. F. Diedrich and H. Walther, Phys. Rev. Lett., 58, 203 (1987).

7. J. J. Sanchez-Mondragon, N. B. Narozhny and J. H. Eberly, Phys. Rev. Lett. 51, 550 (1983); G. S. Agarwal Phys. Rev. Lett. 53, 1732 (1984); G. S. Agarwal, J. Opt. Soc. Am. B2, 480 (1985).

8. R. J. Thompson, G. Rernpe and H. J. Kimble, Phys. Rev. Lett., 68, 1132 (1992); M. G. Raizen, R. J. Thompson, R. J. Brecha, H. J. Kimble and H. J. Carmichael, Phys. Rev. Lett., 63, 240 (1989).

9. For excellent reviews on cavity QED; see (a) H. I. Yoo and J. H. Eberly, Physics **Reports 118, 239 (1985) (b) S. Haroche in** *Fundamental Systems in Quantum Optics,* edited by J. Dalibard, J. M. Raimond and J. Zinn-Justin, p. 768 (Elsevier, Amsterdam,1992) (c) P. Meystre, Physics Reports **219,** 243 (1992) (d) G. Raithel, C. Wagner, H. Walther, L. M. Narducci, M.O. Scully in a special volume of Adv. At. Mol. Phys. edited by P. Berman (Academic, NY, 1994).

10. B. W. Shore and P. L. Knight, J. Mod. Optics 40, 1195-1238 (1993); S. M. Barnett and P. L. Knight, Opt. Acta **31,** 435 (1984); S. M. Barnett and P. L. Knight, Phys. Rev. A33, 2433 (1986), S. M. Barnett, P. Filipowicz, J. Javaninen et al in *Frontiers in Quantum Optics* ed. by E. R. Pike and S. Sarkar. Adam-Hilger. (1986).

11. K. Aron and P. M. Johnson, J. Chem. Phys. 67, 5099 (1977).

12. J.C. Miller and R. N. Compton, Phys. Rev. A25, 2056 (1982); J. C. Miller, R. N. Compton, M. G. Payne and W.R. Garrett, Phys. Rev. Lett. 45, 114 (1980).

13. M.S. Malcuit, D. J. Gauthier and R.W. Boyd, Phys. Rev. Lett. 55, 1086 (1985).

14. P.L. Knight, Physica Scripta **T12,** 51 (1986); S.J.D. Phoenix and P.L. Knight, J. Opt. Soc. Am. B7, 116 (1990); L. Schoendorff and H. Risken, Phys. Rev. **A31,** 5147 (1990); G. S. Agarwal and R. R. Puri, Phys. Rev. **A43,** 3949 (1991).

15. J.J. Wynne, in Proc. IV International Conference on Multiphoton Processes, eds. S. J. Smith and P. L. Knight (Cambridge Press, 1988), p. 329; D. J. Jackson and J. J. Wynne, Phys. Rev. Lett. 49, 543 (1982).

16. J.C. Maxwell, *A Treatise, on Electricity and Magnetism,* Vol 1 (Dover, New York, 1954, 3rd ed.) p. 408.

17. G. S. Agarwal Phys. Rev. Lett. 57, 827 (1986); G. S. Agarwal and F. Rattay, Phys. Rev. A 37, 3351 (1988).

18. H. C. Baker, Optics Commun. 75, 154 (1990).

19. Liwei Wang, R. R. Puri and J. H. Eberly, Phys. Rev. **A46,** 7192 (1992); C. K. Law, Liwei Wang, and J. H. Eberly, Phys. Rev. **A45,** 5089 (1992).

20. F. M. Faisal, *Theory of Multiphoton Processes,* (Plenum, New York).

21. M. Brune, J. M. Raimond and S. Haroche, Phys. Rev. A35, 154 (1987).

22. J. M. A. Danby, *Computing Applications to differential equations* (Reston Publishing Company, 1985) p. 32-48.